A MIDDLE CEREBRAL ARTERY OCCLUSION MODELLING STUDY OF COMBINATORIAL TREATMENT (ACUTE PHASE) AND POST-ISCHEMIC EXERCISE (CHRONIC PHASE) IN RATS

ELGIN YAP EE LIN

NATIONAL UNIVERSITY OF SINGAPORE

2011

A MIDDLE CEREBRAL ARTERY OCCLUSION MODELLING STUDY OF COMBINATORIAL TREATMENT (ACUTE PHASE) AND POST-ISCHEMIC EXERCISE (CHRONIC PHASE) IN RATS

ELGIN YAP EE LIN
(*B. Sc (Merits)*, NUS)

A THESIS SUBMITTED

FOR THE DEGREE OF DOCTOR OF PHILOSOPHY

DEPARTMENT OF ANATOMY

NATIONAL UNIVERSITY OF SINGAPORE

2011

Acknowledgements

I would like to express my most humble but profound gratitude to A/P Ng Yee Kong (Department of Anatomy, NUS) and A/P Ivan Ng (Department of Neurosurgery, NNI) for their generous faith and unflinching support in my dreams and pursuits.

I would also like to extend my most sincere appreciation to Prof Bay Boon Huat (Department of Anatomy, NUS), Prof Ling Eng Ang (Department of Anatomy, NUS) and A/P Samuel Tay Sam Wah (Department of Anatomy, NUS) for their valuable aid and guidance.

And I would like to give thanks to the fellow staff and students from the department of Anatomy for their help and friendship.

Finally, I would like to acknowledge my wonderful Wife (Tan Wan Loo) who has been inspiring and assisting me from the beginning to the completion of this thesis with absolute profundity.

Dedications

Following an unfathomably long gestational PhD candidature, I know only too well that I am just about to take my very first step.

The Russian author Leo Tolstoy (1828-1910) said: “Those who live life in perfection look only forwards, those who have stopped moving forwards look back on their achievements.”

This thesis is the distillation of the earlier phases in my life through the anticipation, inspiration, patience, support and understanding from my family and teachers.

I am dedicating this “part of my life” to my Wife (Tan Wan Loo), my Parents (Yap Cheong Eng and Goh Siew Hong), my Brother (Yap Victor), and my family member (Egan Yap).

Now I am looking forward to dedicate the latter part of my life to many more personalities that I am about to meet.

Lastly “If realism gives me short-sightedness; let me stick to idealism.”

Publications and Abstracts

Publications

Yap E, Tan WL, Ng I, Ng YK. Combinatorial-approached neuroprotection using non-selective pan-caspase inhibitor and poly (ADP-ribose) polymerase (PARP) inhibitor following experimental stroke in rats; is there additional benefit? Brain Res. 2008; 1195: 130-138.

Yap E, Tan WL, Ng I, Ng YK. Long Term Moderate Forced Treadmill Exercise Increased Pecam-1 Expression in Brain Cortex via Changes to PDGF Level (Submitted)

Abstracts

4th European Society for Neuroscience Meeting Conference on "Advances in Molecular Mechanisms of Neurological Disorders" 2009 (Leipzig, Germany) Title: Effects of long term moderate forced treadmill exercise on angiogenic factors in the rat hippocampus

3rd European Society for Neuroscience Meeting Conference on “Advances in Molecular Mechanisms of Neurological Disorders” 2007 (Salamanca, Spain) Title: The benefits of post-ischemic exercise; a look into TGF-β signaling pathway

7th Bienniel Meeting of the Asian Pacific Society for Neurochemistry 2006 (Singapore, Singapore) Title: The benefits of exercise following stroke; the role of smad7

7th Bienniel Meeting of the Asian Pacific Society for Neurochemistry 2006 (Singapore, Singapore) Title: Dual modality neuroprotection using non-selective poly (ADP-ribose) polymerase (PARP) and pancaspase inhibitors following experimental stroke in rats; is there additional benefit?

Table of Contents

Summary

Stroke is the third leading cause of death and disability both locally and internationally. Despite the enormous availability of scientific literatures on brain ischemia, currently, only intravenous recombinant tissue-type plasminogen activator (rt-PA, Alteplase) thrombolytic treatment and antiplatelet therapy are approved pharmacological managements which induce the degradation of the arterial thrombus and restoration of vessel patency and blood flow to improve clinical prognosis. In the present study, experimental brain ischemia was modeled with intraluminal suture technique induced middle cerebral artery occlusion in rats (MCAo). Stroke can be temporally classified into varying phases where pharmacological intervention plays an important mediating role in the early phase and physiotherapy in addition to medication are proven clinical approach for managing brain ischemia later.

Studies showed that in early phases of MCAo, cell death advances via a continuum between apoptotic and non-apoptotic modes that hinged on cellular energy level. In the current acute phase study, concomitant administration of both z-VAD-fmk and 3-AB yielded better outcome with bigger infarct volume reduction in comparison with single inhibitor administration following MCAo. In addition, combinatorial treatment remained effective even when administered at 24hr post MCAo. Although there was no general correlation between intracellular ATP level and infarct size, only treatment

with PARP inhibitors had showed that intracellular ATP level was inversely related to the size of infarct.

Although physiotherapy has been clinically proven, its molecular basis has not been well elucidated. The present chronic phase study demonstrated that eight weeks of moderate forced treadmill post-ischemic exercise were able to reduce secondary damages, and achieved better clinical outcome following brain ischemia via multi-modal neuroprotective and angiogenic (in turn supporting neuroregeneration) mechanisms. The elevated level of activated caspase-3 seen in the MCAo rats was reduced subsequent to post-ischemic exercise when TGF-β1 was further increased and smad7 was reduced concomitantly in the ipsilateral cortices of the MCAo-runner rats suggesting an anti-caspase-dependent-apoptosis property of TGF-β1's role in neuroprotection. Paradoxically, up-regulated positive TUNEL staining within the ipsilateral cortices of the MCAo-runner rats may be taken as an indication as the body's effort to modulate imminent cell death via apoptotic pathways which will be less prone to inflammatory events.

In addition to neuroprotection, neuroregeneration after ischemic insults is pivotal for a more favorable prognosis. For neuroregeneration to happen, increase in angiogenic and erythropoietic activities are needed to form new and effective oxygen delivery vascular structures. Interestingly, distinct Pecam-1 immunoreactivities were seen with marginal PDGFB increased in sham-runner rats. However, opposite observations

could be observed in the ipsilateral cortices of the MCAo-runner rats with up-regulated PDGFB expressions that were not reciprocated by strong Pecam-1 immunoreactivities. Thus suggested that brain ischemia may produce or remove another unidentified factor that may form either inhibitive or necessary condition for the angiogenic property of PDGFB to work. With changes to the angiogenic/erythropoietic factors and vasculatures, antioxidants' profiles were also dissimilar in the rats possibly reflecting the differential conditions.

In its essence, the present study has shown that combinatorial administration of both z-VAD-fmk and 3-AB was better than if the inhibitors were given individually in the acute phase stroke. The current data from the chronic phase of brain ischemia experiments also showed that post-ischemic exercises could induce endogenous factors that may confer neuroprotection and possibly neuroregeneration.

List of Tables

List of Figures

List of abbreviations

•OH	hydroxyl radical
3-AB	3-Aminobenzamide
AD	Alzheimer’s disease
Akt (aka PKB)	protein kinase B
ATP	Adenosine-5'-triphosphate
Bad	Bcl-2-associated death promoter
BBB	blood-brain barrier
Bcl-2	B-cell leukemia/lymphoma 2
BMP	bone morphogenic protein
CA1	Cornu Ammonis 1
Ca^{2+}	calcium
CBF	cerebral blood flow
CBV	cerebral blood volume
CCA	common carotid artery
cAMP	cyclic adenosine monophosphate
cDNA	complementary DNA
cm/sec	centimeter per second
CNS	central nervous system
Cu/ZnSOD	copper/zinc SOD
DAB	3,3'-diaminobenzidine
DAPI	4',6-diamidino-2-phenylindole

DG	dentate gyrus
DNA	deoxyribonucleic acid
ECA	external carotid artery
ECSOD	extracellular SOD
EPO	erythropoietin
EPOR	erythropoietin receptor
Erk	extracellular-signal regulated kinase
Fig.	figure
GPx	glutathione peroxidase
GSH	glutathione
H_2O_2	hydrogen peroxide
HDB	horizontal diagonal band of Broca
HIF-1α	hypoxia inducible factor-1alpha
HIV	human immuno-deficiency virus
hr	hour
HuEPO	human erythropoietin
IACUC	Institutional Animal Care and Use Committee
ICA	internal carotid artery
IFN-γ	interferon-gamma
JAK2	janus kinase-2
kD	kiloDalton
m	metre

μg	microgram
μl	microlitre
MAPK	mitogen-activated protein kinase
MCAo	middle cerebral artery occlusion
mg/kg	milligram per kilogram
min	minutes
Mn-SOD	manganese SOD
moles/mg	moles per milligram
mRNA	messenger ribonucleic acid
NAD^+	nicotinamide adenine dinucleotide
NeuN	Neuronal Nuclei
NF-κB	nuclear factor kappa B
NGF	nerve growth factor
$OONO^-$	peroxynitrite
One-way ANOVA	One-way analysis of variance
PARP	poly (ADP-ribose) polymerase
PBS	phosphate-buffered saline
PDGF	platelet derived growth factor
PDGFR	platelet derived growth factor receptor
PET	positive emission tomography
PI3k	phosphatidylinositol-3-OH kinase
PPA	pterygopalatine artery

PVDF	polyvinylidene difluoride
rHuEPO	recombinant human erythropoietin
RIPA	RadioImmuno Precipitation Assay
ROS	reactive oxygen species
rt-PA	recombinant tissue-type plasminogen activator
sec	second
SAH	subarachnoid hemorrhage
SDS-PAGE	sodium dodecyl sulfate polyacrylamide gel electrophoresis
smad	Sma and Mad protein
SOD	superoxide dismutase
TGFBR-I/II	transforming growth factor-beta receptor type I/II
TGF-β	transforming growth factor-beta
TNF-α	tumor necrosis factor- alpha
TTC	2,3,5-triphenyltetrazolium chloride
TUNEL	terminal deoxynucleotidyl transferase dUTP nick end labeling
V	voltage
VEGF	vascular endothelial growth factor
VEGFR	vascular endothelial growth factor receptor
z-VAD-fmk	Carbobenzoxy-Val-Ala-Asp-fluoromethylketone

INTRODUCTION

CHAPTER ONE

1.1 Epidemiology of Stroke

Stroke is the third leading cause of death and disability both locally and internationally. Approximately 11% of all deaths in Singapore are contributed by stroke related deaths; these are predominantly elderly patients and remain a priority for the health of the nation (Venketasubramanian et al., 2005). Although the incidence of stroke is reducing with improved public health measures, the prevalence is increasing within the aging population. In addition, although stroke is a clinical term used to describe a sudden cerebrovascular accident causing major physical disability, a large number of events are silent and are a recognized cause of multi-infarct dementia associated with progressive cognitive decline and dependency (Caplan and Schoene, 1978; Fields, 1986). The true burden on the community is incalculable, and set to increase.

1.2 Clinical Classification of Brain ischemia

Stroke can be broadly divided into two major categories – hemorrhagic and ischemic. In Singapore, approximately 75% of all strokes are of ischemic origin which is the interest of this thesis. Ischemic stroke can be further dichotomized into thrombotic and embolic cerebral ischemia. Ischemic stroke occurs when a blood vessel leading to the brain is occluded, thus resulting in a reduction of cerebral perfusion. Within minutes of reduced cerebral perfusion, brain infarction that is characterized by an irreversibly necrotic core formed within an area of hypoperfused brain tissue will develop. The hypoperfused

regions are viable tissue of varying degree and are termed as the ischemic penumbra (Astrup et al., 1981; Heiss et al., 1994; Heiss, 2000) which represents the target for most therapeutic interests and interventions. Clinical interpretation of normal cerebral blood flow in grey matter and white matter are in the range 60–70 ml/100 g/min and 20–30 ml/100 g/min respectively. When the flow rate went below a threshold of 10–12 ml/100 g/min, it is called absolute ischemia and develops irreversible neuronal structural damage (ischemic core) (Hossmann, 1994).

Temporally, stroke can be stratified into the following phases: hyper-acute, acute, sub-acute and chronic brain ischemia. In human, the four phases for stroke are defined as between symptomatic onset and six hours for hyper-acute phase, within 24hr to approximately seven days post-stroke for acute phase (Page et al., 2005; Bader et al., 2006), one week to three months post-stroke for sub-acute phase (Page et al., 2001; Page et al., 2002; Kalra et al., 2007) and more than three months post-stroke for chronic phase (Page et al., 2004; Nudo et al., 2007). Understanding the mechanisms of these various and distinct phases are pivotal in delivering an effective rehabilitation intervention because cellular events that are triggered by insults to the brain during the acute and sub-acute phases are likely to be independent of the processes in the chronic phases.

The regions of brain infarction are characterized by a necrotic core, in which all cell death occurs rapidly. This core of irreversible damage is surrounded by an ischemic penumbra in which neurons die over days to weeks (Schellinger et al., 2001a; 2001b) likely through

apoptotic processes and the potential area of developing therapeutic interventions (Rami et al., 2008). Apoptosis and necrosis have long been recognized and documented as two distinct forms of cell death where apoptosis is an energy requiring programmed process and necrosis is presumably an unregulated mode (Wyllie et al., 1980). Not only apoptosis and necrosis are considered biochemically and morphologically different, they hold different implications for the surrounding tissues as well.

1.3 Types of Experimental Brain Ischemia Rodent Model

Extensive studies have shown that apoptosis and necrosis occurred in brain of the experimental cerebral ischemic rodent model following middle cerebral artery occlusion (MCAo), where apoptosis occurs surrounding the necrotic core, in the penumbra region (Ferrer and Planas, 2003). Most in vivo rodent models of experimental brain ischemia that are used today were developed between the late 1970s and early 1980s. They are generally divided into two categories, global and focal ischemia. MCAo is a focal ischemic model, was first introduced by Kozuimi and coworkers (Kozuimi et al., 1986) and subsequently modified by Longa and co-workers (Longa et al., 1989) and many others to reduce subarachnoid haemorrhage (SAH) by blunting the end of the nylon suture and premature reperfusion by coating the suture with poly-L-lysine or silicone (Belayev et al., 1996; Schmid-Elsaesser et al., 1998). MCAo model can be further defined by period of occlusion. In temporary MCAo, vascular occlusion is induced up to three

hours followed by prolonged reperfusion, while in permanent MCAo vascular occlusion is maintained throughout the experiment.

1.4 Clinical Relevance of Middle Cerebral Artery Occlusion (MCAo) Rodent Model

In permanent ischemic model, there is significant variation in the extent of the different infarcted regions documented with the different strains of rodents such as Sprague-Dawley rats, spontaneously hypertensive rats, and Wistar rats (Brint et al., 1988; Buchan et al., 1992; Markgraf et al., 1993; Back et al., 1995). At the same time, infarction can be first observed between the third to the twelfth hour following MCAo. This wide time range further supports the existence of fundamental difference in each strain's properties. Sprague-Dawley rats was seen with an earlier circumscribed area of infarct as compared to Wistar rats, which possibly be due to the less uniform lesion in the latter (Peter, 1999).

As in human, permanent MCAo in rodents produce core ischemic cell death in striatum that progress into the other regions of neocortex, entorhinal cortex and medial caudate-putamen which make up the penumbra (Bolander et al., 1989; Nagasawa et al., 1989; Memezawa et al., 1992; Belayev et al., 1997). The infarcted core area in the striatum is presented with a necrotic character that occurs rapidly upon ischemic insult (Garcia et al., 1995; Li et al., 1995b) and the devastation in this core region has reached a

irreversible point that render most administered neuroprotective agents ineffective (Mohamed et al., 1985; Buchan et al., 1991; Minematsu et al., 1993; Yrjanheikki et al., 1999; Sydserff et al., 2002). At the other end of the spectrum, the infarcted area in penumbra contains a greater degree of delayed apoptotic cell death than in striatal infarction (Garcia et al., 1995; Li et al., 1995a; 1995b; Linnik et al., 1995). This delayed progression of cell death in the penumbra (cortex) following MCAo presents an opportunity for this model to be employed in identification of new targets for neuroprotective therapies (Gladstone et al., 2003; Cheng et al., 2004).

However, studies using positron emission tomography (PET) scans showed that blood flow rates varies widely in terms of space and time within the penumbral region in different MCAo models resulting in modeling inconsistency (Nagasawa et al., 1989; Heiss et al., 1994; Zhao et al., 1994; Belayev et al., 1997). Modification of the MCAo model with occlusion of the MCA together with ipsilateral common carotid artery (CCA) reduces cerebral blood flow (CBF) leading to the core and periphery of the MCA territory and has been reported to successfully produce more consistent infarct volumes (Chen et al., 1986; Ginsberg and Busto, 1989; Buchan et al., 1992; Avendano et al., 1995; Soriano et al., 1997). Pan-necrosis, occurs during the final stage of infarct development in focal ischemia, refers to the complete loss of cellular elements approximately seven days following ischemic insult. In this stage, the neuronal death is found together with glial and vascular cell death and loss of cellular elements.

1.5 Post-Ischemic Cellular Events and Responses in the Central Nervous System (CNS)

Brain ischemia elicits an array of cellular response and activates a convoluted cellular signaling. The normal physiological function of nervous system is orchestrated by different cell types with differing roles. The neurons are the functional cells whereas the astrocytes, microglia and oligodendrocytes play the supporting role in the brain. In the event of an ischemic incident onset, neuronal cell can be degenerated by energy failure caused by rapid loss of blood supply, or by the activation of calcium (Ca^{2+}) - dependent pathways (Mattson, 2000). When blood supply to the brain is impeded in stroke, neuronal cells in the core lesion die immediately from oxygen and glucose starvation, mainly necrosis. Necrotic neuronal cell death within the core ischemic region can trigger immune responses that lead to microglial activation and infiltration of peripheral inflammatory cells usually with a negative connotation (Siesjo and Siesjo, 1996; Dirnagl et al., 1999). These inflammatory cells can release a variety of cytotoxic agents including more cytokines and more reactive oxygen species (ROS) in response to ischemia which may play a crucial role in further development of ischemic neuronal damage (Ishibashi et al., 2002).

1.6 Intracellular Adenosine-5'-Triphosphate (ATP) Level Following Brain Ischemia

At the immediate site of the ischemic region during an acute phase of a stroke, lower blood flow rate trigger necrosis as a result of an energy failure, or drastic decrease in intracellular (adenosine-5'-triphosphate) ATP levels (Eguchi et al., 1997; Leist et al., 1997). Intracellular ATP levels are fundamentally decided by three parameters: material supply (glucose uptake), ATP synthesis (mostly in the mitochondria) and consumption. Poly (ADP-ribose) polymerase (PARP) is a deoxyribonucleic acid (DNA) repair enzyme that is primarily activated by DNA strand breaks. Berger et al. (1986) proposed a "suicide" concept whereby PARP overactivation occurs when there was massive level of DNA damage, leading to intracellular ATP depletion in an attempt to restore nicotinamide adenine dinucleotide (NAD^+), is implicated for participation in DNA damage-induced necrotic death (Ha and Snyder, 1999).

1.7 Roles of Transforming Growth Factor-β1 (TGF-β1) and Sma and Mad Protein 7 (smad7) in Brain Ischemia

Transforming Growth Factor-β1 (TGF-β1) is a member of super-family of multifunctional cytokines orchestrates various critical physiological processes, including proliferation, differentiation, growth inhibition, and apoptosis (Schuster and Krieglstein, 2002). TGF-β isoforms (TGF-β1, 2 and 3) elicit their cell type-specific responses through

the ligand induced formation of a heteromeric receptor complex between the serine/threonine kinases TGF-β receptor type I (TGFBR-I) and TGFBR-II: the type II receptor binds TGF-β by its own, then recruits the type I receptor, allowing the transphosphorylation-mediated activation of TGFBR-I. The TGFBR-I then interact and phosphorylate smad protein transcription factor, smad2 and smad3, which form heterotrimeric complexes with smad4 and translocate into the nucleus to regulate key target gene transcription cascade (Shi and Massague, 2003; ten Dijke and Hill, 2004). smad7, an inhibitory smad, acts by occupying ligand-activated TGFBR-I and interfering with the phosphorylation of smad2 and smad3 in a negative feedback loop preventing over-stimulation of the cell by TGF-β. Up-regulation of smad7 has been associated with an inhibition of TGF-β1-induced signaling (Hayashi et al., 1997).

TGF-b1 mRNA and protein have been shown to increase and have also demonstrated neuroprotective activity (Ruocco et al., 1999; Zhu et al., 2002) following experimental hypoxia (Klempt et al., 1992), global (Zhu et al., 2000) or focal (Ata et al., 1999) ischemia, and in cultured neurons after various stimuli (Ren and Flanders, 1996). The neuroprotective mechanism of this cytokine to antagonize neuronal apoptosis has been coupled to the up-regulation of B-cell leukemia/lymphoma 2 (Bcl-2) and Bcl-xl (Prehn et al., 1994), and the inhibition of caspase-3 activation (Zhu et al., 2001). It was proposed that a mechanistic loop, involving Bcl-2 and caspase-3, where inhibition of caspase-3 activation by TGF-β1 is mediated through the up-regulation of Bcl-2. And because of suppressed caspase-3 activation, the cleavage of Bcl-2, a substrate of caspase-3, could in

turn be reduced. In view of this point, reduced activation of caspase-3 by TGF-β1 may contribute to up-regulation of Bcl-2 expression. Besides the classic receptor-activated smad signaling, increasing studies have demonstrated that TGF-β1 activates other pathways such as mitogen-activated protein kinase (MAPK) and phosphatidylinositol-3-OH kinase (PI3k)/Akt signaling pathways (Xiao et al., 2002; Yu et al., 2002). And It has been demonstrated recently that TGF-β1 inactivates the pro-apoptotic protein Bcl-2-associated death promoter (Bad) via activation of mitogen-activated protein kinase (MAPK)/extracellular-signal regulated kinase (Erk)1,2 pathway (Zhu et al., 2002).

The cytoprotective effect of TGF-β1 produced in the central nervous system (CNS) following various insults may be consistent with the low numbers of apoptotic microglia found in in vivo models of CNS inflammatory diseases (Pender et al., 1991), as abnormal overactivation and resultant death of microglial cells may cause more neurotoxicity in various neurodegenerative diseases (Gebicke-Haerter et al., 1996). Microglia are functionally equivalent to peripheral macrophages in the CNS (Giulian, 1987). Activated microglia which secrete bioactive molecules, such as reactive oxygen or nitrogen species and inflammatory cytotoxins, have been closely associated with various neurodegenerative diseases such as stroke, trauma, Alzheimer's disease (AD), multiple sclerosis, and human immuno-deficiency virus (HIV)-associated dementia (Ransohoff et al., 1996; Gonzalez-Scarano and Baltuch, 1999). Sustained overproduction of those molecules via microglia over-activation would cause severe damage to both the normal

and pathological brain region. Nonetheless, the role of TGF-β1 in relation to anti-inflammatory and anti-apoptotic functions in the CNS remains controversial as it is extremely dependent on the cell type, the pathological stimuli and the experimental conditions (De Luca et al., 1996)

In the smad signaling pathway, smad7 expression is increased in response to TGF-β, bone morphogenic protein (BMP), and activin, providing a mechanism for negative feedback regulation (Massague´ and Chen, 2000). Interestingly, smad7 expression can also be induced by interferon-γ (IFN-γ) and by tumor necrosis factor- α (TNF-α), which suggest that smad7 may fulfill other cellular functions independent of its inhibitory role (Ulloa et al., 1999; Bitzer et al., 2000). Overexpression of smad7 has also been reported, in several studies which pronounce TGF-β1 as pro-apoptotic, to sensitize various cell types to many forms of cell death via a yet defined mechanism (Landstrom et al., 2000; Lallemand et al., 2001), where smad7 could possibly be involved in the activation of the Jun N-terminal kinase (JNK) signaling pathway, which appears to play a critical role in mediating the apoptotic function of smad7 (Maire et al., 2005).

1.8 Roles of Erythropoietin (EPO) and Erythropoietin Receptor (EPOR) in Brain Ischemia

During hypoxia and ischemia, expressions of erythropoietin (EPO) and its receptor (EPOR) are enhanced as a result of hypoxia inducible factor-1α (HIF-1α) accumulation.

Human erythropoietin (HuEPO), a glycoprotein growth factor, is the main regulator of erythropoiesis. The HuEPO gene was cloned in the early 1980s: a recombinant human form of erythropoietin (rHuEPO) was subsequently developed. EPO, increases red cell mass to improve tissue oxygenation, is produced by the kidney and the liver (in fetuses) in response to hypoxic and ischemic insults to stimulate erythropoiesis (Jewell et al., 2001; Sirén et al., 2001a).

EPO has also been shown to exert neuroprotective effects against neurological injury in several experimental models both *in vitro* and *in vivo* (Grasso et al., 2001). EPO may protect neurons from glutamate toxicity by activation of calcium channels, increasing the activity of antioxidant enzymes in neurons, modulation of angiogenesis in the ischemic brain, and by anti-apoptotic effects via the activation of janus kinase-2 (JAK2) and nuclear factor κB (NF-κB) signaling pathways (Digicaylioglu and Lipton, 2001; Chong et al., 2002)

Treatment with rHuEPO in hypoxic and ischemic animal experimentation have shown significantly reduced delayed neuronal death in the Cornu Ammonis 1 (CA1) area of the hippocampus (Zhang et al., 2006) and prevented cognition impairment in the passive avoidance test (Catania et al., 2002). The “Göttingen EPO-Stroke-Trial” which took place in 1998 is the first clinical trial that suggested rHuEPO, in addition to erythropoiesis, has therapeutic advantages that can alleviate ischemic and traumatic CNS damages and these findings were supported by subsequent clinical trial.

Jelkmann (2005) with his elegant review has dichotomized the effects of EPO to be direct and indirect. Indirectly, EPO improves sensory, cognitive and endocrine functions of the CNS through its erythropoiesis-stimulating effect, because it increases the oxygen supply to the brain. The alleviation of anaemia in patients suffering from renal insufficiency or malignancy ameliorates attention difficulties and psychomotor slowing and may cure from depressing fatigue. The direct effects of EPO are independent of erythropoiesis. Both EPO and its receptor (EPOR) are expressed in the CNS where EPO prevents hypoxia- and glutamate-induced neuronal cell death.

There is increasing evidence that EPO has a protective function in cerebral ischemia. Enthusiasm for rHuEPO as a potential neuroprotective therapeutic must be tempered, however, by the knowledge it also enlarges circulating red cell mass and increases platelet aggregability. When using rHuEPO for treatment, high EPO plasma levels associated with increases in blood viscosity, however, may counteract beneficial effects of EPO in brain ischemia (Wiessner et al., 2001). Therefore, production of endogenous EPO from brain and endothelial cells are particularly important for neuroprotection as only low levels of rHuEPO appear to be able to cross the blood-brain barrier (BBB) when administered at high dose intravenously.

1.9 Roles of Hypoxia Inducible Factor-1 (HIF-1) in Brain Ischemia

HIF-1 is a wide spectrum transcription factor that encodes for various proteins that mediate molecular responses to reduced oxygen availability (Stroka et al., 2001; Shao et al., 2005). HIF-1 protein is a heterodimer consisting of a α- and β-subunit. The HIF-1β subunit is expressed constitutively in the nucleus, whereas the HIF-1α subunit expresses variably under normoxic and hypoxic conditions. During normoxia, HIF-1α subunit is subjected to ubiquitination and proteasomal degradation (Salceda and Caro, 1997; Huang et al., 1998). However, these processes are inhibited under hypoxic conditions to allow accumulation of HIF-1α subunit which then translocate into the nucleus from the cytoplasm and form heterodimerization of the HIF-1α and HIF-1β subunits (Jiang et al., 1996; Jewell et al., 2001). This complex, together with its transcriptional co-activators, will then bind to the hypoxia response elements of various HIF-1 target genes such as vascular endothelial growth factor (VEGF) and EPO (Ratcliffe et al., 1998; Semenza et al., 2001; Fandrey et al., 2006) to elicit an appropriate response.

1.10 Roles of Vascular Endothelial Growth Factor (VEGF) and VEGF Receptor (VEGFR) in Brain Ischemia

VEGF is a major family of angiogenic growth factor that induces vascularisation (Carmeliet and Storkebaum, 2002), currently consisting of various isoforms such as VEGF-A, VEGF-B, VEGF-C, VEGF-D, and PLGF (Katoh and Katoh, 2006; Ladomery

et al., 2007). Among the different isoforms, VEGF-A is the best described and often referred to as VEGF. VEGF ligand binds to the vascular endothelial growth factor receptors (VEGFR), a tyrosine kinase receptor, to elicit several intracellular signaling pathways to promote cell proliferation and induce cell survival (Takahashi et al., 1999; Kilic et al., 2006). VEGFR are dichotomized into VEGFR-1 and VEGFR-2 with VEGFR-2 being the primary transducer of VEGF signals. VEGF expression level is increased following a variety of brain insults. Although VEGF is expressed largely by neurons and astrocytes following experimental seizure (Nicoletti et al., 2008), under hypoxic conditions VEGF is secreted mostly by astrocytes (Chow et al., 2001). During seizure VEGFR expression has been observed in endothelial cells of blood vessels, astrocytes and neurons where VEGFR-2 is overexpressed by neurons following epileptic insult (Croll et al., 2004a; 2004b; Rigau et al., 2007). In the case of hypoxia, VEGFR-2 expression was found to co-localise with the endothelial cells of blood vessels, astrocytes, and neurons at 48hr post-stroke and persist up to ten days (Kovacs et al., 1996; Kilic et al., 2006). Neo-vascularisation may take place following ischemic insult via VEGF. However, neo-angiogenesis usually refers to newly formed capillaries which were "leaky" and poorly perfused (Greenberg et al., 2008; Karamysheva, 2008). On top of its angiogenic property, VEGF signals have been documented to play a neuroprotective and neurotrophic roles and exert direct effects on different cell types such as neurons, astrocytes, and microglia (Carmeliet and Storkebaum, 2002).

1.11 Roles of Platelet-derived Growth Factors (PDGF) and PDGF Receptor (PDGFR) in Brain Ischemia

Platelet-derived growth factors (PDGFs) consist of four different ligands denoted as PDGFA, PDGFB, PDGFC and PDGFD (Fredriksson et al., 2004; Reigstad et al., 2005). PDGF is expressed as an inactive monomeric form, and is then activated proteolytically to form homodimeric or heterodimeric complexes. Among all the known ligands, only PDGF-A and PDGFB has been observed in a hetero-configuration. Active PDGF ligands interact with two distinct, but related structurally, membrane bound receptor tyrosine kinases, PDGF receptor A (PDGFRA) and PDGF receptor B (PDGFRB) (Fredriksson et al., 2004; Reigstad et al., 2005). This ligand-receptor interaction induces either homodimerization or heterodimerization with the two types of receptor to give a total of three distinct permutations. Each PDGFR has been shown to have different affinity with different PDGF ligands (Heldin and Westermark, 1999; Li et al., 2000; Bergsten et al., 2001; LaRochelle et al., 2001), where PDGF-BB has a greater binding affinity for PDGFRB. Similar to VEGF and VEGFR, PDGFB and its receptor, PDGFRB displayed a complementary role in the maturation process of newly formed blood vessels (Folkman and D'Amore, 1996; Lindahl et al., 1997; Yancopoulos et al., 2000). In the CNS, PDGFB and its receptor, PDGFRB were found to be expressed strongly in neurons (Sasahara et al., 1991; Smits et al., 1991). Following cerebral ischemia, expression of the ligand has been up-regulated in neurons and macrophages, and expression of its receptor has been observed in neurons, astrocytes and macrophages which suggest an additional role to the

angiogenic maturation; possibly neuroprotection (Iihara et al., 1994; Cheng and Mattson, 1995; Iihara et al., 1996; Krupinski et al., 1997; Kaneko et al., 1998).

1.12 Roles of Antioxidants in Brain Ischemia

Reactive oxygen species (ROS) or free radicals are generated via aerobic metabolism, although with short half-life, have been implicated in the pathophysiology of many neurologic disorders and brain dysfunctions such as stroke (Kontos, 1985; Siesjö et al., 1989; Chan, 1994). For example free radicals can alter the structural and functional integrity of cells by lipid peroxidation, thus making CNS especially susceptible (Dringen, 2000; Adibhatla and Hatcher, 2006), which eventually lead to cell death by either necrosis or apoptosis. This malice against the individual cell by the ROS is scavenged and controlled by a variety of antioxidant enzymes such as superoxide dismutase (SOD), catalase and glutathione peroxidase (GPx). Acting at different point in a cascade of defense, SOD, GPx and catalase have been found to inhibit the formation of hydroxyl radical (•OH) and peroxynitrite ($OONO^-$), via converting $OONO^-$ to hydrogen peroxide (H_2O_2) and then into water and oxygen molecules (Crack et al., 2003). SOD reduces superoxide ($•O_2$-) to H_2O_2, whereby H_2O_2 is converted into water at the expense of glutathione (GSH) by either GPx or catalase. There are three subtypes of SODs, copper/zinc SOD (Cu/ZnSOD, SOD1), manganese SOD (Mn-SOD, SOD2), and extracellular SOD (ECSOD, SOD3), where Cu/ZnSOD have been shown to be more crucial in brain ischemia (Kondo et al., 1997a; 1997b; Chan et al., 1998; Kawase et

al.,1999). GPx enzymes belong to a family of selenoproteins includes various isoforms of varying substrate specificity (Ursini et al., 1995; Brigelius-Flohe, 1999), cytosolic GPx1 being the predominantly expressed isoform (Ho et al., 1997; De Haan et al., 1998; Lei and Cheng, 2005) and have shown to be very important for the antioxidative defense of brain cells (Zhang et al., 2000; Crack et al., 2001; Flentjar et al., 2002). Albeit sharing the same role of detoxification of H_2O_2 with GPx in the brain (Dringen and Hamprecht, 1997; Dringen et al., 1999; Baud et al., 2004; Liddell et al., 2004), catalase has been documented with lower activity in brain than in kidney or liver (Ho et al., 1997). Even with a rigorous multi-layer of antioxidant enzyme activities, oxidative stress can still occur when the level of antioxidant enzyme activities are overwhelmed by the excessive production of the free radicals during brain ischemic insult.

1.13 **Clinical Management of Brain Ischemia**

Although with wide inter-individual variability, both hyper-acute phase and acute phase of brain ischemia characteristically develop from the initial symptoms of neurologic impairment which is then followed by further deterioration of the neurologic impairment before realizing clinical stability with or without medical intervention. Pharmacological interventions during the early phase (hyper-acute phase and acute phase) are aimed to be administered within a therapeutic window of three hours upon confirmed non-hemorrhagic stroke onset (Clark and Madden, 2009). Currently, the goals of arterial thrombus degradation and restoration of vessel patency and blood flow to improve

clinical prognosis are achieved with intravenous recombinant tissue-type plasminogen activator (rt-PA, Alteplase) thrombolytic treatment and antiplatelet therapy. After going through the hyper-acute phase and acute phase of stroke, the subject enters the sub-acute phase and chronic phase of brain ischemia when signs of recovery in neurological functions are evident. Usually, 95% of the subjects will reach their optimal recovery by the third month (Jorgensen et al., 1995). The goals of pharmacological interventions in these phases are to prevent a recurrence of similar ischemic insult thus differ much in intentions as opposed to the acute phase. However the pharmacological interventions are commonly combined with implementation of physical rehabilitation such as physical, occupational, and speech therapy to improve neurological function. This comprehensive program is to help a person to attain as close as possible to a pre-stroke level of functioning allowing independence for the activities of daily routine (Dobkin, 2004).

1.14 Pharmacological Intervention in Acute Phase of MCAo

3-Aminobenzamide (3-AB), a poly (ADP-ribose) polymerase (PARP) inhibitor, has been shown to be effective in reducing neuronal death in cortical cultures and infarct size following MCAo in rats (Ding et al., 2001). However another study showed that PARP inhibition had increased caspase-3-like activity (Cole and Perez-Polo, 2002) which indicates that there may be a switch of cellular death mode from necrosis to apoptosis.

In the apoptotic penumbra, caspases play an essential role in apoptosis (Cohen, 1997; Nicholson and Thornberry, 1997). Though three major apoptotic pathways have been proposed (mitochondrial, death receptors mediated and endoplasmic reticulum (ER) initiated pathways) (Danial and Korsmeyer, 2004), all these mechanisms converge to caspase-3 activation and nuclear fragmentation as the final step.

All caspases are synthesized as proenzymes activated by proteolytic cleavage at Asp-X sites and contain a conserved pentapeptide QACXG sequence. Caspases are essential for apoptosis to proceed (Cohen, 1997; Nicholson and Thornberry, 1997). Among the family of capases, caspase-3 holds a pivotal position in the downstream of the cascade pathway. Caspase-3 is activated via the proteolytic processing of its inactive zymogen into activated p17 and p12 subunits.

PARP is a DNA repair enzyme, a substrate of caspase-3 as well, is primarily activated by DNA strand breaks. Berger et al. (1986) proposed a “suicide” concept whereby PARP overactivation occurs when there is massive level of DNA damage, leads to cellular ATP depletion, is implicated for participation in DNA damage-induced necrotic death (Ha and Synder, 1999).

Carbobenzoxy-Val-Ala-Asp-fluoromethylketone (z-VAD-fmk) a broad spectrum irreversible caspase inhibitor can modulate apoptotic cell death. In some cell lines, caspase inhibition has been shown to increase cell survival (Endres et al., 1998), whereas

other cells show an increased level of death by switching the mode of death to necrosis (Lemaire et al., 1998; Vercammen et al., 1998; Ruemmele et al., 1999). Thus caspase inhibition may not prevent cell death, instead induce a switch from apoptosis to necrosis.

Traces of apoptosis have been observed in the pro-necrotic core of MCAo animals (Choi, 1996; Guegan and Sola, 2000). This has led to the controversial theory that cell death advances via a number of hybrid pathways among a continuum between the two extremes (Roy and Sapolsky, 1999) called aponecrosis or necrapoptosis (Formigli et al., 2000). The cellular energy producing factory, the mitochondria, is now increasingly being implicated in the cell's decision to live or die (Murphy et al., 1999) and may even influence the mode of cell death chosen (i.e. apoptosis or necrosis), depending on their functional state (Tsujimoto, 1997). Leist et al. (1997) have shown in their experiment that ATP level is a determinant of cell death by apoptosis or necrosis.

Attempts in using pan-caspase inhibitor, z-VAD-fmk, has been explored and shown promising results in reducing infarct size when administered into ischemic rodents (Endres et al., 1998), but caspase inactivation has also been proposed to be crucial for the switch mechanism from apoptosis to necrosis (Melino et al., 1997; Lemaire et al., 1998). While another group in a separate study successfully employed 3-AB, a PARP enzyme inhibitor in reducing the brain injury volume (Cole and Perez-Polo, 2002) using rat pheochromocytoma PC12 cells subjected to H_2O_2 injury. However, blocking the depletion of both NAD^+ and ATP by PARP allow energy-dependent apoptosis to occur

(Berger et al., 1986). Currently there is no report on brain ischemia using MCAo rodent model with concomitant dosages of pan-caspase inhibitor and PARP inhibitor with reference to ATP availability.

1.15 Effects of Pre- and Post-ischemic Exercise as Physical Rehabilitation in Brain Ischemia

The lead time from ischemic injury to cognitive and functional recovery requires a prolonged course of interventions; however the current pharmacological intervention has only a short therapeutic window within the hyper-acute and acute phase of stroke onset. Therefore, rehabilitation through physical therapy forms a complementary long-term program for stroke management into the latter phases of stroke.

More recently, both human and animal studies have shown that exercises can also produce beneficial effects endogenously necessary to maintain a healthy and functional ageing brain (Larson et al., 2006; Cotman et al., 2007). These broad spectrums of positive effects were outcomes of induced neurogenesis (Pereira et al., 2007) and reduced neurodegenerative processes (Ang et al., 2004) sustained by increased cerebral blood volume (CBV) (Pereira et al., 2007) to meet the increased demand in cellular metabolism. Studies have shown forced treadmill exercise may ameliorate neurologic impairment by impeding neuronal loss, through suppression of the ischemia-induced increases in apoptosis following various brain insults. These studies suggest the possibility that

treadmill exercise aids the recovery from CNS sequelae following stroke (Ang et al., 2003; Sim et al., 2005). Although it has been demonstrated that exercise training has an anti-apoptotic effect on post ischemic brain tissues, the mechanisms responsible for this effect are still largely unclear.

Previously it was shown that pre-ischemic forced treadmill exercise has neuroprotective effect and reduced infarct volume in rats following MCAo. At the molecular level, reverse transcription polymerase chain reaction revealed that the treadmill exercise prior to MCAo increased gene expression for nerve growth factor (NGF). In addition, treadmill exercise showed a significantly higher number of cholinergic neurons, which constitutively expressed p75, in the horizontal diagonal band of Broca (HDB). The findings suggested that neuroprotection after physical exercise may be a result of an increase in an endogenous neurotrophic factor, NGF and the proliferation of its receptive cholinergic neurons (Ang et al., 2003). In another study, forced treadmill exercise preconditioning was shown to induce angiogenesis with newly established microvessel bed that could increase neuronal tolerance to ischemic insults with an adequate blood flow into the area during reperfusion and possibly establishing a collateral circulation (Ding et al., 2004).

At the other end of the spectrum with more clinical relevance, post-ischemic exercise study has shown forced treadmill exercise to significantly suppress the ischemia-induced caspase-3 expression and terminal deoxynucleotidyl transferase dUTP nick end labeling

(TUNEL) positive cells in gerbils. And in the same experiment, ischemia-induced short-term memory impairment was improved following the exercise regime (Sim et al., 2005). However, there is no consensus in data concerning effects of exercise on cerebral ischemia in both humans and animals studies. These dissimilarities may be due to the differences in severity of insults and the distinct types and intensities of physical activities protocols being endorsed (Risedal et al., 1999; Ramsden et al., 2003). Currently, there is no data that look at the effects of post-ischemic exercises on the expression of antioxidants such as Cu/ZnSOD, GPx1 and catalase, and growth factors such as TGF-β1, EPO and PDGF which influence apoptosis, erythropoiesis and angiogenesis following brain ischemia.

1.16 Aims and Scope of the Project

The objectives of this study are to employ the well established MCAo rodent model (Longa et al., 1989) to study the effects of pharmacological intervention in the acute phase of stroke and the effects of post-ischemic exercise in the chronic phase of stroke.

1.16.1 Pharmacological intervention in the acute phase of stroke

Pharmacological interventions during the early phase (hyper-acute phase and acute phase) are usually administered within a therapeutic window of three hours upon confirmed non-hemorrhagic stroke onset (Clark and Madden, 2009). Currently, only rt-PA for

thrombolytic treatment and antiplatelet therapy are approved intravenous medications for the goals of arterial thrombus degradation and restoration of vessel patency and blood flow to improve clinical prognosis. In numerous publications on the topic of preventing cell damage or death following experimental hypoxia or ischemia, both pan-caspase inhibitor (z-VAD-fmk) and non-selective PARP inhibitor (3-AB) have showed potential in provision of alternative remedy in addition to the traditional thrombolytic treatment. As stroke presents a multi-pathway cell death mode which lead to infarcted brain, therapy of brain ischemic may not have to be restricted to single indication. However, there is no data at present looking at the effects of combinatorial treatment on experimental MCAo with combined administration of z-VAD-fmk and 3-AB. Thus,

"Hypothesis 1 states that combined inhibitors administration of both z-VAD-fmk and 3-AB can yield better outcome with bigger infarct volume reduction in comparison with single inhibitor administration following acute phase of experimental MCAo."

To prove the hypothesis 1, the study aims to

1) compare the effects of single and combined inhibitors administration of both pan-caspase inhibitor, z-VAD-fmk and non-selective PARP inhibitor, 3-AB in the infarct volume reduction post-MCAo,

2) ascertain the possible benefit of combined inhibitors treatment up to 24hr after MCAo,

3) determine the possible correlation of the intracellular ATP level with infarct volume.

1.16.2 Post-ischemic exercise in the chronic phase of stroke

As the recovery from stroke require an extended duration therefore a long term management plan, physiotherapy has often been prescribed as a complementary therapeutic program in addition to pharmacological remedy. Lee and coworkers (Lee et al., 2006) have shown that under pathological conditions, increased physical exercises can reduce expression of activated caspase-3 that is pivotal in apoptotic mechanism. Moreover, various studies have shown that increased physical activities can up-regulate endogenous neurotrophic factors with functions that have been known to be able to decrease caspase-3 activation (Wu et al., 2008; Nguyen et al., 2009; Stranahan et al., 2009). In order to reinstate orders subsequent to brain ischemia, the program must be able to reduce apoptosis and enhance angiogenesis which in turn will create a favorable environment for neurogenesis. However, at present there is no data looking at the overall effects of eight weeks of moderate post-ischemic exercise on mediation of apoptosis and angiogenic potential via TGF-β1-signaling, VEGF/PDGF system, EPO/EPOR system and antioxidant enzyme activities. Thus,

"Hypothesis 2 states that eight weeks of moderate post-ischemic exercises increase anti-apoptotic activities of TGF-β1-signaling"

To prove hypothesis 2, the study aims to

1) determine the effects of eight weeks of moderate exercise on:
    a. TGF-β1 and smad7 expression in both hippocampus and cortex.

b. correlation between changes in TGF-β signaling and apoptotic markers/TUNEL in both hippocampus and cortex.

2) ascertain the effects of eight weeks of moderate post-ischemic exercise on:

a. TGF-β1 and smad7 expression in ischemic cortex.

b. correlation between changes in TGF-β signaling and apoptotic markers/TUNEL in ischemic cortex.

"Hypothesis 3 states that eight weeks of moderate exercises increase angiogenesis in non-ischemia and ischemia via VEGF/PDGF system"

To prove hypothesis 3, the study aims to

1) determine the effects of eight weeks of moderate exercise on HIF-1α, VEGF, VEGFRB, PDGFB and PDGFRB expression in both hippocampus and cortex.

2) ascertain the effects of eight weeks of moderate post-ischemic exercise on expression of HIF-1α, VEGF, VEGFRB, PDGFB, PDGFRB and angiogenesis in ischemic cortex.

"Hypothesis 4 states that eight weeks of moderate post-ischemic exercises increase erythropoetic potential via EPO/EPOR system"

To prove hypothesis 4, the study aims to

1) determine the effects of eight weeks of moderate exercise on EPO and EPOR expression in both hippocampus and cortex.

2) ascertain the effects of eight weeks of moderate post-ischemic exercise on EPO and EPOR in ischemic cortex.

"Hypothesis 5 states that eight weeks of moderate post-ischemic exercises reduce secondary damages by moderating antioxidant enzyme activities"

To prove hypothesis 5, the study aims to

1) determine the effects of eight weeks of moderate exercise on enzyme activities of Cu/ZnSOD, GPx1 and catalase in both hippocampus and cortex.

2) ascertain the effects of eight weeks of moderate post-ischemic exercise on enzyme activities of Cu/ZnSOD, GPx1 and catalase in ischemic cortex.

MATERIAL AND METHODS

CHAPTER TWO

2.1 Animals

One hundred and fifty eight male Sprague-Dawley rats (200 to 250g approximately 6 weeks old) obtained from the University Laboratory Animal Centre were used in the study. All experiments were carried out in accordance with the guidelines set by the Institutional Animal Care and Use Committee (IACUC), National University of Singapore (NUS) and all efforts were made to minimize the number of rats used and their suffering. Animals were age-matched and divided into various groups for the different purposes in both early and late phases of experimental MCAo. All the rats were housed in individual cages in order to fulfill strict solitary confinement requirement. This was to minimize other possible confounding factors such as environmental and social interaction influences.

2.1.1 Acute phase grouping

In this experiment, the study was sub-divided into two phases. For the first phase of the study, the rodents were randomly divided into four groups (n=10): a) sham group, b) untreated MCAo control group, c) pan-caspase inhibitor group and d) PARP inhibitor group. The untreated MCAo control group was administered intraperitoneally with saline 30min post-MCAo. The rats were administered intraperitoneally with 1mg/kg, 3mg/kg and 5mg/kg z-VAD-fmk (#V-116, Sigma, St Louis, MO, USA) 30min post-MCAo for the pan-caspase inhibitor group. Intraperitoneal injection of 10mg/kg, 30mg/kg and

50mg/kg 3-AB (#A0788, Sigma, St Louis, MO, USA) were given 30min post-MCAo for the PARP inhibitor group. Rats were euthanized 48hr following MCAo. For the second phase combined inhibitors treatment study, the concentration of pan-caspase inhibitor and PARP inhibitor used in combination were based on the dosages that yielded the highest infarct size reduction from the earlier study. Temporal profile of pharmacological intervention at 30min, 6hr, and 24hr post-MCAo were analyzed. The rats were sacrificed at 48hr post-MCAo. These timings were selected based on the activities of PARP, caspase-8 and caspase-3 following permanent MCAo (LaPlaca, 1999; Velier et al., 1999; Harrison et al., 2001).

2.1.2 Chronic phase grouping

In this experiment, the rats were randomly assigned to four individual groups: a) sham group, b) sham-runner group, c) MCAo group, and d) MCAo-runner group. The animals in both sham-runner group and MCAo-runner group are subjected to one week familiarization with the treadmill plus eight weeks of forced treadmill exercise following a one week interval post-surgery. The sham rats and MCAo rats were exposed to the same set up daily for the duration that the runners were trained on the treadmill. Earlier studies had shown that rats subjected to moderate post-ischemic exercise are able to achieve better outcome as compared with sedentary rats from second week onwards (Lee et al., 2009b).

2.2 Surgical Procedure

Animals were anesthetized with 0.2ml/100g cocktail of ketamine and xylazine (75 mg/kg + 10 mg/kg) mixture before surgery or sacrifice. The femoral artery was cannulated for monitoring of blood pressure (ML 785 Powerlab 8SP, ADInstrument, AOC, USA) and rectal temperature (Homeothermic Blanket System, Harvard Apparatus Inc., MA, USA) was monitored and maintained at 37°C. MCAo was carried out as described by Longa et al. (1989) with modifications (Fig. 1). A ventral midline incision was made and the carotid arteries were exposed. The pterygopalatine artery (PPA) was identified and ligated. A 4/0 suture with the tip blunted by heating was inserted via a hole created on external carotid artery (ECA), with temporarily clipped common carotid artery (CCA), and then via the internal carotid artery (ICA) which continue till the junction of anterior and middle cerebral artery. The suture was left in the animal till sacrifice. For the sham-operated rats, no vessel occlusion was carried out after exposure of the arteries. Within a 24 hrs period after the MCAo procedure, the number of sham and MCAo rats that did not survive was recorded.

(Refer to Appendix 1 for Instruments needed for MCAo surgery)

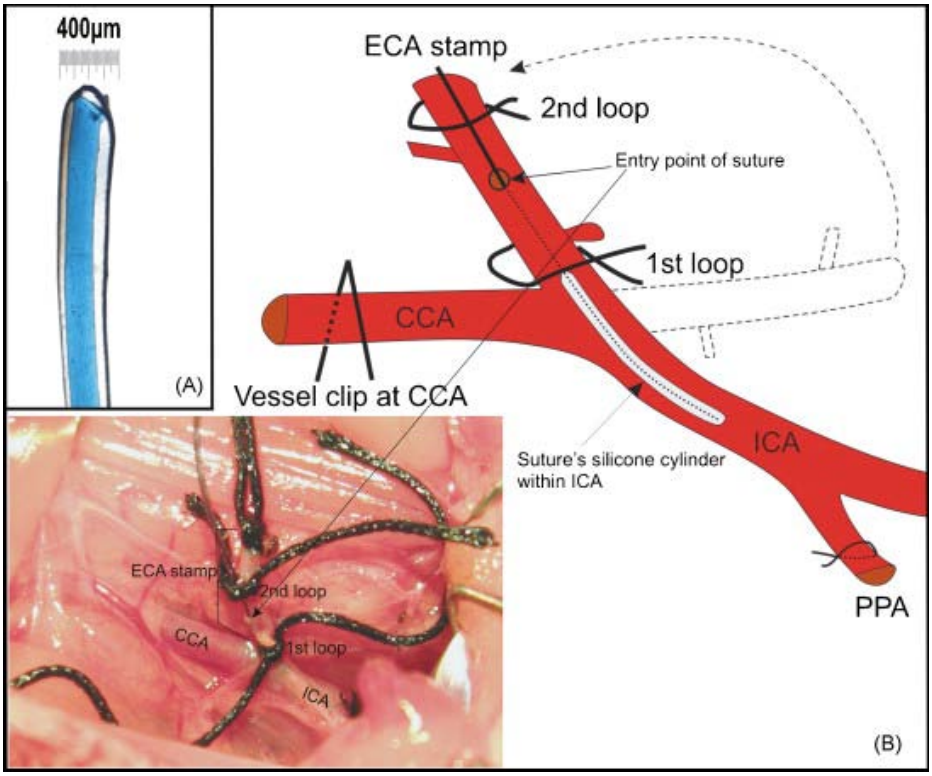

(Adapted from Lourbopoulos et al. 2008)

Fig. 1. Schematic diagram and photograph of intraluminal suture technique MCAo. Shown here is (A) an example of 4/0 polypropylene monofilament suture and (B) the operating field of the ventral midline incision with the carotid arteries exposed and ligated for inducing the experimental MCAo according to Longa et al. 1989 with modifications.

2.3 Neurological Evaluation and Weight Changes

The individual weight and neurological status of the rats from the sham (n=4), sham-runner (n=4), MCAo (n=4) and MCAo-runner (n=4) rats were assessed weekly over a ten weeks period after the MCAo surgery using a scoring system detailed by Menzies and colleagues (1992). A scale of 0 to 4 was used to evaluate the rats after recovery from anesthesia (Table 1). The test consisted of the following steps: rats were held by the tail and the forelimbs posture was noted. Normal rats extended both forelimbs towards the floor and were given a score of 0. If the contralateral forelimb to the stroke side was noted to be flexed during suspension, the rat was given a score of 1. The rats were then placed on an absorbent surface and pulled by the tail. If there were signs that the contralateral forelimb grip was decreased, the rat was given a score of 2. The rats were then placed on the floor but still held by the tail. The rat that showed signs of moving towards the stroke side but could also move in other directions was given a score of 3. Rats that consistently moved in circles towards the stroke side were given a score of 4. This neurological test was consecutively repeated three times for each rat and the highest score was recorded.

Table 1: Neurological examination score chart

Description	Score
When suspended by the tail, both forelimbs of the rat extended symmetrically towards the floor.	0
The contralateral forelimb is consistently flexed towards the body.	1
Decreased grip of the contralateral forelimb when pulled by the tail. This is done on an absorbent surface.	2
Established a tendency to move in circles towards the paralytic side though they appear to have the abilities to move in all directions.	3
Consistently moves in circles towards the paralytic side.	4

(Adapted from Menzies et al., 1992)

2.4 Infarct Size Analysis

The rats for the acute phase experiment were reanesthesized with ketamine + xylazine mixture and decapitated. The brain were removed and then coronally sectioned into slices with 1mm thickness using a brain matrix (Harvard Apparatus Inc., MA, USA). The brain slices were then incubated with 0.1% solution of 2,3,5-triphenyltetrazolium chloride (TTC) (Sigma, catalog number T4375) at 37°C for 30min, and then fixed by immersion in 4% paraformaldehyde. TTC stains viable brain tissue purple and, while infarcted tissue

remains unstained (Fig. 2). The TTC stained brain slices were photographed and the digitized images of infarct area were analyzed and quantified using an image processing software package (Scion Image for Windows, Version 4.0.2). The infarct volume were then calculated and corrected for edema based on a formula suggested by Swanson et al. (1990).

True infarct volume = [right hemisphere area - (left hemisphere area - infarct area)] × thickness of the section

Data were presented as mean ± SEM. Statistical comparisons are made with one-way analysis of variance (ANOVA), Newman-Keuls Multiple Comparison Test, where $p<0.05$ is considered statistically significant.

Fig. 2. Brain sections with TTC staining. The MCAo models (n=4) revealed that areas of infarction were restricted only to the territories supplied by the left MCA. These infarcted regions were represented by the unstained tissue, while the unaffected areas were stained purple.
(c - cortex and h - hippocampus)

(Refer to Appendix 2 for essential reagents used for TTC staining)

2.5 Intracellular ATP Level Determination

The cellular ATP levels of the rats for the acute phase experiment were quantified using a luciferin/luciferase-based assay. The whole brain was removed to create a tissue suspension and tissues were lysed with ATP releasing buffer (Sigma). ATP content was measured with ATP assay kit (#119108 ATP Assay Kit, Calbiochem, CA, USA) and a luminometer (BD Monolight™ 3096 Microplate Luminometer) according to manufacturer's instruction manual.

2.6 Treadmill Exercise

After surgery, the sham-operated or MCAo rats for the chronic phase experiment were randomly assigned to either non-runner or runner group and were given a week of resting period before being placed in initial exercise regime, which was designed to allow the animals to be familiarize with the treadmill machine (Panlab S.L., LE 8710R, Barcelona, Spain) (Fig. 3). In the week of familiarization, the rats began with 10min of running at the speed of 15cm/sec at 0 degree inclination and progressively increased to 30min session at the same speed, with daily increased duration of 5min interval (Table 2A). Subsequently the rats from the runner groups were being forced to run on a treadmill machine for 45min, once a day, five days per week, for the following eight consecutive weeks. The exercise workload consisted of running at the speed 25cm/sec for the first 5min, 35cm/sec for the next 35min, and then back to 25cm/sec for the last 5min with 0 degree inclination

(Table 2B). Animals in the non-runner groups were left on the treadmill for 45min and were not made to run. A dose–response correlation between exercise duration/intensity and beneficial effects has been reported, whereby the best outcomes were associated with moderate exercise (Shen et al., 2001). Running distances covered in the present study were well above the threshold level of 500m/day which was considered as moderate exercise regime and reported to be needed for up-regulation of some key gene products believed to mediate effects of exercise on the brain (Shen et al., 2001). All the runners were sacrificed two days after the last run for allowance of wash-out period.

Table 2A: Treadmill exercise familiarization program

Week 0	Speed (cm/s)	Duration (min)
Day 1	15	10
Day 2	15	15
Day 3	15	20
Day 4	15	25
Day 5	15	30

Table 2B: Treadmill moderate exercise regime

Week 1 to 8	Speed (cm/sec)	Duration (min)
Day 1	25 ⇨ 35 ⇨ 25	5 ⇨ 35 ⇨ 5
Day 2	25 ⇨ 35 ⇨ 25	5 ⇨ 35 ⇨ 5
Day 3	25 ⇨ 35 ⇨ 25	5 ⇨ 35 ⇨ 5
Day 4	25 ⇨ 35 ⇨ 25	5 ⇨ 35 ⇨ 5
Day 5	25 ⇨ 35 ⇨ 25	5 ⇨ 35 ⇨ 5

Fig. 3. Photographs showing the five lanes motorized treadmill. This treadmill adapted for adult rats was used in the experiment. Note the metal grid at the rear end (green arrow) of the treadmill served to enforce running with adjustable strength of electric shock.

2.7 Real Time-Polymerase Chain Reaction (RT-PCR)

The ipsilateral and contralateral cortices and hippocampi were harvested from rats ten weeks after the onset of global ischemia and allowed wash-out period two days after completion of the last treadmill exercise. RNA was extracted from the snap-frozen tissue using RNeasy Lipid Tissue Midi Kit (Qiagen, GmbH, Germany). The total RNA was quantified with ND-1000 spectrophotometer (Nanodrop, Fisher Thermo, Wilmingyon, DE, USA). For reverse transcription, 1µg of RNA was incubated at 70°C for 10min. Single-stranded cDNA was synthesized from the RNA by adding reaction mixture

containing 4µl of MgCl2 (24mM), 2µl of reverse transcriptase 10X buffer, 2µl of dNTP mixture (10mM), 0.5µl of Recominabant RNasin® inhibitor, 15U of AMV reverse transcriptase (high concentration), 0.5µg of Oligo (dT)15 primers, 1µg of RNA and nuclease free water (Promega, Madison, WI, USA) in total volume of 20µl. The reaction mixture was incubated for 1hr at 42°C and the reaction was terminated by heating for 5min at 95°C. Finally, reaction mixture was incubated at 0°C. The samples were store at -20°C for subsequent PCR analysis. Quantitative real time-PCR was carried out on a Light Cycler 2.0 instrument (Roche Diagnostics, Indianapolis, IN) using QuantiTect® SYBR® Green RT-PCR kit (Qiagen, Valencia, CA, USA) according to the manufacturer's instructions. An aliquot of 1µl of the reverse transcription products (cDNA) was added to the reaction mixture of 10µl containing RNase free water and SYBR Green. Reaction mixture was pre-incubated at 85°C for 10min, PCR was completed with 50 cycles of denaturation at 95°C for 15sec, annealing at 63°C for 10sec and elongation at 72°C for PCR product size per 25sec. Specific forward and reverese primers and amplicon size for each gene are provided in Table 3. β-actin was adopted as the internal control and for normalizing the quantities in each sample. Gene expression was quantified using $2^{-\hat{}\hat{}ct}$ method. Data were analyzed by unpaired t-test or One Way ANOVA Tukey's test was presented as mean ± standard errors. Statistical significance is accepted at $P<0.05$.

(Refer to Appendix 3 for essential reagents used for quantitative real time PCR)

Table 3: List of primer sequences

Gene	Primer sequence		Amplicon Size (bp)
	Forward primer (5'–3')	Reverse primer (5'–3')	
TGF-b1	TGG ACC GCA ACA ACG CCA TCT ATG AGA AAA CC	TGG AGC TGA AGC AAT AGT TGG TAT CCA GGG CT	426
TGFBR-II	CTG TCT GTG GAT GAC CTG GC	CTG GTG GTT GAG CCA GAA GC	303
Smad2	AAA ATG TCG TCC ATC TGC C	GAG CTC ATG ATG GTC GTG AA	431
Smad7	ATG DTG TGC CTT CCT CCG CT	CGT CCA CGG CTG CTG CAT AA	494
HIF-1α	TCA AGT CAG CAA CGT GGA AG	TAT CGA GGC TGT GTC GAC TG	198
VEGF	CGG GCC CAC CAG CTC TGA ACA	GGG CGG CTG CTC CAA GGT CA	121
VEGFR2	ATT TGG CAC CAC ACT TTC TAC	TCA CGC ACG ATT TCC CTC TCA G	379
PDGFB	CTG CCT CTC TGC TGC TAC CT	GAT GAG CTT TCC GAC TCG AC	206
PDGFRB	TGT TCG TGC TAT TGC TCC TG	TCA GCA CAC TGG AGA AGG TG	201
EPO	GAT CGC CCG GCT AGA GGA AAA AG	TCG CAA CCC AGT CCA TCT TGT GT	305
EPOR	CTG GTG GAC AAC ATC GCT CTG	GGT CTG CTG ACC TCA CTT GTG	226
β-actin	GTA TGT CGT GGA GTC TAC TGG	CAT CAT ACT TGG CAG GTT TCT C	488

2.8 Western Blot Analysis

For Western blotting, the ipsilateral and contralateral cortices and hippocampi were harvested from rats ten weeks after the onset of global ischemia and allowed wash-out period two days after completion of the last treadmill exercise. The specimens were homogenised in 1X RIPA lysis buffer with complete protease inhibitor cocktail (Santa Cruz Biotechnology Inc., CA, USA). The protein concentrations were determined by BCA (bicinchoninic acid) protein assay kit (Pierce, Thermo Scientific, IL, USA). 75μg of each sample homogenate was loaded onto a 10%, 12% or 15% SDS-PAGE gel and separated using Mini Protein II apparatus (Bio-Rad, CA, USA) for about 2hr at 100V. Proteins were subsequently electroblotted onto a PVDF membrane (Bio-Rad Laboratories) for 50min at 23V. The membrane was then blocked for one hour at room temperature with 5% dried milk in PBS with 1% Tween 20 (PBST), followed by overnight incubation with primary antibody at 4°C. The primary antibodies used were listed in table 4. After washing with PBST for three times (15min each time), the membrane was incubated with appropriate species-specific horseradish peroxidase-conjugated secondary antibody: goat anti-rabbit immunoglobulin G (sc-2004, 1:1000; Santa Cruz Biotechnology Inc., CA, USA) or goat anti-mouse immunoglobulin G (sc-2005, 1:1000; Santa Cruz Biotechnology Inc., CA, USA). The membrane was then washed with PBST for three times (15min each time). Protein expression was detected with an enhanced chemiluminescence detection system (ECL+Plus; Amersham Pharmacia Biotech, Piscataway, NJ). Protein bands were quantified by densitometry

method and ImageQuant™ 350 (GE Healthcare UK Limited, Bucks, UK). All samples were normalized against the same value of expression for the housekeeping β-actin.

The data were presented as relative expression, with sham-operated brain. Data were analyzed by unpaired t-test or One Way ANOVA Tukey's test was presented as mean ± standard errors. Statistical significance is accepted at $P<0.05$

(Refer to Appendix 4 for essential reagents used for Western blotting)

Table 4: List of primary antibodies and dilution factor

Antibodies	Dilution	Manufacturer
TGF-β1	1:2000	#3709 rabbit polyclonal antibody; Cell Signaling Technology Inc., MA, USA
smad7	1:500	sc-11392 rabbit polyclonal antibody; Santa Cruz Biotechnology Inc., CA, USA
Cleaved Caspase 3	1:1000	#9661 rabbit polyclonal antibody; Cell Signaling Technology Inc., MA, USA
PARP	1:1000	#9542 rabbit polyclonal antibody; Cell Signaling Technology Inc., MA, USA
HIF-1α	1:1000	#3716 rabbit polyclonal antibody; Cell Signaling Technology Inc., MA, USA
PDGF	1:1000	ab53716 rabbit polyclonal antibody; Abcam Inc., MA, USA
EPO	1:500	sc-7956 rabbit polyclonal antibody; Santa Cruz Biotechnology Inc., CA, USA
EPOR	1:1000	sc-697 rabbit polyclonal antibody; Santa Cruz Biotechnology Inc., CA, USA
Cu/ZnSOD	1:250	ab13498 rabbit polyclonal antibody; Abcam Inc., MA, USA
Catalase	1:1000	ab1877 rabbit polyclonal antibody; Abcam Inc., MA, USA
GPx1	1:1000	ab59546 rabbit polyclonal antibody; Abcam Inc., MA, USA
β-actin	1:1000	A5316 mouse monoclonal antibody (clone 74); Sigma-Aldrich Co., MO, USA

2.9 Immunohistochemistry and Double Staining

Rats from the four groups (sham, sham-runner, MCAo, and MCAo-runner) were anesthetized using ketamine + xylazine mixture. Transcardial perfusion was performed with Ringer's solution (200 ml) and then 4% paraformaldehyde in 0.1M phosphate buffer (PB; pH 7.4; 200–300ml). Subsequently, the brain was removed, post fixed in the same fixative for an additional 4hr at 4°C, and then cryoprotected in 0.1M PB containing 15% sucrose overnight at 4°C. The brain was embedded in Lipshaw M-1 embedding matrix and treated with liquid nitrogen. Every fifth frozen section of 30μm, 2mm from the frontal pole was harvested and mounted onto gelatinized slides. Tissue sections were then washed three times (10min for each time) with PBS and blocked with 5% normal goat serum for 1hr to minimize nonspecific adsorption. The sections were then incubated with primary antibody such as anti-TGF-β1 (V) rabbit polyclonal antibody (sc146) (Santa Cruz Biotechnology Inc., CA, USA) (1:100), anti-Smad7 (H-79) rabbit polyclonal antibody (sc11392) (Santa Cruz Biotechnology Inc., CA, USA) (1:100), anti-Pecam-1 rabbit polyclonal antibody (sc-18892) (Santa Cruz Biotechnology Inc., CA, USA) (1:200), anti-EPO rabbit polyclonal antibody (sc-7956) (Santa Cruz Biotechnology Inc., CA, USA) (1:200) or anti-EPOR rabbit polyclonal antibody (sc-697) (Santa Cruz Biotechnology Inc., CA, USA) (1:200). All the sections incubated with various primary antibody listed above, with the exception of anti-Pecam-1 sections, were also co-incubated with anti-NeuN mouse monoclonal antibody (MAB377) [Chemicon (Millipore), MA, USA] (1:100) overnight at room temperature (25°C). Sections were then

washed three times (10min each time) with PBS and incubated with species-specific fluorescein labeled secondary antibodies: goat anti-rabbit immunoglobulin (IgG) Cy3 conjugate (AP132C) [Chemicon (Millipore), MA, USA] (1:200) and goat anti-mouse IgG, F(ab')2, FITC conjugate (AQ303F) [Chemicon (Millipore), MA, USA] (1:200) for 1hr at room temperature. After washing three times (10min for each time) with PBS, the slides were mounted and visualized by confocal microscopy (Olympus FV1000 inverted microscope IX81).

(Refer to Appendix 5 for essential reagents used for immunohistochemistry)

2.10 TUNEL Staining

Rats from the four groups (sham, sham-runner, MCAo, and MCAo-runner) were anesthetized using ketamine + xylazine mixture. Transcardial perfusion was performed with Ringer's solution (200 ml) and then 4% paraformaldehyde in 0.1M phosphate buffer (PB; pH 7.4; 200–300ml). Subsequently, the brain was removed, postfixed in the same fixative for an additional 4hr at 4°C, and then cryoprotected in 0.1M PB containing 15% sucrose overnight at 4°C. The brain was embedded in Lipshaw M-1 embedding matrix and treated with liquid nitrogen. Every fifth frozen section of 30μm, 2mm from the frontal pole was harvested and mounted onto gelatinized slides. Tissue sections were pretreated with 0.1% Triton X-100 in 0.1% sodium citrate for 2min on ice. The sections were then washed three times (10min each time) with PBS and incubated with anti-NeuN

mouse monoclonal antibody (MAB377) [Chemicon (Millipore), MA, USA] (1:100) overnight at room temperature (25°C). Sections were then washed three times (10min each time) with PBS and incubated with species-specific fluorescein labeled secondary antibodies: goat anti-mouse immunoglobulin IgG, Cy3 conjugate (AP124C) [Chemicon (Millipore), MA, USA] (1:200) for 1hr at room temperature. The sections were then washed three times (10min each time) with PBS and incubated with TUNEL reaction mixture from the *in situ* cell death detection kit [Roche Diagnostics Corporation (Roche Applied Science), IN, USA] that contains TdT and fluorescein-dUTP for 60min at 37°C in a humidified chamber in the dark. Subsequently, the tissue sections were washed three times (10min each time) with PBS before the cover slips were mounted. The label incorporated at the damaged sites of the DNA was visualized by confocal microscopy (Olympus FV1000 inverted microscope IX81).

2.11 Statistical Analysis

Data were presented as mean ± SEM. Statistical comparisons were made with upaired t-test and one-way ANOVA (Newman-Keuls/Tukey's Multiple Comparison Test) where $p<0.05$ is considered statistically significant.

Experimental markers assessed and quantified in this thesis are summarized in Table 5.

Table 5: Summary of experimental markers addressed and quantified

Acute phase of MCAo: Effects of combined treatment versus single modality with pan-caspase and PARP inhibitors

	Inhibitor administration following		
Marker assessed	30min p.s.	6hr p.s.	24hr p.s.
Infarct size	z-VAD-fmk	Combined	Combined
	3-AB		
	Combined		
ATP level	z-VAD-fmk	Combined	Combined
	3-AB		
	Combined		
Caspase-3 activation/ PARP cleavage	WB, z-VAD-fmk	WB, Combined	WB, Combined
	WB, 3-AB		
	WB, Combined		

Chronic phase of MCAo: Effects of post-ischemic exercises, ten weeks post-surgery

Marker assessed	Hippocampus			Cortex		
TGF-β1	RT-PCR	WB	IHC (CA1, DG)	RT-PCR	WB	IHC
TGFBR-II	RT-PCR			RT-PCR		
Smad7	RT-PCR	WB	IHC (CA1, DG)	RT-PCR	WB	IHC
Smad2	RT-PCR			RT-PCR		
Caspase-3 activation/ PARP cleavage					WB	
TUNEL						IHC
HIF-1α	RT-PCR	WB		RT-PCR	WB	
VEGF	RT-PCR			RT-PCR		
VEGFR2	RT-PCR			RT-PCR		
PDGFB	RT-PCR	WB		RT-PCR	WB	
PDGFRB	RT-PCR			RT-PCR		
Pecam-1						IHC
EPO		WB	IHC (CA1, DG)		WB	IHC
EPOR		WB	IHC (CA1, DG)		WB	IHC
Cu/Zn-SOD		WB			WB	
Catalase		WB			WB	
GPx1		WB			WB	

p.s., post-surgery; RT-PCR, Real Time Polymerase Chain Reaction; WB, Western Blot; ICH, Immunohistochemistry; CA1, Cornu Ammonis 1; DG, Dentate Gyrus

RESULTS

CHAPTER THREE

3.1 Effects of Pharmacological Intervention in Acute Phase of MCAo

3.1.1 Effects of pan-caspase inhibition on infarct size

To determine the optimized z-VAD-fmk concentration that showed the maximum infarct size reduction administered at 30min post-MCAo, rats were divided into three groups, receiving different concentration (1mg/kg, 3mg/kg and 5mg/kg) for the study. Fig. 4 showed that of the three groups, rats injected with 1mg/kg (35.78% ± 1.95%) and 3mg/kg (24.13% ± 3.89%) z-VAD-fmk showed statistically significant reduction in the infarct size following MCAo. Whereas 5mg/kg (39.80% ± 2.69%) z-VAD-fmk group did not show significant reduction in infarct size comparing to the saline control group (45.97% ± 1.86%).

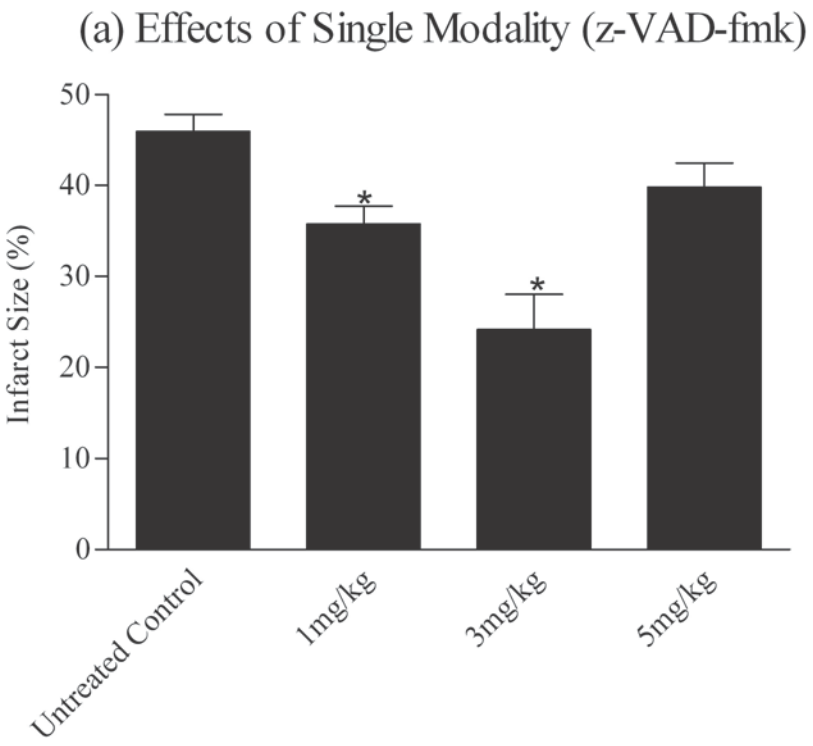

Fig. 4. Infarct size reduction following single inhibitor administration of pan-caspase inhibitor (z-VAD-fmk). Reduction of infarct sizes with single modality pan-caspase inhibitor (z-VAD-fmk) treatment following 48hr MCAo. Each group of animals (n=4) was treated with different doses of z-VAD-fmk, while the untreated control group was given saline. The infarct sizes were determined by TTC staining. Data were analysed by One-way ANOVA, Newman-Keuls Multiple Comparison Test (*p-value<0.05).

3.1.2 Effects of PARP inhibition on infarct size

The 3-AB treated rats were also divided into three groups administered with either 10mg/kg, 30mg/kg or 50mg/kg 30min post-MCAo. Only animals treated with 30mg/kg (26.98% ± 2.22%) 3-AB showed statistically significant reduction in the infarct size following MCAo (Fig. 5). The animals treated with 10mg/kg (39.99% ± 1.15%) and 50mg/kg (38.14% ± 3.70%) 3-AB did not show significant reduction as compared with the saline control group (45.97% ± 1.86%).

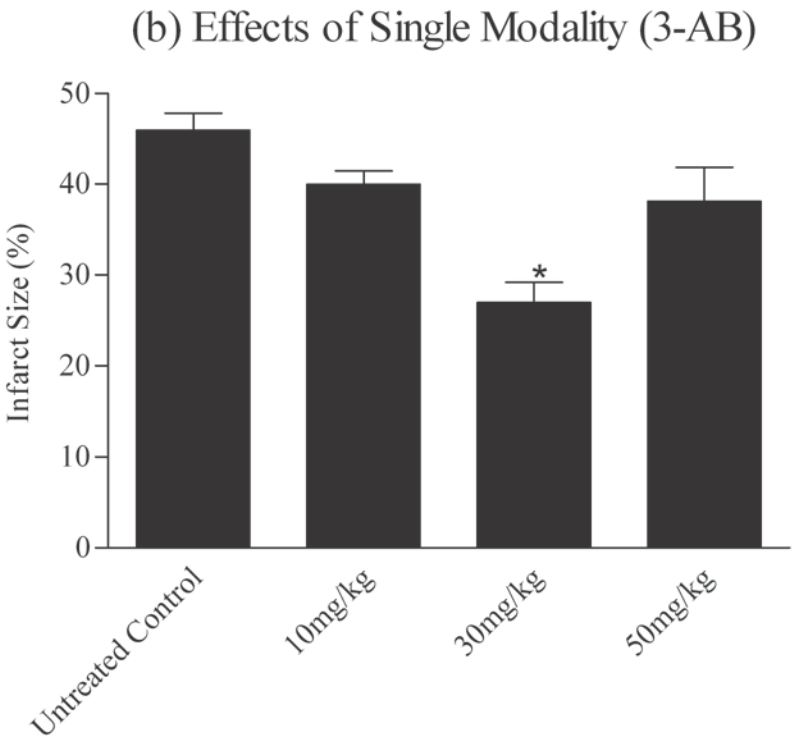

Fig. 5. Infarct size reduction following single inhibitor administration of PARP inhibitor (3-AB). Reduction of infarct sizes with single modality PARP inhibitor (3-AB) treatment following 48hr MCAo. Each group of animals (n=4) was treated with different doses of 3-AB, while the untreated control group was given saline. The infarct sizes were determined by TTC staining. The infarct sizes were determined by TTC staining. Data were analysed by One-way ANOVA, Newman-Keuls Multiple Comparison Test (*p-value<0.05).

3.1.3 Effects and temporal profile of combined inhibitors treatment on infarct size

In the second phase of the study, most efficacious dosages of both pan-caspase and PARP inhibitors (3mg/kg z-VAD-fmk and 30mg/kg 3-AB) were used in the combined inhibitors treatment group after the MCAo. Fig. 6 showed that the concomitant administration of both inhibitors showed further reduction in the infarct size (7.228% ± 1.988%) at 30min post-MCAo as compared to brains of rats treated with specific inhibitor separately. The timing of the insult was prolonged from 30min to 6hr (21.02% ± 1.06%) and 24hr (24.40% ± 2,12%), before treatment intervention (Fig. 7). The combined inhibitors treatment showed effectiveness in reducing infarct size up to the 24hr limit set in this study.

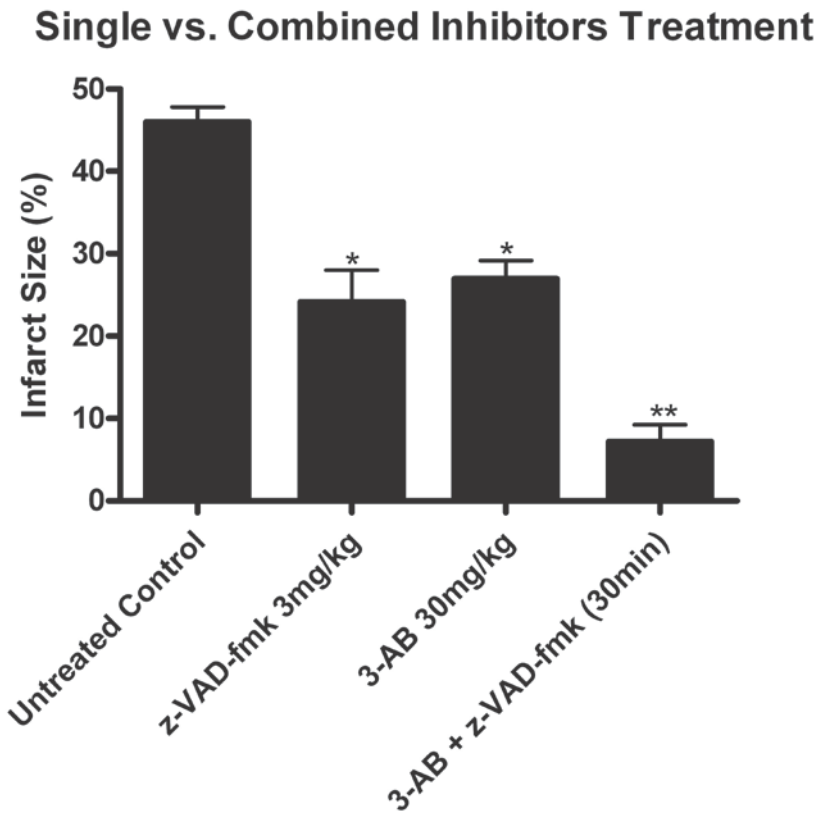

Fig. 6. Effects of single and combined inhibitors treatment on infarct size. Graph showing infarct sizes in ipsilateral brain, 48hr after MCAo in rats from various groups (n=4): untreated control; z-VAD-fmk; 3-AB; combined inhibitors treatment. The infarct sizes were determined by TTC staining and showed further reduction with combined inhibitors treatment. Data were analysed by One-way ANOVA, Newman-Keuls Multiple Comparison Test (*p-value<0.05, **p-value<0.01).

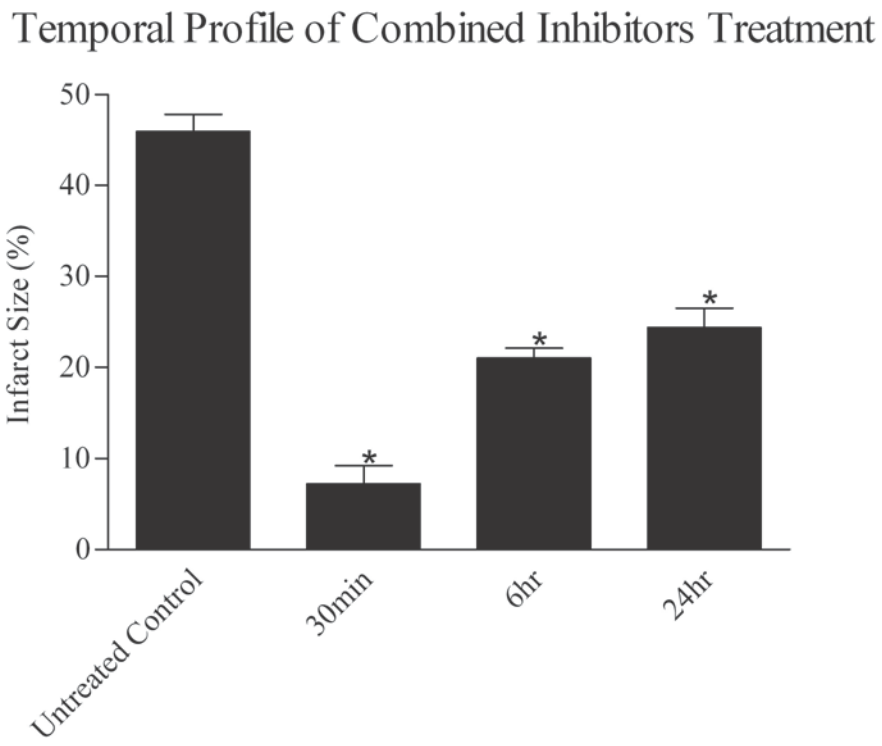

Fig. 7. Temporal profile of infarct sizes in rats with combined inhibitors treatment. Infarct sizes temporal profiles at 48hr after MCAo in rats treated with combined inhibitors (z-VAD-fmk and 3-AB) treatment (n=4). The infarct sizes were determined by TTC staining. Data were analysed by One-way ANOVA, Newman-Keuls Multiple Comparison Test (*p-value<0.05).

3.1.4 Effects of pan-caspase and PARP inhibition on intracellular ATP level

To quantify the intracellular ATP level, 33 rats were randomly divided into the following groups: sham-operated; untreated control; pan-caspase inhibitor (with the three varying dosages); PARP inhibitor (with the three varying dosages) and the combined inhibitors treatment (with three different time profiles) groups. They were used to analyze the intracellular ATP level in the lesioned cerebral cortex 48hr after MCAo. Fig. 8a showed that intracellular ATP level in sham-operated animals were measured at $1.01\times10^{-2} \pm 9.87\times10^{-4}$moles/mg, and the untreated control group were determined at $3.36\times10^{-3} \pm 2.09\times10^{-4}$moles/mg. Animals which received 1mg/kg ($3.39\times10^{-3} \pm 1.23\times10^{-4}$moles/mg), 3mg/kg ($3.94\times10^{-3} \pm 2.59\times10^{-4}$moles/mg) and 5mg/kg ($4.58\times10^{-3} \pm 7.97\times10^{-4}$moles/mg) z-VAD-fmk did not raise the intracellular ATP level significantly. Rats administered with 30mg/kg ($7.56\times10^{-3} \pm 1.25\times10^{-3}$moles/mg) and 50mg/kg ($6.05\times10^{-3} \pm 8.72\times10^{-4}$moles/mg) of 3-AB were able to increase the intracellular ATP level significantly, but not the animal treated with 10mg/kg 3-AB ($2.61\times10^{-3} \pm 9.42\times10^{-5}$moles/mg) (Fig. 8a). Fig. 8a further showed the temporal profile of the combinatorial administration of both inhibitors on the intracellular ATP level at 30min ($5.21\times10^{-3} \pm 5.94\times10^{-4}$moles/mg), 6hr ($5.86\times10^{-3} \pm 5.67\times10^{-4}$moles/mg) and 24hr ($4.52\times10^{-3} \pm 2.72\times10^{-4}$moles/mg). Combined inhibitors treated animals brought slight increase, though not statistically significant, in the intracellular ATP level as compared to the untreated group.

The results showed that there were clear distinction between the sham-operated brain tissue and the saline controlled brain tissue intracellular ATP level. However, as depicted in Fig. 8b, only the animal treated with 3-AB, have shown that the intracellular ATP level was inversely correlated with the size of the infarct in the ischemic brain (r^2 = -0.41, $p<0.05$).

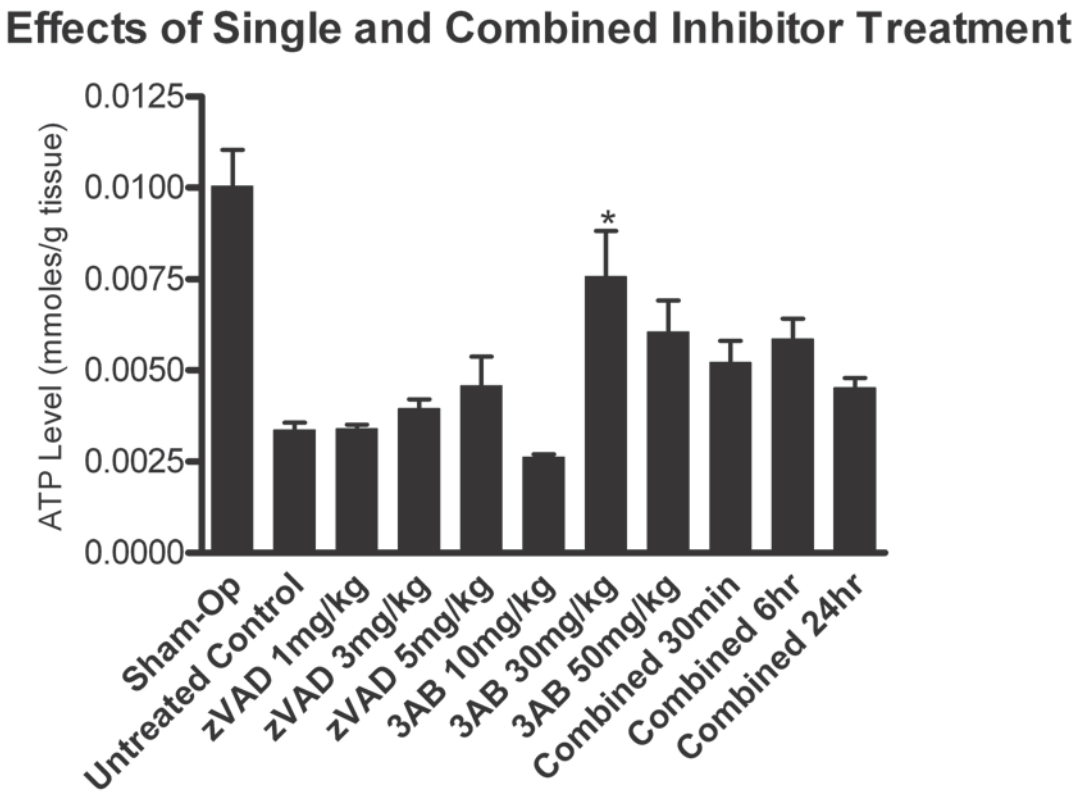

Fig. 8a. Intracellular ATP level following single and combined inhibitors administration of pan-caspase inhibitor (z-VAD-fmk) and PARP inhibitor (3-AB). Intracellular ATP levels of lesioned cerebral cortices subjected to z-VAD-fmk, 3-AB and combined inhibitors treatments evaluated at 48hr following MCAo. Each group of rats (n=3) was treated with different doses of z-VAD-fmk and 3-AB, while the untreated control group was given 0.9% saline. Combined administration of z-VAD-fmk and 3-AB were given at different time intervals. Intracellular ATP level were determined using ATP assay kit and luminometer. Data were analysed by One-way ANOVA, Newman-Keuls Multiple Comparison Test (*p-value<0.05).

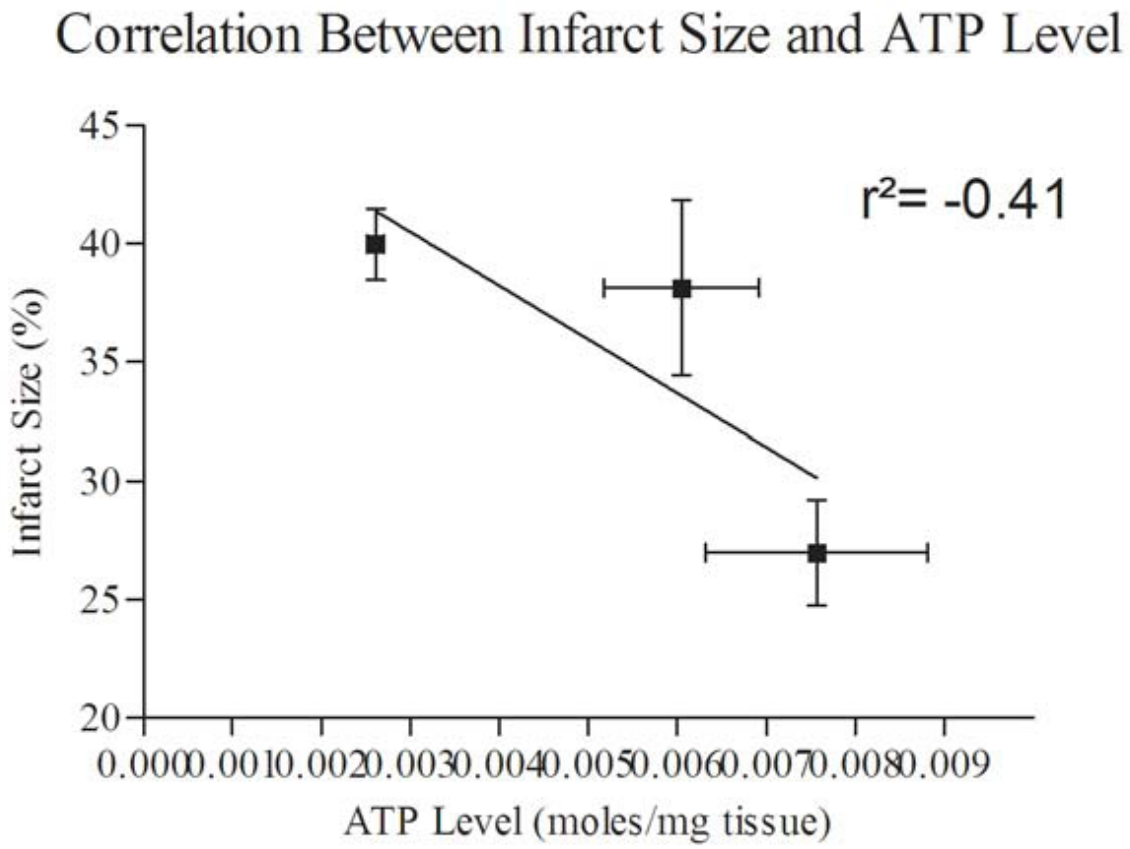

Fig. 8b. Coefficient of determination for infarct size and intracellular ATP level for rats treated with 3-AB. Intracellular ATP level and size of infarct of brains (n=7) which were subjected to different doses of 3-AB measured at 48hr following MCAo. Linear regression analysis showed an inverse correlation between intracellular ATP level and size of infarct at $r^2 = -0.41$ with p-value<0.05.

3.1.5 Effects of pan-caspase and PARP inhibition on intracellular apoptotic markers

Caspase-3 exists in cells as inactive 36kD proenzyme which are proteolytically cleaved into 19kD and 17kD fragment. PARP (116kD), a substrate for activated caspase-3, are cleaved into 89kD and 24kD fragments. Cleaved caspase-3 (active) and PARP cleavage are commonly used as apoptotic marker (Han et al., 2003). Fig. 9a to 9c show the protein expression changes in the lesioned cerebral cortices of rats with cleaved caspase-3 and PARP cleavage being absent in groups receiving 10mg/kg 3-AB, 3mg/kg z-VAD-fmk and 5mg/kg z-VAD-fmk treatments, while 30mg/kg, 50mg/kg 3-AB and 1mg/kg z-VAD-fmk treatments showed cleaved caspase-3 and PARP cleavage clearly. The combined inhibitors treatment showed PARP cleavage independent of caspase-3 activation.

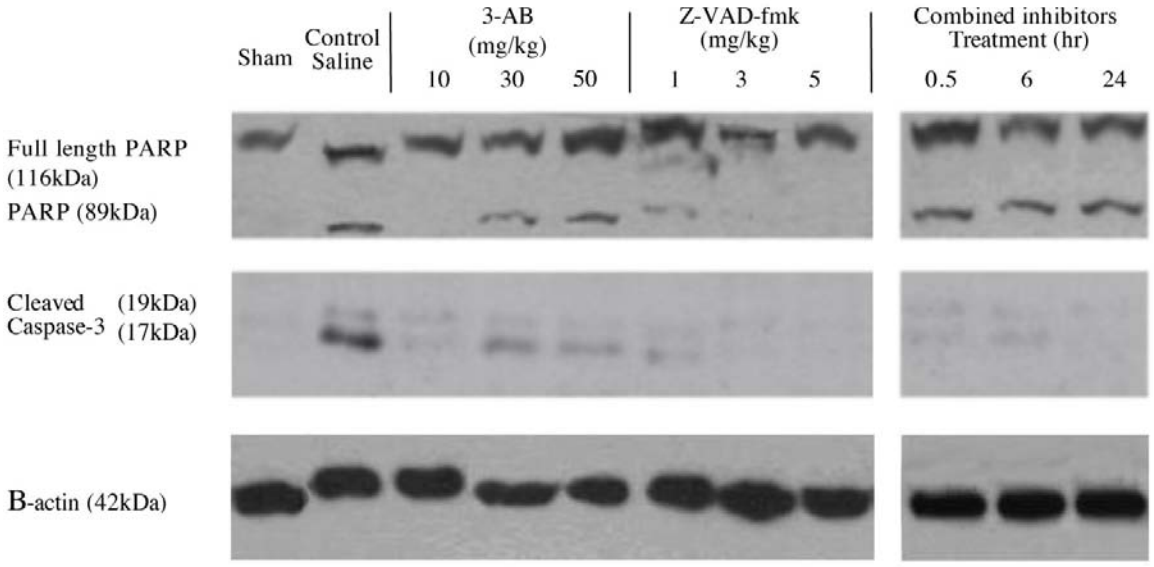

Fig. 9a. Western blots of cleaved caspase-3 and cleaved PARP following MCAo. The various treatments were administered at 30min post-surgery unless otherwise stated as in the combined treatment groups. The lesioned cerebral cortices were excised for analysis 48hr following MCAo. Western blot membranes were labeled with cleaved caspase-3 antibody and cleaved PARP antibody, which were then developed with the ECL system. β-actin was used for normalisation purpose.

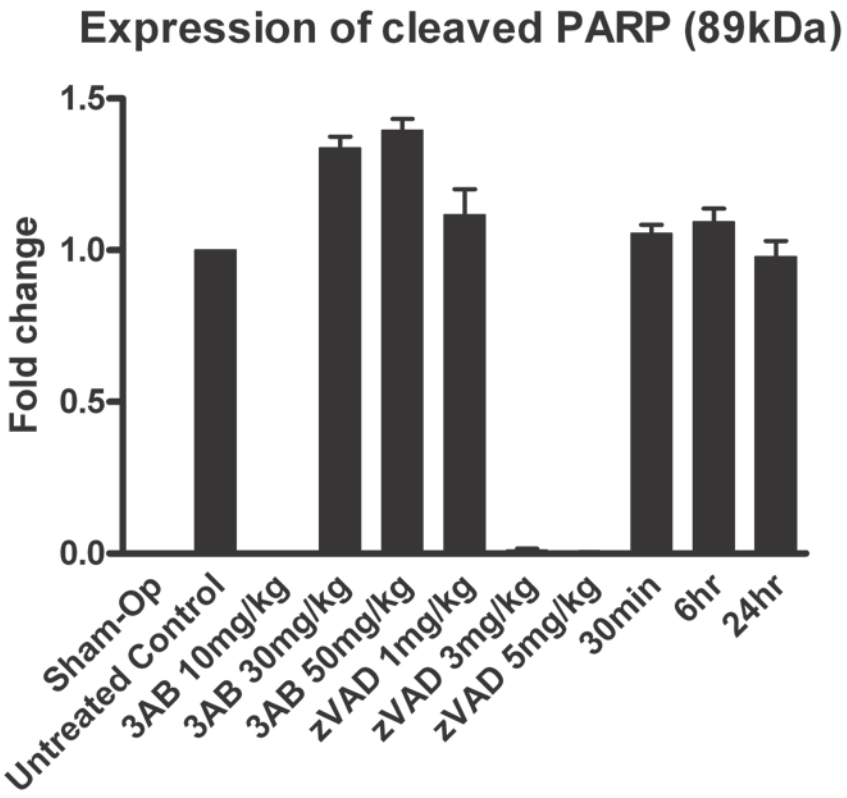

Fig. 9b. Western Blot analysis of PARP cleavage following MCAo. Each group of rats (n=3) was treated with different doses of 3-AB (PARP inhibitor), and control were given saline. Optimized doses of both inhibitors were administered concurrently in the combined inhibitors treatment group. 30 and 50mg/kg 3-AB and 1mg/kg z-VAD-fmk show cleaved caspase3 and PARP cleavage which suggests apoptosis process is present. In the combined inhibitors treatment, only PARP cleavage is observed.

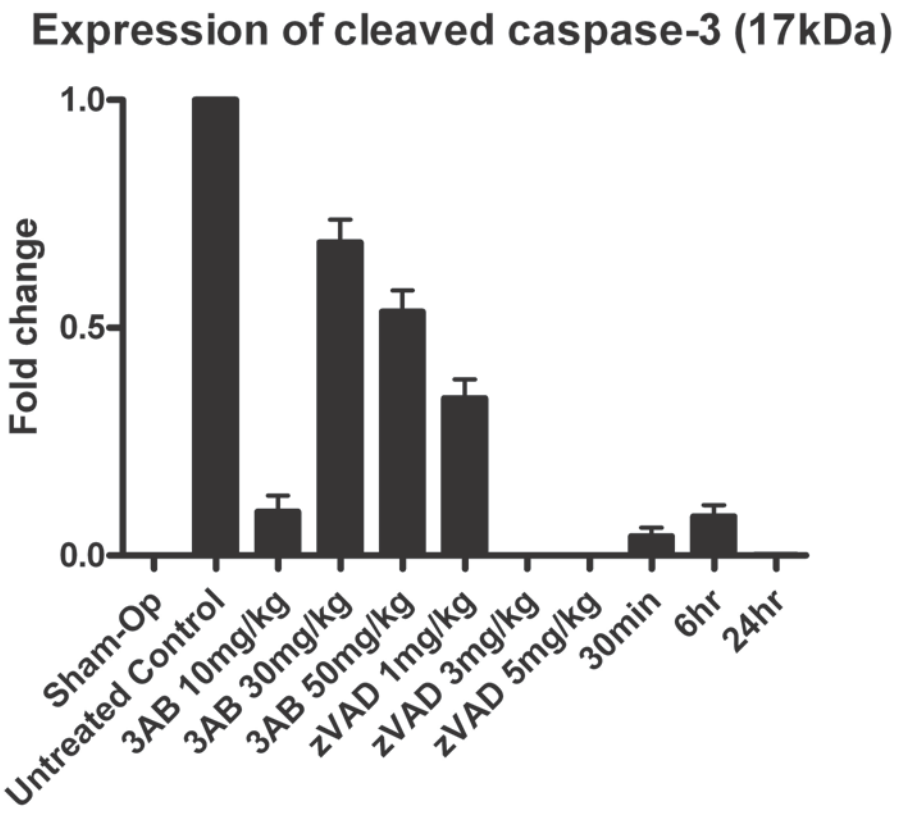

Fig. 9c. Western Blot analysis of cleaved caspase-3 following MCAo. Each group of rats (n=3) is treated with different doses of z-VAD-fmk (pan caspase inhibitor), and control are given saline. Optimized doses of both inhibitors are administered concurrently in the combined inhibitors treatment group. 30 and 50mg/kg 3-AB and 1mg/kg z-VAD-fmk show cleaved caspase3 and PARP cleavage which suggests apoptosis process is present. In the combined inhibitors treatment, only PARP cleavage is observed.

3.2 Effects of Post-ischemic Exercise in Chronic Phase of MCAo

3.2.1 Mortality rate

Mortality rate within 24hr after surgery was 30% (12/36) for MCAO rats (consists of MCAo and MCAo-runner) and 0% (0/24) for the sham-operated rats (consists of sham and sham-runner) (Fig. 10). It was suggested by Venketasubramanian et al. (2005) that most of the death was due to the brain ischemia and not surgery.

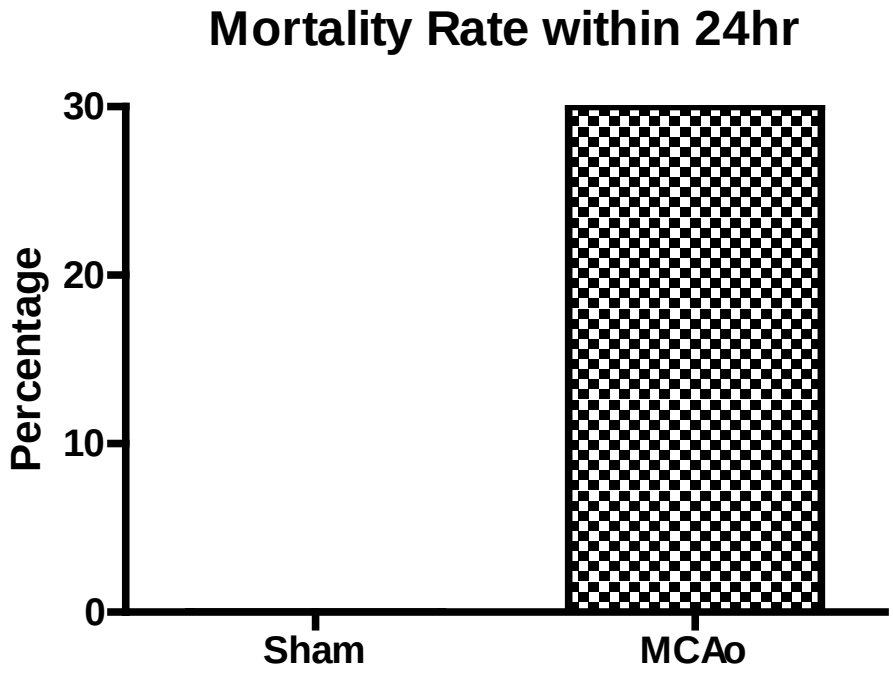

Fig. 10. Mortality rate within 24hr after sham-operation and experimental MCAo surgery. Mortality rate within 24hr after experimental MCAo surgery is 30% (12/36) for MCAo rats and 0% (0/24) for the sham-operated rats. It is apparent that the death is due to brain ischemia and not surgery.

3.2.2 Estimation of path length run on the treadmill

Both sham-runner rats and MCAo-runner rats were acclimatized to the treadmill machine (Panlab S.L., LE 8710R, Barcelona, Spain) progressively from 10 to 30min at the speed of 15cm/sec with 0 degree inclination, thus covered a total of 90 to 270m/day (Table 2A). Rats from the runner group were then subjected to the actual forced exercise program on the treadmill machine for 45min, once a day, five days per week, for eight consecutive weeks. The exercise workload consisted of running at the speed 25cm/sec for the first 5min, 35cm/sec for the next 35min, and then back to 25cm/sec for the last 5min with 0 degree inclination (Table 2B). The total distance covered at each session was 885m/day which was above the threshold of 500m/day indicated for any up-regulation of BDNF and activated cyclic adenosine monophosphate (cAMP) response element-binding protein (Shen et al., 2001). Both sham rats and MCAo rats were exposed to the same set-up with the treadmill turned off for the above duration thus did not cover any significant distance except distance for instinctive exploration.

3.2.3 Weight changes

The weights of all rats (n = 16) were observed to register a decline following surgery. The lost weights were presented in percentage instead of absolute value. One day post-operatively the weight changes were recorded with a drop of 5.57 ± 0.63%, 5.21 ± 0.68%, 14.53 ± 1.07% and 13.97 ± 0.8% in sham, sham-runner, MCAo and MCAo-runner rats respectively (Fig. 11). Rats subjected to MCAo experienced weight lost (in percentage) approximately 2.5 times more than the sham-operated rats with p-value<0.001.

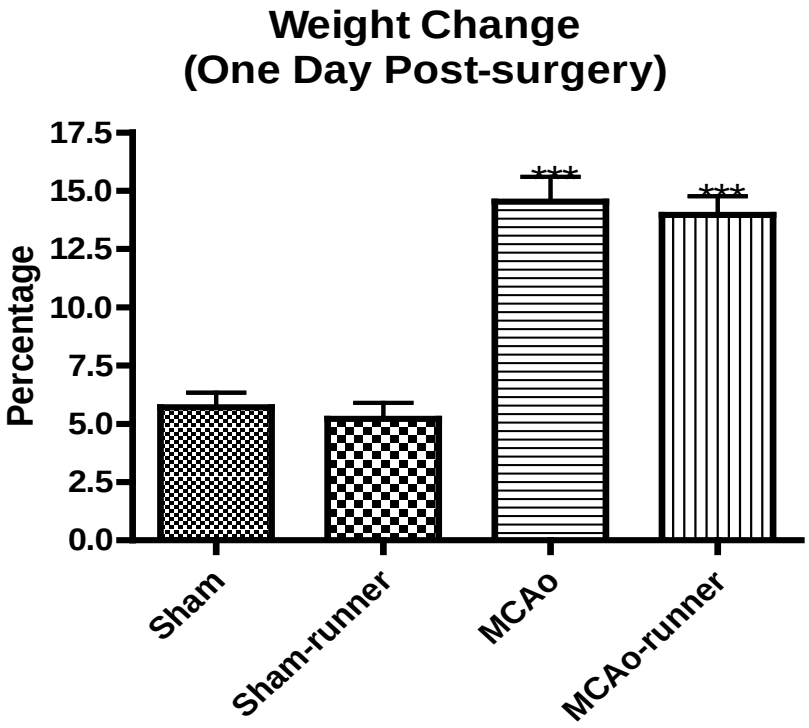

Fig. 11. Weight change (loss) 24hr post surgery. Weight change (loss) is evaluated with a reduction of 5.57 ± 0.63%, 5.21 ± 0.68%, 14.53 ± 1.07% and 13.97 ± 0.8% in sham, sham-runner, MCAo and MCAo-runner rats respectively. Weight loss is observed in all the groups, and the animal with MCAo registered higher weight loss. Data are analyzed with One-way ANOVA, Tukey's Multiple Comparison Test with ***p-value<0.001.

The rats were weighed again at 10th week post-surgery, and without exception, all the rats registered weight gain across-the-board. The gained weights were presented in percentage. The weights gained were recorded as 121.8 ± 10.93%, 57.5 ± 8.45%, 124.7 ± 8.52% and 68.34 ± 8.66% in sham, sham-runner, MCAo and MCAo-runner rats respectively (Fig. 12). Interestingly, sham rats and MCAo rats, which were not subjected to forced treadmill exercise occlusion, experienced weight gain (in percentage) approximately 2.5 times more as compared to the rats which were subjected to forced treadmill exercise with p-value<0.001. However, no difference was seen between sedentary or runner groups regardless whether they were subjected to MCAo or sham-operations.

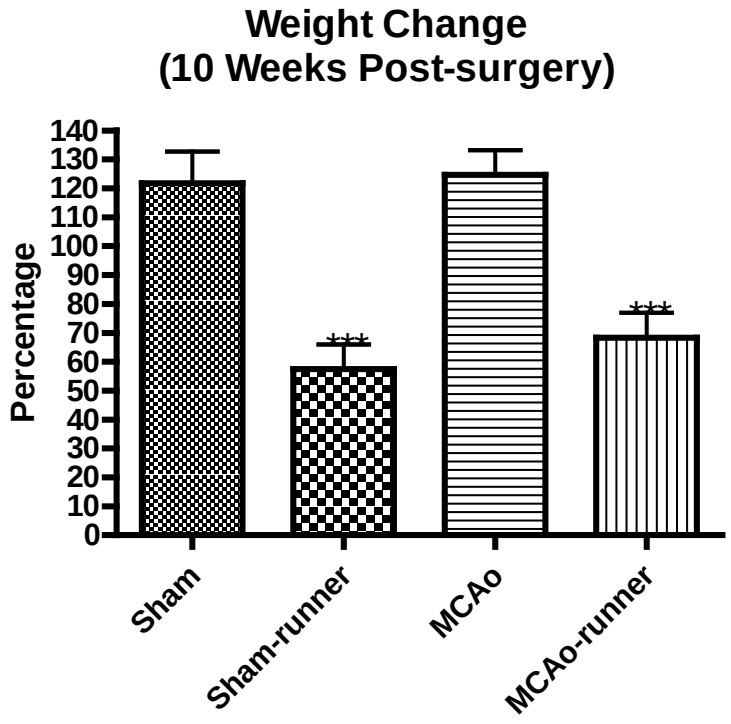

Fig. 12. Weight change (gain) ten weeks post surgery. Sham, sham-runner, MCAo and MCAo-runner rats are observed with weight increased by 121.8 ± 10.93%, 57.5 ± 8.45%, 124.7 ± 8.52% and 68.34 ± 8.66% respectively. The results show that exercise could reduce weight gain in animal with or without MCAo. Data are analyzed with One-way ANOVA, Tukey's Multiple Comparison Test with ***p-value<0.001.

3.2.4 Neurological scores

All the rats were subjected to neurological evaluation following experimental MCAo for a total of ten weeks. The animals showed some signs of paralysis which included abnormal posture and hemiplegia and a reduction in spontaneous movements after MCAo. Typically, this was maximal during the 1st week, and then gradually improved at varying degrees over the following nine weeks with or without any forced treadmill exercise. However, from 4th week onwards, MCAo-runner rats began to show some functional recovery, as reflected in the lower score, as compared the MCAo rats. And at the end of 10th week, the MCAo-runner rats showed distinct functional recovery in contrast with the MCAo rats (Fig. 13).

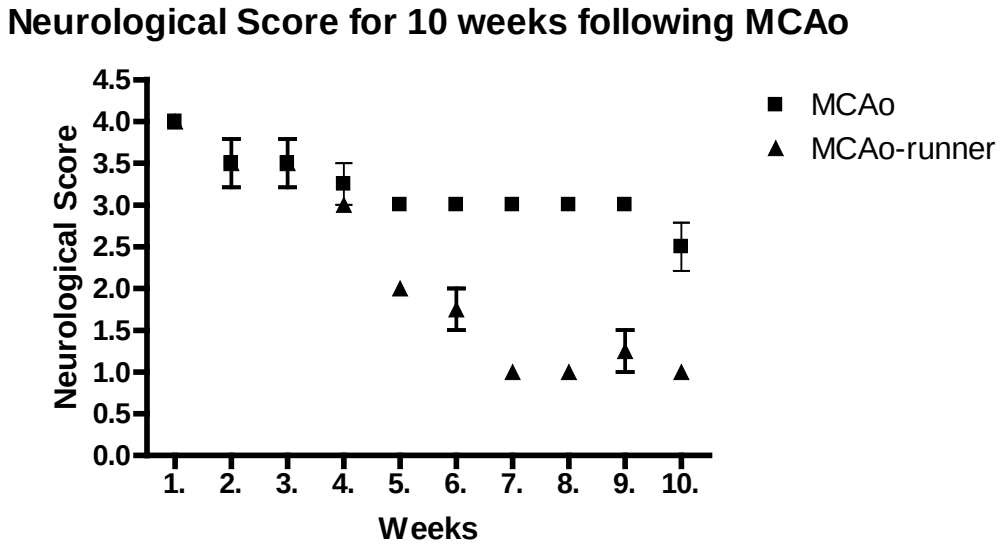

Fig. 13. Neurological evaluation scores for MCAo (n=4) and MCAo-runner (n=4) rats ten weeks post-surgery (one week rest; one week treadmill familiarization; eight weeks moderate forced treadmill exercise). A lower score is indicative of better status for functional recovery. The data show that MCAo-runner rats can achieve a distinct improvement at week five as compared with the MCAo rats.

3.2.5 TGF-β signaling in hippocampus

All animals were sacrificed at ten weeks (included trainings and eight weeks of actual exercise regime) with two days wash-out period after the last run.

3.2.5.1 Effects of exercise on TGF-β1, TGFBR-II, smad2 and smad7 mRNA and protein expression in hippocampus

Following eight weeks of forced treadmill exercise, TGF-b1 and smad7 mRNA expressions were significantly increased by 1.40 ± 0.06 and 2.30 ± 0.45 fold respectively in the sham-runner rats as compared with the sham rats, p-value<0.05 (Fig. 14a and 14d). TGFBR-II and smad2 mRNA expressions in the sham-runner rats flanked the mRNA expression levels in sham rats by 0.88 ± 0.08 and 1.35 ± 0.22 fold respectively following forced treadmill exercise, however, the changes were not statistically significant (Fig. 14b and 14c).

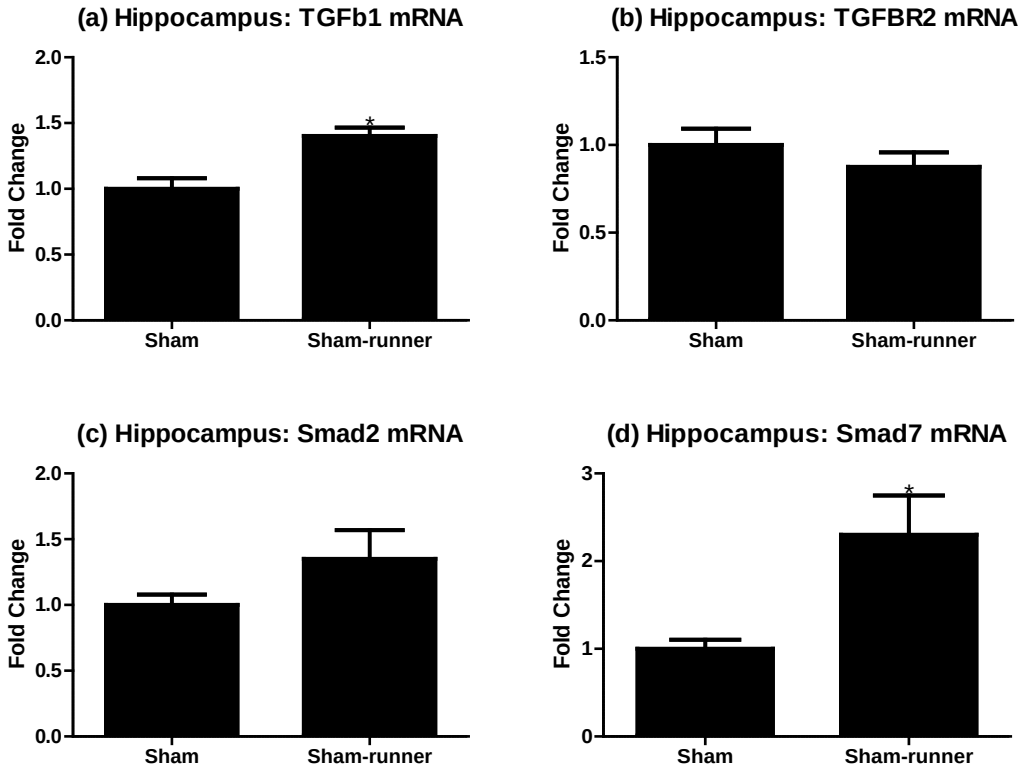

Fig. 14. mRNA expressions of TGF signaling in the hippocampus following eight weeks forced treadmill exercise. The brain homogenates are prepared from animals (n=4) sacrificed at ten weeks (whereby first two weeks are allocated for acclimatization and familiarization) and two days (as wash-out period for rats' the last run). Changes in mRNA levels are evaluated by quantitative real-time PCR and the result show that forced exercise increases both (a) TGFb1 and (d) smad7 mRNAs by 1.40 ± 0.06 and 2.30 ± 0.45 fold respectively in the sham-runner as compared with sham. However the exercise regime do not induce any significant changes to the (b) TGFBR2 and (c) smad2 mRNAs which are calculated at 0.88 ± 0.08 and 1.35 ± 0.22 fold respectively in the sham-runner. All data are analysed using unpaired t-test with *p-value<0.05.

Exposure to prolonged forced treadmill exercise produced increase in both TGF-β1 and smad7 protein expression by 1.38 ± 0.05 and 1.54 ± 0.07 fold respectively in the sham-runner rats as compared with the sham rats, p-value<0.05 (Fig. 15a and 15b). However, this regimented exercise program did not register any significant change in both cleaved caspase-3 and cleaved PARP protein expression which was recorded at 0.99 ± 0.08 and 1.17 ± 0.10 fold respectively for the sham-runner rats as compared with the sham rats (Fig. 15c and 15d). All data were analyzed with unpaired t-test.

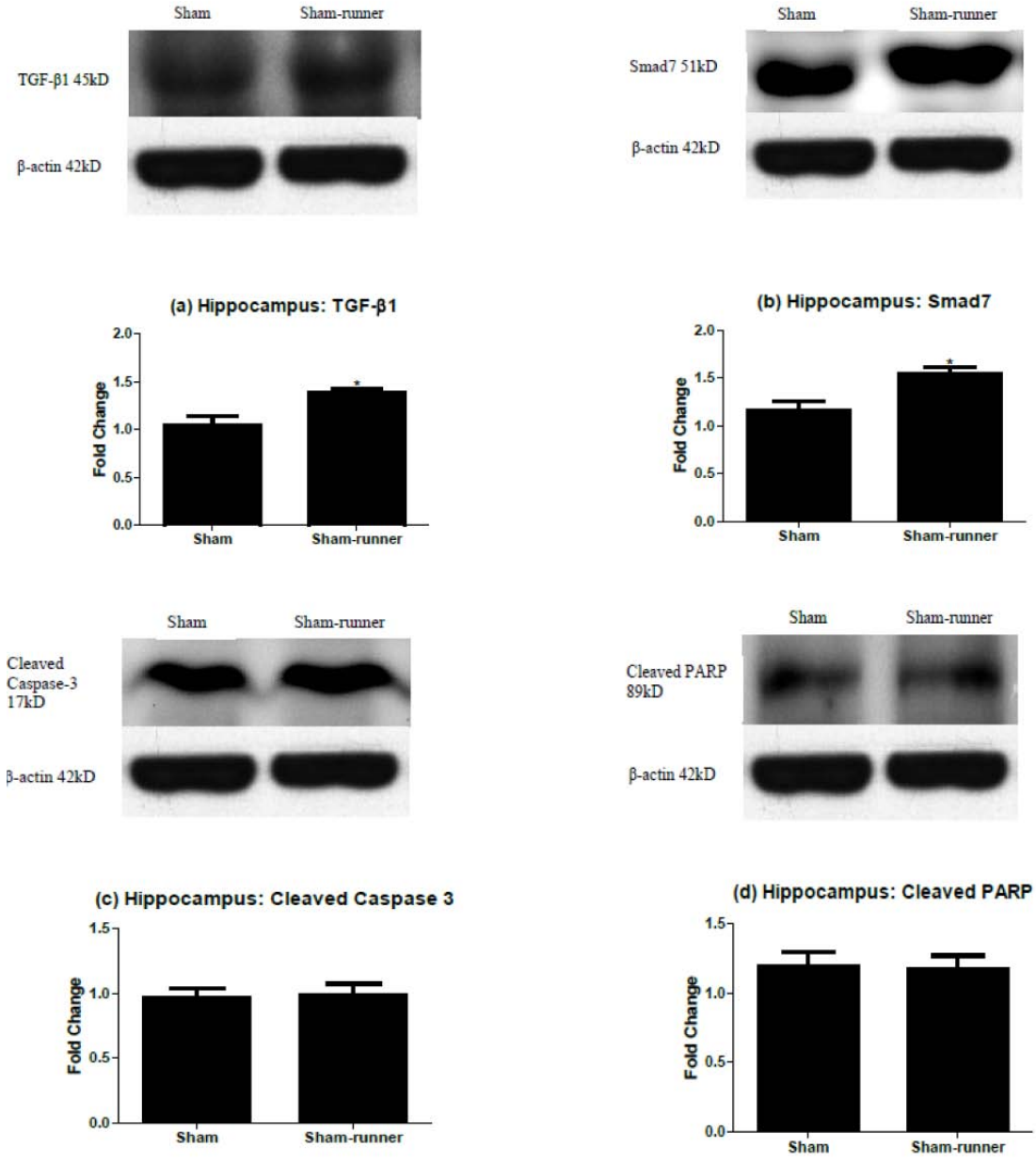

Fig. 15. Western blots and protein expressions of TGF signaling and capase-3 activity in the hippocampus following eight weeks forced treadmill exercise. The TGF-β1, smad7, cleaved caspase-3 and cleaved PARP antibodies detect the specific bands at 45kD, 51kD, 17kD and 89kD respectively with *β*-actin (42kD) used for normalisation. Forced treadmill exercise increases both (a) TGF-β1 and (b) smad7 protein levels in the sham-runner by 1.38 ± 0.05 and 1.54 ± 0.07 fold respectively as compared with the sham. These results suggest that forced exercise can have an effect on the hippocampal TGF signaling pathway. However, the experiment shows that forced exercise does not have any significant impact on caspase-dependent apoptosis. All data are analysed using unpaired t-test with *p-value<0.05.

3.2.5.2 Effects of exercise on TGF-β1 protein expression in the CA1 region

These confocal images in Fig. 16 depicted the CA1 region (bregma -2.0 to -5.0mm ± 0.5mm) immunostained with TGF-β1 and NeuN antibodies under different experimental conditions. Constitutively, punctated pattern of TGF-β1 expressions were found in the sham rats' CA1s and the adjacent oriens layer and stratum radiatum (Fig. 16A to C). Following forced treadmill exercise, TGF-β1 expressions appeared diffused and present in more NeuN neurons within the CA1 of sham-runner rats when compared with the control rats (Fig. 16D to F).

Subsequent to experimental brain ischemia, the TGF-β1 expressions in the MCAo rats were also presented in some NeuN neurons in the ipsilateral CA1s but seemingly subdued in the oriens layer and stratum radiatum (Fig. 16G to I), when compared with sham rats. Similarly, in the contralateral CA1s of the MCAo rats (Fig. 16J to L), more TGF-β1 expression were co-localised with the CA1s' neurons while the intensity of TGF-β1 expression in the oriens layer and stratum radiatum, although with higher immunoreactivities than their counter sides, appeared to be lower than sham rats.

The immunoreactivity profiles of the TGF-β1 expression in the MCAo-runner rats, when compared with the MCAo rats, remained relatively unchanged in the ipsilateral CA1's neurons (Fig. 16M to O) following post-ischemic exercise. The ipsilateral CA1's neurons in the MCAo-runner rats although shared similar regions of positive TGF-β1 expression

with sham-runner rats, the TGF-β1 immunoreactivities in the oriens layer and stratum radiatum from the ipsilateral hippocampi were less intense in the MCAo-runner rats than both sham-runner and MCAo rats. TGF-β1 expressions were also less intense in the contralateral hippocampi of the MCAo-runner rats (Fig. 16P to R) when compared with the same side of MCAo and sham-runner rats.

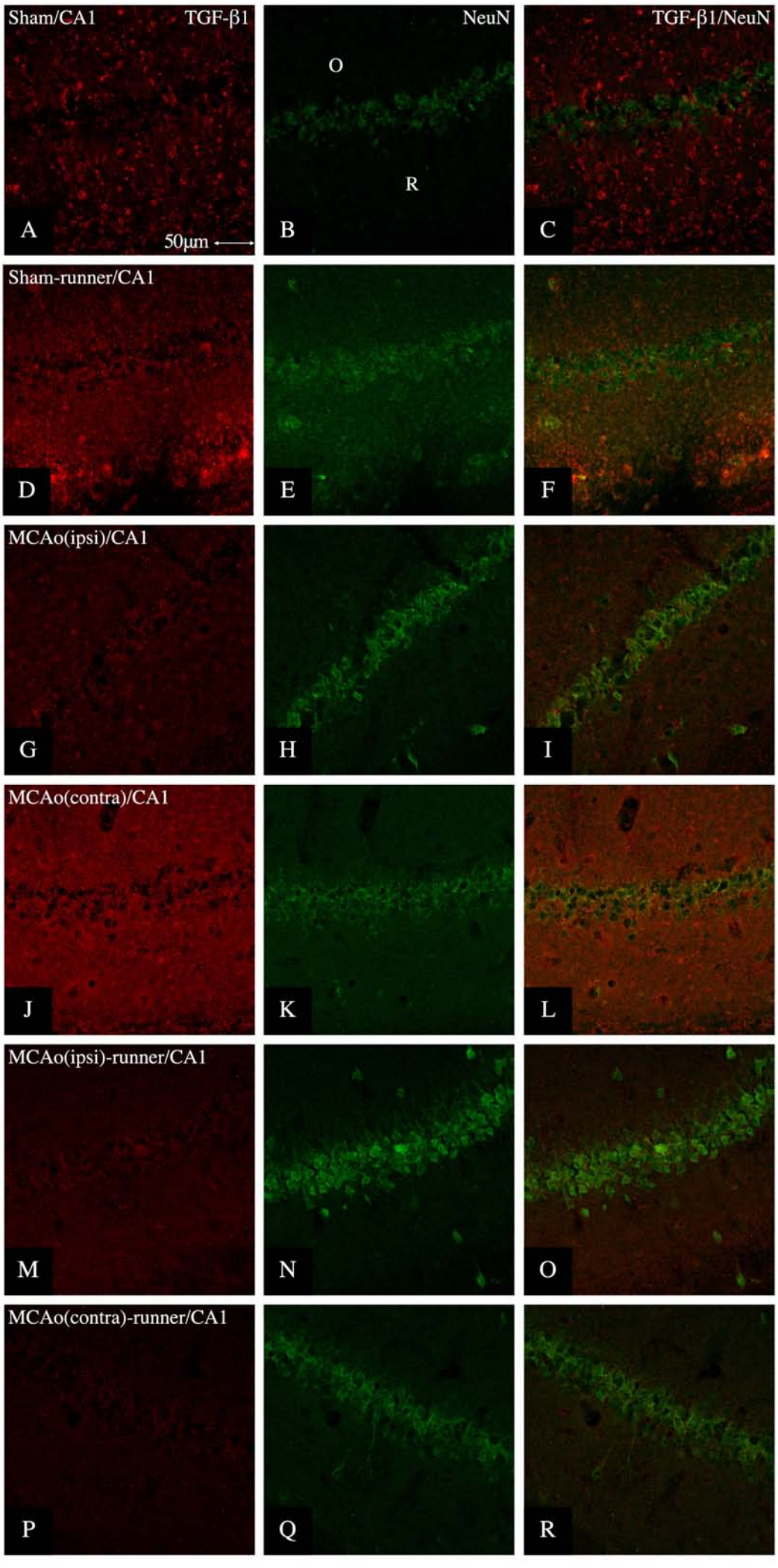
Sham/CA1
TGF-β1
A
50μm
NeuN
O
R
B
TGF-β1/NeuN
C
Sham-runner/CA1
D
E
F
MCAo(ipsi)/CA1
G
H
I
MCAo(contra)/CA1
J
K
L
MCAo(ipsi)-runner/CA1
M
N
O
MCAo(contra)-runner/CA1
P
Q
R

Fig. 16. Double staining of TGF-β1 and NeuN in CA1. These brain sections are from either sham-operated or MCAo rats following eight weeks with or without forced treadmill exercise. The 30μm brain sections were prepared from both sedentary and exercised animals (n=4) sacrificed at ten weeks (whereby first two weeks were allocated for acclimatization and familiarization) and two days (as wash-out period for rats subjected to the last run) post-surgery with or without MCAo. These confocal images depict the CA1 region at bregma -2.0 to -5.0mm ± 0.5mm under different experimental conditions. The tissues were double stained with TGF-β1 (red) and NeuN (green). Sham rats are displayed in Panel A to C and sham-runner rats are presented in Panel D to F. The ipsilateral and contralateral CA1 of MCAo rats are shown in Panel G to I [MCAo(ipsi)] and Panel J to L [MCAo(contra)] respectively. The ipsilateral and contralateral CA1 of MCAo-runner rats are exhibited in Panel M to O [MCAo(ipsi)-runner] and Panel P to R [MCAo(contra)-runner] respectively. Immunoreactivities of TGF-β1 are shifted to NeuN positive neurons in the CA1s following either increased physical activity or brain ischemia. Forced exercise appear to reduce the intensity of TGF-β1 expressions in oriens layer and stratum radiatum. O, oriens layer and R, stratum radiatum.

3.2.5.3 Effects of exercise on TGF-β1 protein expression in the DG

These confocal images in Fig. 17A to R depicted the DG from different experimental and control rats were immunostained with TGF-β1 and neuronal marker, NeuN antibodies.

As in the case of the CA1 region, punctated staining patterns of TGF-β1 expression were observed in the DGs of the sham rats (Fig. 17A to C). Instead of repeating what was observed in the CA1, TGF-β1 expressions in the DGs were noticeably reduced as compared with the sedentary rats following eight weeks of regimented treadmill in the sham-runner rats (Fig. 17D to F). Therefore, may suggest that TGF-β1 had specific roles to fulfill within the hippocampus' sub-structures.

In both ipsilateral (Fig. 17G to I) and contralateral (Fig. 17J to L) hippocampi of the MCAo rats, TGF-β1 expression pattern appeared more diffused yet with comparable intensity to the sham rats following ischemic insults.

Likened to the sham-operated scenarios, TGF-β1 staining patterns appeared subdued after post-ischemic exercise in both ipsilateral (Fig. 17M to O) and contralateral (Fig. 17P to R) hippocampi of the MCAo-runner rats as compared with the MCAo rats. These changes rendered the TGF-β1 staining patterns in MCAo-runner rats analogous to the observations made in the sham-runner rats.

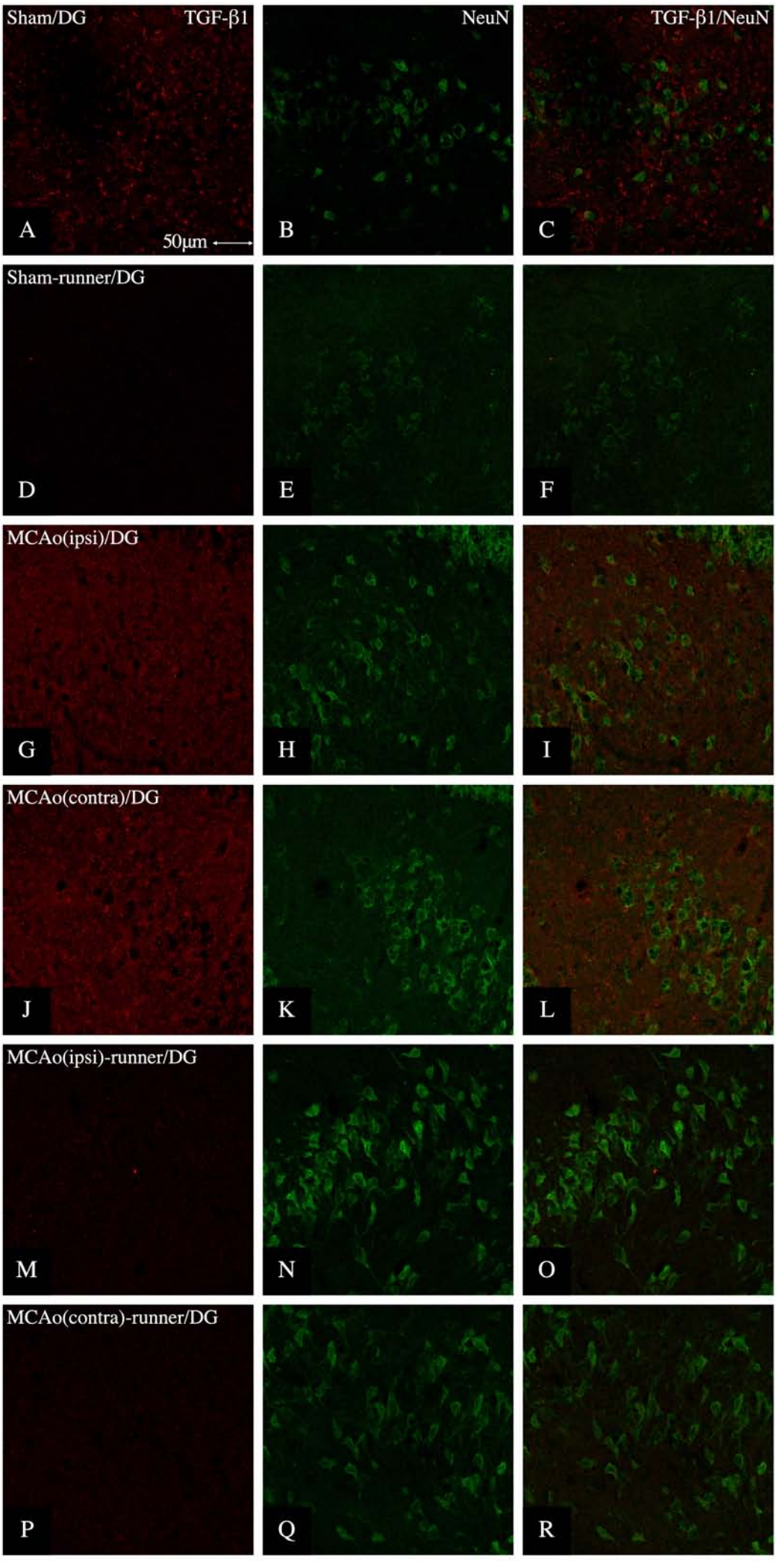
Sham/DG
TGF-β1
NeuN
TGF-β1/NeuN
A
50μm
B
C
Sham-runner/DG
D
E
F
MCAo(ipsi)/DG
G
H
I
MCAo(contra)/DG
J
K
L
MCAo(ipsi)-runner/DG
M
N
O
MCAo(contra)-runner/DG
P
Q
R

Fig. 17. Double staining of TGF-β1 and NeuN in DG. Brain sections are prepared from either sham-operated or MCAo rats following eight weeks with or without forced treadmill exercise. These confocal images depict the DG at bregma -2.0 to -5.0mm ± 0.5mm under different experimental conditions. The tissues were double stained with TGF-β1 (red) and NeuN (green). Intensity of TGF-β1 staining pattern was noticeably suppressed following increased physical activity in both sham-operated and MCAo rats. (D; G; J; M; P)

3.2.5.4 Effects of exercise on smad7 protein expression in the CA1 region

These confocal images in Fig. 18 depicted the CA1 region immunostained with smad7 and NeuN antibodies in various experimental conditions. Smad7 expression was hardly recognized in the sham rats' CA1 regions (Fig. 18A to C). However, following eight weeks of regimented treadmill exercise smad7 was detected and found to be co-localised with NeuN immunoreactive neurons in the CA1 region of the sham-runner rats (Fig. 18D to F). In addition, smad7 expression was also seen in the oriens layer and stratum radiatum.

In both ipsilateral (Fig. 18G to I) and contralateral (Fig. 18J to L) hippocampi of the MCAo rats, smad7 expressions were also detected and co-localised with NeuN positive neurons in the CA1 region, oriens layer and stratum radiatum.

Post-ischemic exercise marginally reduced smad7 staining intensity in the ipsilateral CA1s of the MCAo-runner rats (Fig. 18M to O) as compared with the same region of the MCAo rats. There was no noticeable change in the smad7 expression in the contralateral CA1 of the MCAo-runner rats (Fig. 18P to R) in contrast with the MCAo rats. Therefore, the effects of post-ischemic exercise on smad7 expression in the CA1 appeared to be restricted to the injured hippocampus.

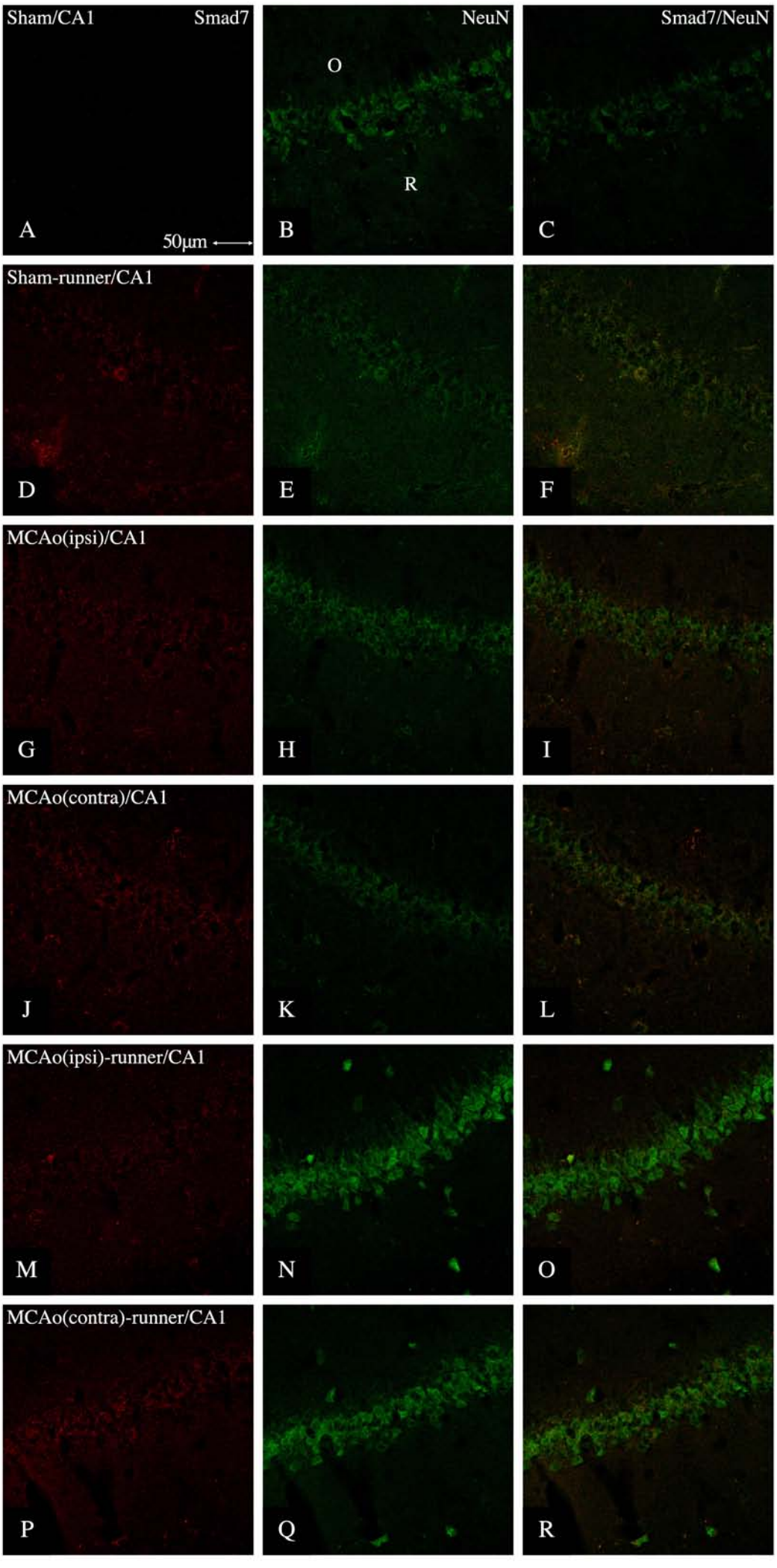
Sham/CA1
Smad7
A
50μm
NeuN
O
R
B
Smad7/NeuN
C
Sham-runner/CA1
D
E
F
MCAo(ipsi)/CA1
G
H
I
MCAo(contra)/CA1
J
K
L
MCAo(ipsi)-runner/CA1
M
N
O
MCAo(contra)-runner/CA1
P
Q
R

Fig. 18. Double staining of smad7 and NeuN in CA1. These brain sections are taken from either sham-operated or MCAo rats following eight weeks with or without forced treadmill exercise. These confocal images depict the CA1 region at bregma -2.0 to -5.0mm ± 0.5mm under different experimental conditions. The tissues were double stained with smad7 (red) and NeuN (green). Smad7 was increased following forced treadmill exercise and experimental brain ischemia (D; G; J; M; P). Interestingly, smad7 expression was subdued in the ipsilateral CA1 region following post-ischemic exercise (M). O, oriens layer and R, stratum radiatum.

3.2.5.5 Effects of exercise on smad7 protein expression in the DG

Immunostaining with smad7 and NeuN antibodies in DG under different experimental conditions were shown in Fig. 19A to R. Smad7 expressions in the DGs were scarce in the sham-operated rats (Fig. 19A to C). Following eight weeks of regimented treadmill exercise, forced exercised rats showed marginal smad7 expression being identified in the DG region and was also co-localised with NeuN positive neurons (Fig. 19D to F).

Smad7 expression was detected in both ipsilateral (Fig. 19G to I) and contralateral (Fig. 19J to L) hippocampi of the MCAo rats with marginal intensity that were co-localised with NeuN positive neurons and as well as extra neuronal structures.

Post ischemic exercise did not alter the smad7 staining profile in the contralateral hippocampus (Fig. 19P to R) of the MCAo-runner rats when compared with sedentary rats. However, smad7 staining intensity in the ipsilateral hippocampus of the forced exercised rats (Fig. 19M to O) appeared to be slightly reduced as compared with the ipsilateral DG of the MCAo rats.

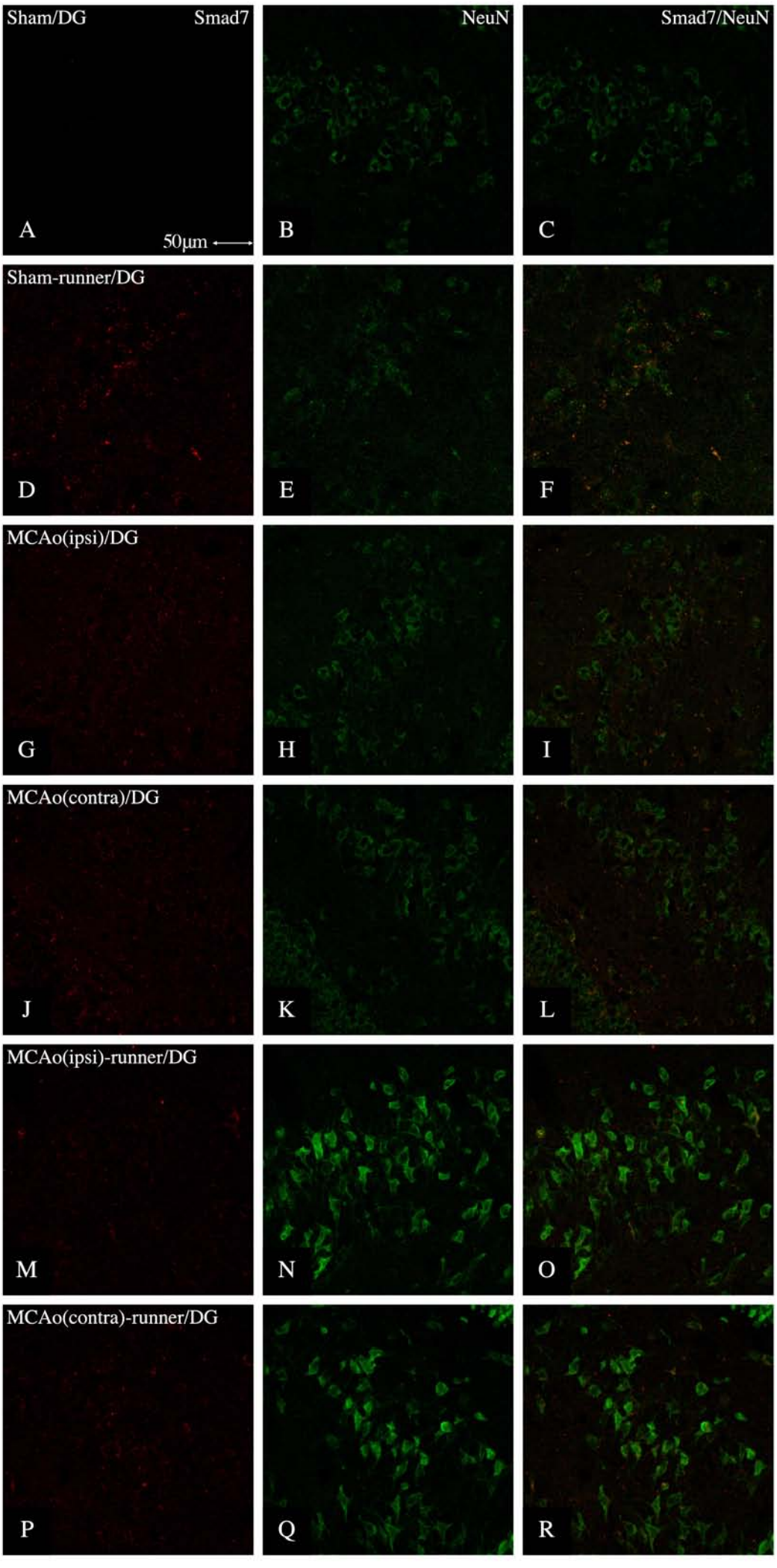
Sham/DG
Smad7
NeuN
Smad7/NeuN
A
50μm
B
C
Sham-runner/DG
D
E
F
MCAo(ipsi)/DG
G
H
I
MCAo(contra)/DG
J
K
L
MCAo(ipsi)-runner/DG
M
N
O
MCAo(contra)-runner/DG
P
Q
R

Fig. 19. Double staining of smad7 and NeuN in DG. Brain sections are prepared from either sham-operated or MCAo rats following eight weeks with or without forced treadmill exercise. These confocal images depict the DG at bregma -2.0 to -5.0mm ± 0.5mm under different experimental conditions. The tissues were double stained with smad7 (red) and NeuN (green). Smad7 expression in the DG is marginally increased subsequent to prolonged running exercise and brain ischemia (D; G; J; M; P). However, when compared to the MCAo rats, smad7 expression appeared slightly suppressed following post-ischemic exercise (M).

3.2.6 TGF-β signaling and apoptosis in cortex

All animals assigned to either exercise or sedentary groups were sacrificed at ten weeks post-surgery (includes the total time allocated for trainings and eight weeks of actual exercise regime for the runner groups), with two days wash-out period after the last run, with or without MCAo .

3.2.6.1 Effects of exercise and brain ischemia on mRNA and protein expression in TGF-β signaling and caspase activity

In Fig. 20a, following eight weeks of forced treadmill exercise, TGF-b1 mRNA expressions were determined at 1.07 ± 0.15 fold in the sham-runner rats thus were not set apart significantly from the sham rats. Under ischemic condition, TGF-b1 mRNA expressions in MCAo rats were also recorded with marginal up-regulations at 1.19 ± 0.04 and 1.17 ± 0.04 in both ipsilateral and contralateral cortices respectively, but these differences were not statistically significant when compared with the sham rats. When forced exercise was introduced on top of ischemic insult, TGF-b1 mRNA expression was statistically increased by 2.53 ± 0.69 fold in the ipsilateral cortices of the MCAo-runner rats in contrast to MCAo rats, p-value<0.05. However, the contralateral cortices of the MCAo-runner rats remained comparable to the MCAo rats and the TGF-b1 mRNA expression was recorded at 1.15 ± 0.12.

As shown in Fig. 20b, TGFBR-II mRNA expressions in the sham-runner rats were recorded with a slight drop at 0.75 ± 0.04 fold after subjected to eight weeks of forced treadmill exercise. Under ischemic condition, TGFBR-II mRNA expressions were documented at 0.88 ± 0.06 and 1.01 ± 0.02 fold in both ipsilateral and contralateral cortices respectively of the MCAo rats. However, these adjustments when compared with the sham rats were not statistically significant. Following eight weeks of post-ischemic forced treadmill exercise, TGFBR-II mRNA expressions were further decreased to 0.59 ± 0.06 and 0.78 ± 0.09 fold in the ipsilateral and contralateral cortices of the MCAo-runner rats but the changes were not statistically significant when compared with the MCAo rats.

In Fig. 20c, smad2 mRNA expression was marginally increased by 1.24 ± 0.11 fold following eight weeks of forced treadmill exercise in the sham-runner rats. Smad2 mRNA expressions following experimental brain ischemia were also recorded with a small increment at 1.38 ± 0.13 and 1.37 ± 0.09 in both ipsilateral and contralateral cortices respectively of the MCAo rats. However, these alterations when compared with the sham animals were not statistically significant. Following eight weeks of post-ischemic forced treadmill exercise, smad2 mRNA expressions were documented with a marginal up-regulation at 1.24 ± 0.14 and 1.10 ± 0.04 in both the ipsilateral and contralateral cortices respectively of the MCAo-runner rats which were comparable to the MCAo rats.

Smad7 mRNA expression in Fig. 20d showed the mRNA level was recorded at 0.98 ± 0.14 fold following eight weeks of forced treadmill exercise in the sham-runner

rats. Smad7 mRNA expression were recorded with a slight increase at 1.15 ± 0.10 and 1.34 ± 0.11 in both ipsilateral and contralateral cortices of the MCAo rats respectively following ischemic insults. Similar to the cases seen in smad2 mRNA expressions, these modifications in contrast to sham rats were not statistically significant. Smad7 mRNA expression, following eight weeks of post-ischemic forced treadmill exercise, in both the ipsilateral and contralateral cortices of the MCAo-runner rats, comparable to the MCAo rats, were documented at 0.73 ± 0.04 and 1.01 ± 0.10 respectively. All data were analysed with One way ANOVA, Tukey's Multiple Comparison Test.

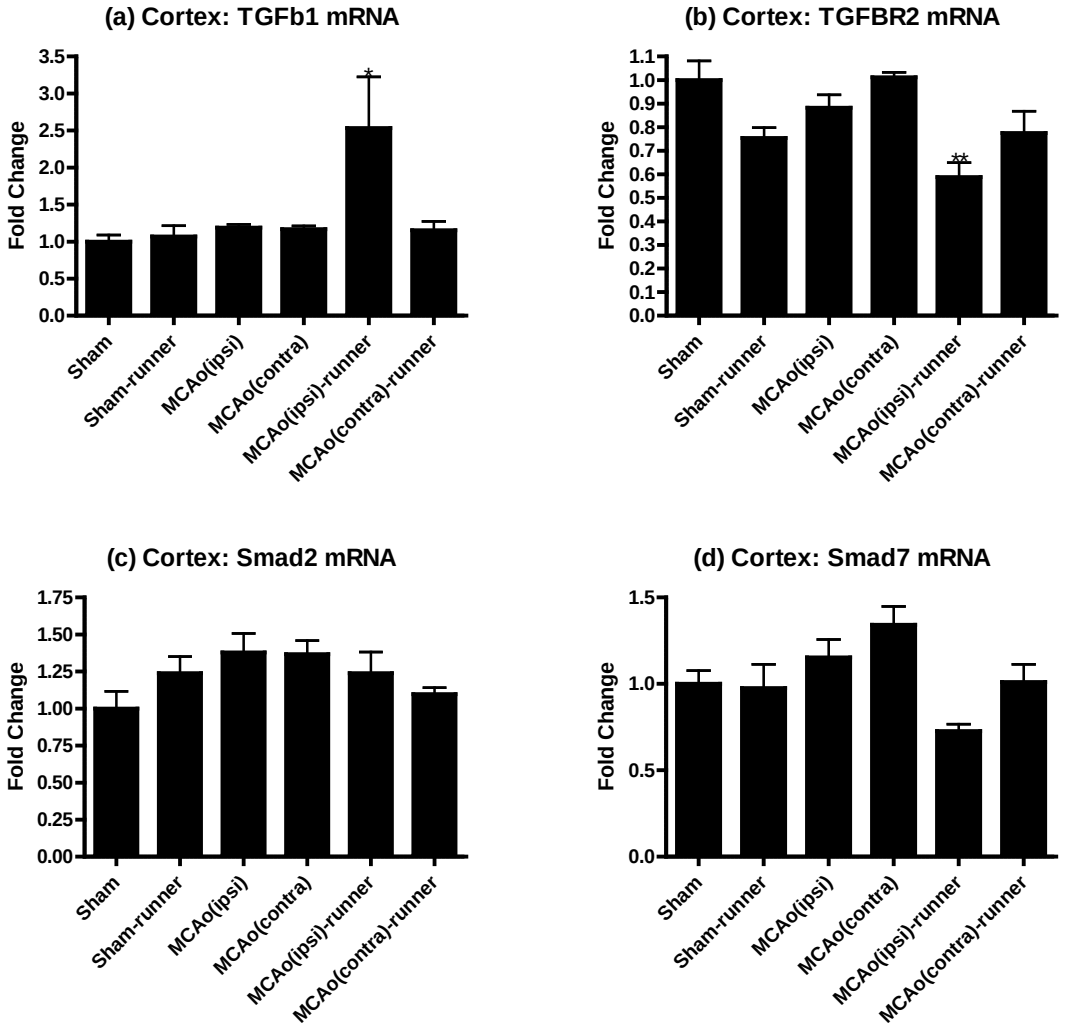

Fig. 20. mRNA expressions of TGF signaling in the cortex. The brain homogenates were prepared from both sedentary and exercised animals (n=4) sacrificed at ten weeks (whereby first two weeks were allocated for acclimatization and familiarization) and two days (as wash-out period for rats subjected to the last run) post-surgery with or without MCAo. Changes in mRNAs levels were evaluated in sham, sham-runner, MCAo (ipsilateral cortex) [MCAo(ipsi)], MCAo (contralateral cortex) [MCAo(contra)], MCAo-runner (ipsilateral cortex) [MCAo(ipsi)-runner] and MCAo-runner (contralateral cortex) [MCAo(contra)-runner] rats. (a) The result showed that the presence of both brain ischemia and forced exercise [in MCAo(ipsi)-runner] can potentiate TGFb1 mRNA expression significantly by 2.53 ± 0.69 fold in the ipsilateral cortex as compared with the MCAo(ipsi) rats. (b) The experiment showed that the presence of both brain ischemia and forced exercise [in MCAo(ipsi)-runner, when compared with the MCAo(ipsi)] can further reduce cortical TGFBR2 mRNA expression to 0.59 ± 0.06 fold albeit not statistically significant. No change in (c) smad2 and (d) smad7 mRNA levels, which suggested that both brain ischemia and forced exercise did not have any influence on their gene expression. All data were analysed with One way ANOVA, Tukey's Multiple Comparison Test with *p-value<0.05 and **p-value<0.01.

In Fig. 21a, eight weeks of forced treadmill exercise did not significantly increase TGF-β1 protein expression for the sham-runner rats and the TGF-β1 level was evaluated at 1.05 ± 0.05 fold which was not statistically significant when compared with the sham rats. Although TGF-β1 protein expression was up-regulated in both cortices of the MCAo rats at 1.28 ± 0.05 and 1.71 ± 0.08 fold for ipsilateral and contralateral cortices respectively, only the contralateral cortices showed significant increase when compared with the sham rats, p-value<0.05. TGF-β1 protein expression seen in the ipsilateral cortices of the MCAo rats were further enhanced in the MCAo-runner rats following eight weeks of post-ischemic forced treadmill exercise documented at 1.55 ± 0.05 fold but the change was not statistically significant. The contralateral cortices of the MCAo-runner rats remained significantly up-regulated at 1.73 ± 0.12 fold and comparable to the increment seen in MCAo rats.

Presented in Fig. 21b, smad7 protein expression showed a slight but not statistically significant upward trend subsequent to eight weeks of forced treadmill exercise in the sham-runner rats (1.18 ± 0.07) when compared with the sham rats. Demonstrably, smad7 protein expression recorded an up-regulation in both ipsilateral and contralateral cortices of the MCAo rats by 1.50 ± 0.09 and 1.43 ± 0.10 fold respectively, and these upward trends were statistically significant when compared with the sham rats, p-value<0.01. Interestingly, smad7 protein levels in the ipsilateral cortices of the MCAo-runner rats were down-regulated (1.03 ± 0.07 fold) when compared with the same side in the MCAo rats, p-value<0.01. Otherwise smad7 protein expression, following eight weeks of

post-ischemic forced treadmill exercise, in the contralateral cortices of the MCAo-runner rats remained around 1.36 ± 0.08 fold as compared with the MCAo rats.

Cleaved caspase-3 protein expressions displayed in Fig. 21c indicated that sham-runner rats were recorded at 1.06 ± 0.04 fold which was comparable to sham rats following eight weeks of forced treadmill exercise. In the ischemic brain, ipsilateral cortices of the MCAo rats recorded a significant increase in cleaved caspase-3 protein expression at 2.84 ± 0.27 fold (p-value<0.01), while the contralateral cortices was noted at 1.18 ± 0.07 fold (not statistically significant) in contrast with the sham rats. This increased cleaved caspase-3 protein levels observed in the ipsilateral cortex of the MCAo rats were down-regulated evidently following eight weeks of post-ischemic forced treadmill exercise to 0.94 ± 0.04 fold as seen in the ipsilateral cortices of the MCAo-runner rats with p-value<0.01. The contralateral cortices of the MCAo-runner rats were recorded at 1.05 ± 0.04 fold which were comparable to the MCAo rats.

As seen in Fig. 21d, cleaved PARP protein expression was recorded with a marginal increase at 1.10 ± 0.04 fold in the sham-runner rats subsequent to eight weeks of forced treadmill exercise but not statistically significant when compared with the sham rats. On the other hand, both ipsilateral and contralateral cortices of the MCAo rats recorded a significant up-regulation of cleaved PARP protein expression (1.50 ± 0.09 and 1.44 ± 0.13 fold respectively) in contrast to the sham rats, p-value<0.05. Post-ischemic exercise brought down the cleaved PARP protein level to 1.13 ± 0.14 (p-value>0.05) and 0.73 ±

0.03 (p-value<0.05) in the ipsilateral and contralateral cortices of the MCAo-runner rats respectively when compared with the MCAo rats.

All data were analyzed with One way ANOVA, Tukey's Multiple Comparison Test.

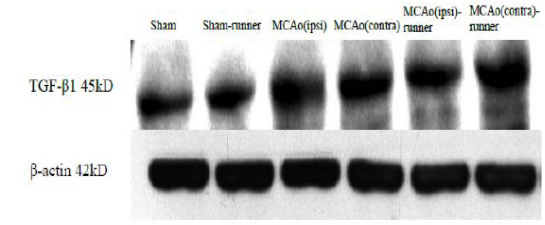

(a) Cortex: TGF-β1

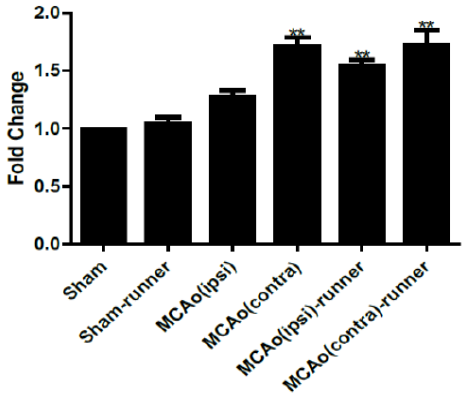

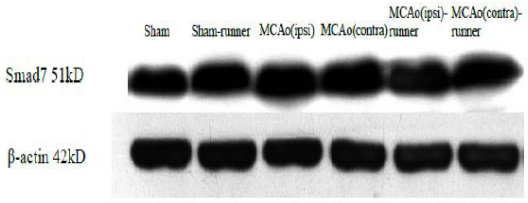

(b) Cortex: Smad7

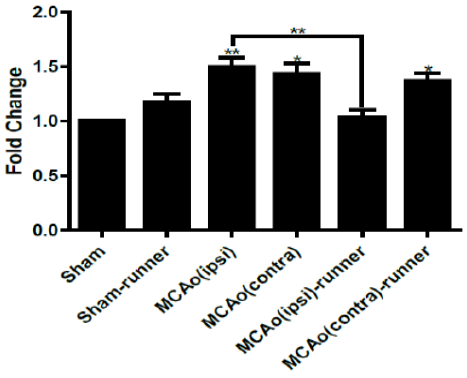

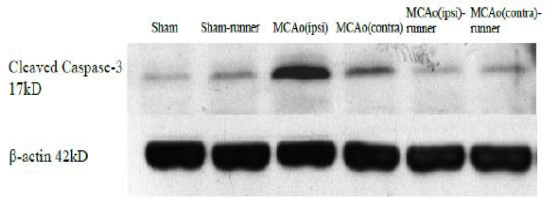

(c) Cortex: Cleaved Caspase-3

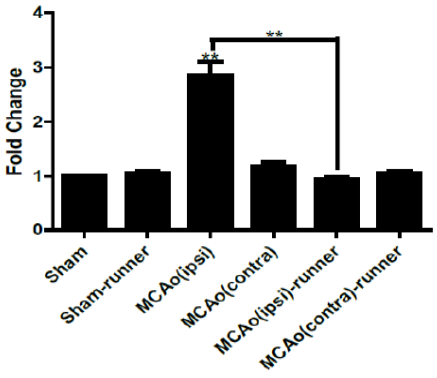

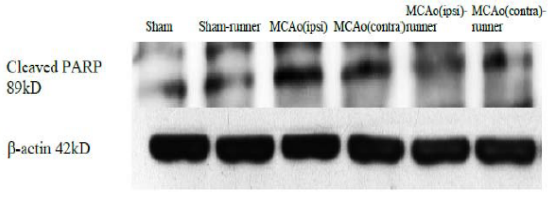

(d) Cortex: Cleaved PARP

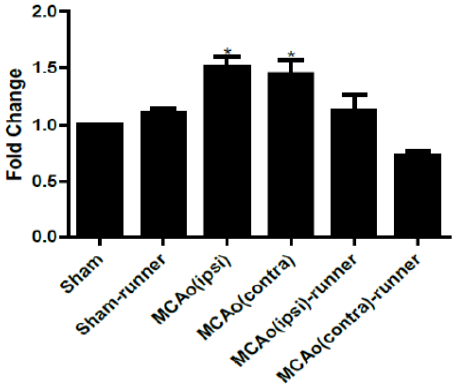

Fig. 21. Western blots and protein expressions of TGF signaling and caspase-3 activity in the cortex. These brain tissues are taken from rats with or without eight weeks forced treadmill exercise under either sham-operated or MCAo conditions. The TGF-β1, smad7, cleaved caspase-3 and cleaved PARP antibodies detect the specific bands at 45kD, 51kD, 17kD and 89kD respectively with *β*-actin (42kD) used for normalisation. (a) TGF-β1 was elevated significantly in MCAo(contra), by 1.71 ± 0.08 fold when compared with the sham. Post-ischemic exercise increased the TGF-β1 level in the ipsilateral cortices by 1.55 ± 0.05 fold. (b) Smad7 can be increased in both ipsilateral and contralateral cortices with brain ischemia by 1.50 ± 0.09 and 1.43 ± 0.10 fold respectively in contrast with the sham-operated rats. And post-ischemic exercise could significantly reduce the protein expression by 1.03 ± 0.07 fold in the ipsilateral cortices when compared with the MCAo rats. (c) Caspase-3 activation was elevated in the ipsilateral cortices of the MCAo rats by 2.84 ± 0.27 fold, and this elevation was down-regulated with post-ischemic exercise to 0.94 ± 0.04 fold. (d) Increased cleaved PARP protein levels were recorded in both ipsilateral and contralateral cortices by 1.50 ± 0.09 and 1.44 ± 0.13 fold respectively in the animals with MCAo. PARP protein levels increment seen in ischemic cortices were reduced after post-ischemic exercise in both ipsilateral and contralateral cortices at varying degree. All data were analysed with One way ANOVA, Tukey's Multiple Comparison Test with *p-value<0.05 and **p-value<0.01.

3.2.6.2 Effects of exercise and brain ischemia on TGF-β1 protein expression

These confocal images in Fig. 22 depicted the parietal cortex (bregma -2.0 to -5.0mm ± 0.5mm) under different experimental conditions. The tissues were double stained with TGF-β1 (red) and NeuN (green) antibodies. Sham rats are displayed in Fig. 22A to C and sham-runner rats are presented in Fig. 22D to F. The ipsilateral and contralateral cortices of the MCAo rats are shown in Fig. 22G to I and Fig. 22J to L respectively. The ipsilateral and contralateral cortices of MCAo-runner rats are exhibited in Fig. 22M to O and Fig. 22P to R respectively.

Constitutively, punctated staining of cortical TGF-β1 expression was observed in the sham rats (Fig. 22A to C). In the sham-runner rats (Fig. 22D to F), the TGF-β1 expression following eight weeks of regimented treadmill exercise retained a punctated staining pattern albeit more diffused, and were present in some NeuN labeled neurons. At the same time, some TGF-β1 immunoreactive structures that resembled vasculatures were demarcated evidently by the punctated staining pattern of the TGF-β1 [Fig. 22D and F (refer to white arrow)].

In the ipsilateral cortices of the MCAo rats (Fig. 22G to I), the immunoreactivity patterns of the TGF-β1 appeared to be diffused in the immediate periphery of the injury site and much coarse when further away the insulted region. Otherwise, TGF-β1s were found within some of the NeuN labeled neurons regardless of the distance from the insulted

area. In the contralateral cortices of the MCAo rats (Fig. 22J to L), TGF-β1 expressions were also detected in a punctated fashion comparable to the outer zone of the injury site in the ipsilateral cortices.

TGF-β1 expression in the ipsilateral cortices of MCAo-runner rats (Fig. 22M to O) appeared to be reduced in staining intensity when compared to the MCAo rats. While the punctated TGF-β1 expression observed in the contralateral cortices of MCAo-runner rats (Fig. 22P to R) seemed to be further intensfied.

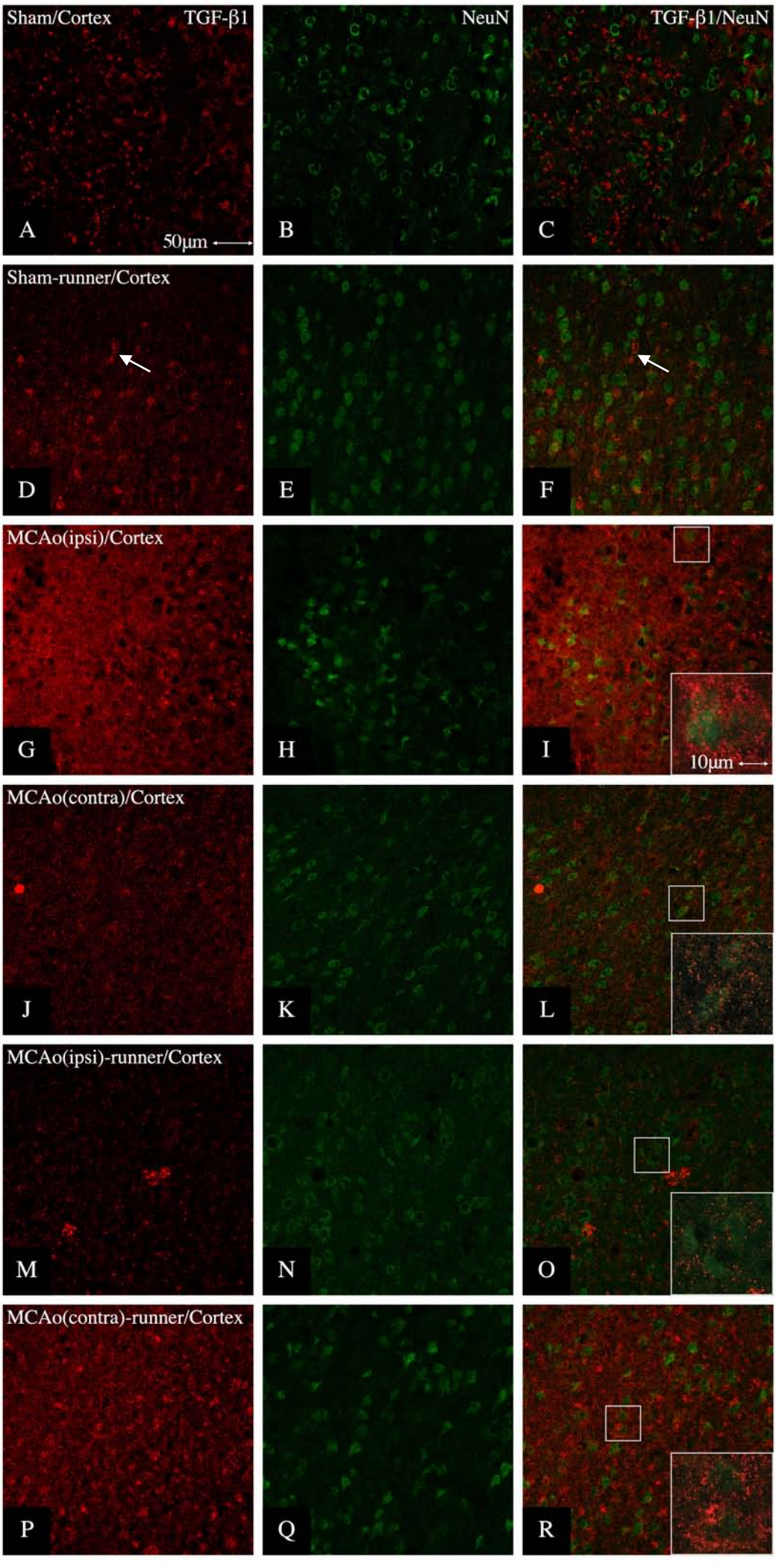
Sham/Cortex
TGF-β1
NeuN
TGF-β1/NeuN
A
50μm
B
C
Sham-runner/Cortex
D
E
F
MCAo(ipsi)/Cortex
G
H
I
10μm
MCAo(contra)/Cortex
J
K
L
MCAo(ipsi)-runner/Cortex
M
N
O
MCAo(contra)-runner/Cortex
P
Q
R

Fig. 22. Double staining of TGF-β1 and NeuN in cortices. These brain sections are from sham-operated or MCAo rats following eight weeks with or without forced treadmill exercise. These confocal images depict the parietal cortex at bregma -2.0 to -5.0mm ± 0.5mm under different experimental conditions. The tissues are double stained with TGF-β1 (red) and NeuN (green). TGF-β1 expressions appear to be more diffused comparing with sham rats following forced treadmill exercise. Experimental MCAo enhances TGF-β1 immunoreactivities in the ipsilateral cortices. However, forced exercise following brain ischemia, seem to reduce TGF-β1 immunoreactivities in the ipsilateral cortices and increase in the opposite sides.

3.2.6.3 Effects of exercise and brain ischemia on staining profile of smad7 protein expression

These confocal images in Fig. 23 depicted the parietal cortex (bregma -2.0 to -5.0mm ± 0.5mm) under different experimental conditions. The tissues were double stained with smad7 (red) and NeuN (green). Sham rats are displayed in Fig. 23A to C and sham-runner rats are presented in Fig. 23D to F. The ipsilateral and contralateral cortices of MCAo rats are shown in Fig. 23G to I and Fig. 23J to L respectively. The ipsilateral and contralateral cortices of MCAo-runner rats are exhibited in Fig. 23M to O and Fig. 23P to R respectively.

In sham rats (Fig. 23A to C), punctated staining patterns of smad7 were observed in the cortices. Following eight weeks of regimented treadmill exercise, the smad7 expressions in the sham-runner rats (Fig. 23D to F) were marginally increased and displayed an even staining pattern in some NeuN labeled neurons.

In the ipsilateral and contralateral cortices of the MCAo rats (Fig. 23G to I and Fig. 23J to L), the distribution of the smad7 in the cortex was observed with punctated staining pattern. In the immediate periphery of the injury site (only ipsilateral cortex), some co-localisation of smad7 with NeuN positive neurons were observed.

In the ipsilateral cortices of the MCAo-runner rats (Fig. 23M to O), the stainings of the smad7 in the cortices seemed less intense, but co-localisation of smad7 with NeuN neurons were more widespread than that of MCAo rats. The contralateral cortices of the MCAo-runner rats (Fig. 23P to R) paralleled observations made in MCAo rats.

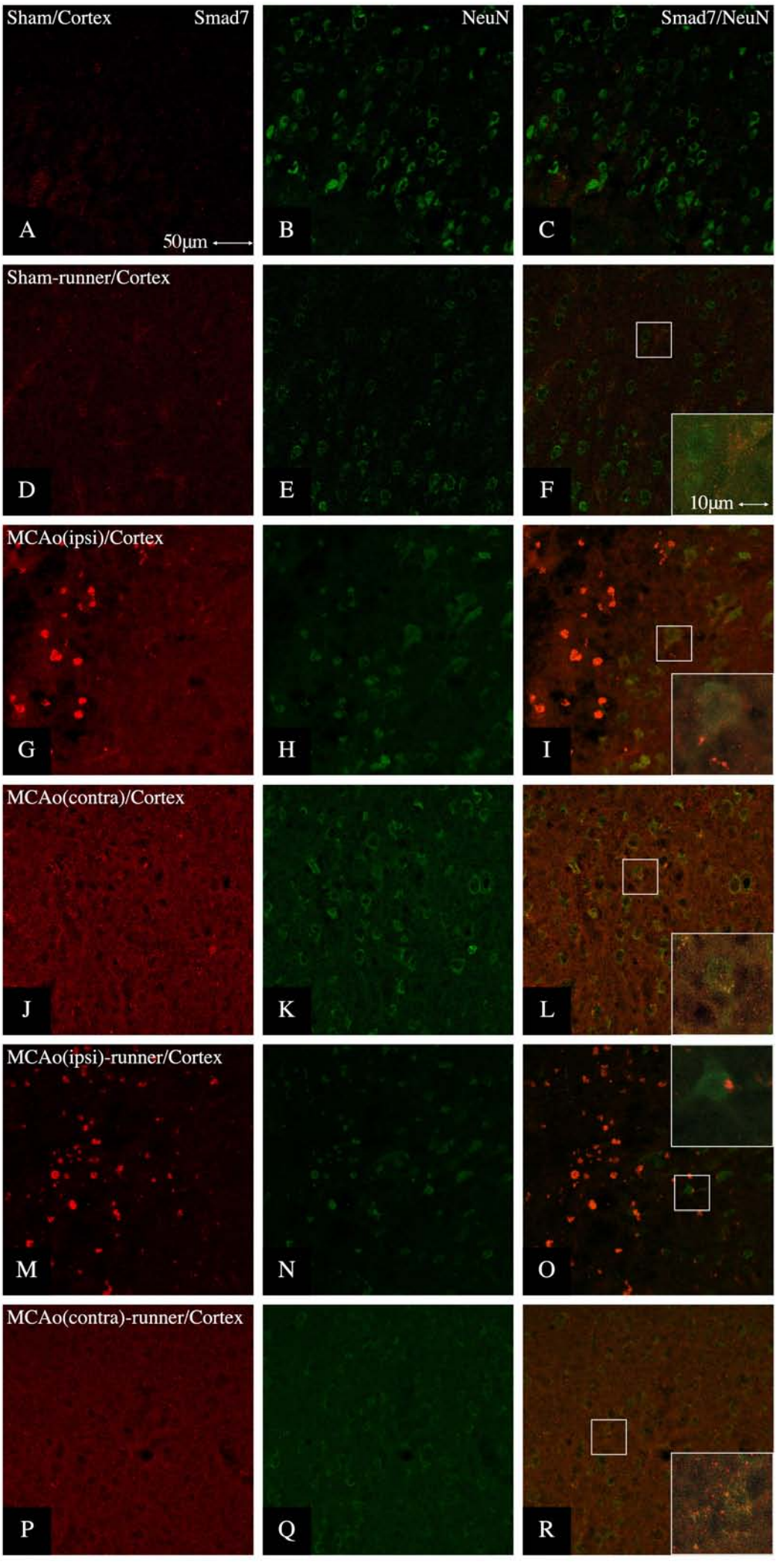
Sham/Cortex
Smad7
NeuN
Smad7/NeuN
A
50μm
B
C
Sham-runner/Cortex
D
E
F
10μm
MCAo(ipsi)/Cortex
G
H
I
MCAo(contra)/Cortex
J
K
L
MCAo(ipsi)-runner/Cortex
M
N
O
MCAo(contra)-runner/Cortex
P
Q
R

Fig. 23. Double staining of smad7 and NeuN in cortices. Brain sections are taken from sham-operated or MCAo rats following eight weeks with or without forced treadmill exercise. These confocal images depict the parietal cortex at bregma -2.0 to -5.0mm ± 0.5mm under different experimental conditions. The tissues are double stained with smad7 (red) and NeuN (green). Smad7 expressional intensities in sedentary sham-operated rats are slightly increased following forced exercise. Smad7 are evidently seen at the border of compromised cortical regions co-localised with NeuN positive neurons in MCAo rats with or without forced exercise. Interestingly, the width of the regions where smad7 are co-localised with NeuN neurons seem to be greater than before the exercise regime imposed.

3.2.6.4 Effects of exercise and brain ischemia on TUNEL staining

These confocal images in Fig. 24 display tissues from the parietal cortices (bregma -2.0 to -5.0mm ± 0.5mm) double stained with TUNEL (green) and NeuN (red) which were subjected to different experimental conditions. Respectively, sham and sham-runner rats are displayed in Fig. 24A to C and Fig. 24D to F. The ipsilateral and contralateral cortices of MCAo rats are shown in Fig. 24G to I and Fig. 24J to L respectively. The ipsilateral and contralateral cortices of MCAo-runner rats are exhibited in Fig. 24M to O and Fig. 24P to R respectively.

TUNEL staining was negative in sham rats (Fig. 24A to C) and sham-runner rats (Fig. 24D to F), contralateral cortices of the MCAo rats (Fig. 24J to L) and contralateral cortices of the MCAo-runner rats (Fig. 24P to R). In the ipsilateral cortices of the MCAo rats (Fig. 24G to I), residing in the borders of ischemic regions, positive TUNEL staining was detected and co-localised with NeuN labeled neurons. Paradoxically, positive TUNEL staining co-localised with NeuN labeled neuron was more pronounced in the ipsilateral cortices of the MCAo-runner rats (Fig. 24M to O) in contrast to sedentary group with brain ischemia.

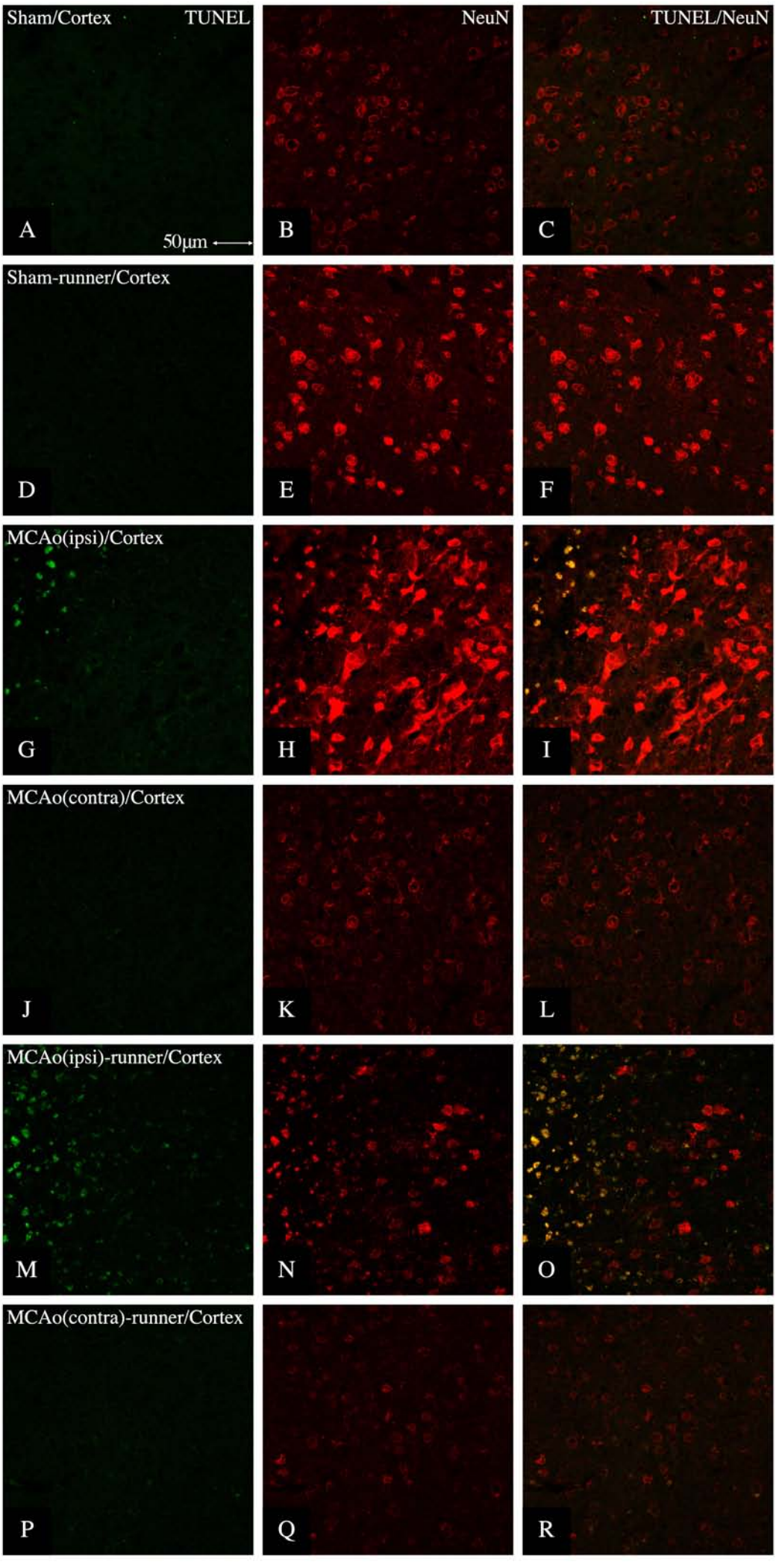
Sham/Cortex
TUNEL
NeuN
TUNEL/NeuN
A
50μm
B
C
Sham-runner/Cortex
D
E
F
MCAo(ipsi)/Cortex
G
H
I
MCAo(contra)/Cortex
J
K
L
MCAo(ipsi)-runner/Cortex
M
N
O
MCAo(contra)-runner/Cortex
P
Q
R

Fig. 24. Double staining of TUNEL and NeuN in cortices. The brain tissues are sectioned from either sham-operated or MCAo rats following eight weeks with or without forced treadmill exercise. These confocal images depict the parietal cortex at bregma -2.0 to -5.0mm ± 0.5mm under different experimental conditions. The tissues are double stained with TUNEL (green) and NeuN (red). Positive TUNEL staining is detected next to borders of the insulted cortices in the MCAo rats. Ironically, TUNEL stainings have their regional width augmented in the MCAo-runner rats following post-ischemic exercise when comparing to the same side of cortices from the MCAo rats.

3.2.7 Changes to expression profile of angiogenic factors in hippocampus following forced treadmill exercise

All animals were sacrificed at ten weeks (includes trainings and eight weeks of actual exercise regime) with two days wash-out period after the last run.

3.2.7.1 Effects of exercise on angiogenic factors' mRNA and protein expression

HIF-1α mRNA expression was recorded with an upward trend by 1.67 ± 0.42 fold following eight weeks of forced treadmill exercise in the sham-runner rats when compared with the sham rats however the difference was not statistically significant (Fig. 25a).

VEGF mRNA expression was documented at 1.38 ± 0.38 fold following eight weeks of forced treadmill exercise in the sham-runner rats in contrast to the sham rats but was not statistically significant (Fig. 25b).

Prolonged forced treadmill exercise in the sham-runner rats, shown in Fig. 25c, increased VEGFR2 mRNA expression by 2.07 ± 0.91 fold as compared with the sham rats however increment was not statistically significant.

Following eight weeks of forced treadmill exercise in the sham-runner rats, PDGFB mRNA expressions were significantly increased by 1.53 ± 0.16 fold as compared with the sham rats, p-value<0.05 (Fig. 25d).

PDGFRB mRNA expressions increased by 2.58 ± 0.35 fold following eight weeks of forced treadmill exercise in the sham-runner rats when compared with the sham rats, p-value<0.05 (Fig. 25e).

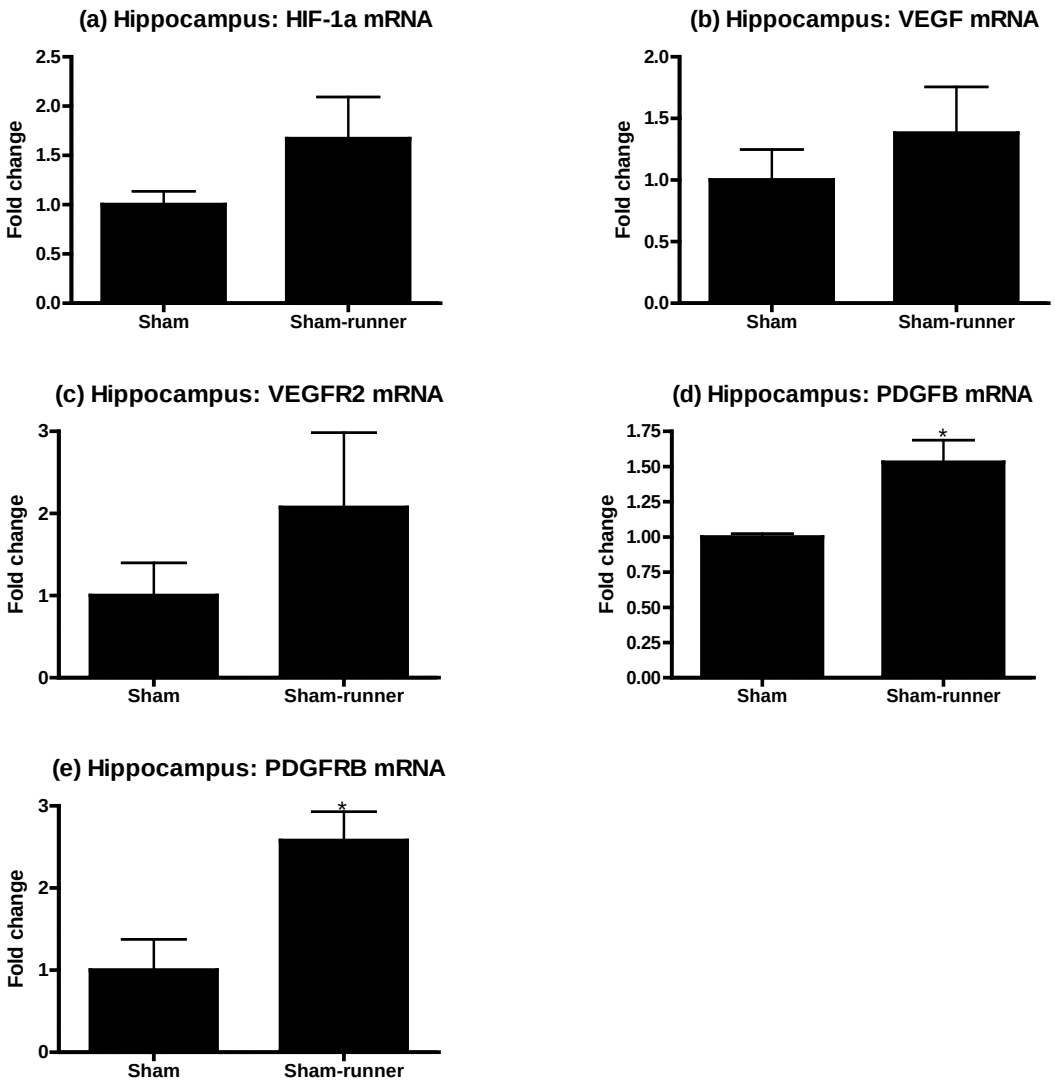

Fig. 25. mRNA expressions of HIF-1α and angiogenic factors in the hippocampus. Changes in mRNA levels were evaluated by quantitative real-time PCR following eight weeks forced treadmill exercise. The increased of the HIF-1α, VEGF and VEGFR2 mRNAs from the sham-runner rats in comparison to sedentary rats was not significant (a, b and c respectively). Significant up-regulation of PDGFB and PDGFRB mRNAs were recorded in the sham-runner rats at 1.53 ± 0.16 and 2.58 ± 0.35 folds respectively when compared with the sham rats (d and e respectively). All data were analysed using unpaired t-test with *p-value<0.05.

HIF-1α protein expressions were considerably up-regulated by 1.82 ± 0.24 fold following eight weeks of forced treadmill exercise in the sham-runner rats and when compared with the sham rats, *p-value<0.05 (Fig. 26a).

PDGFB protein expressions were up-regulated by 1.30 ± 0.03 fold following eight weeks of forced treadmill exercise in the sham-runner rats as compared with the sham rats, **p-value<0.01 (Fig. 26b). All data were analyzed with unpaired t-test.

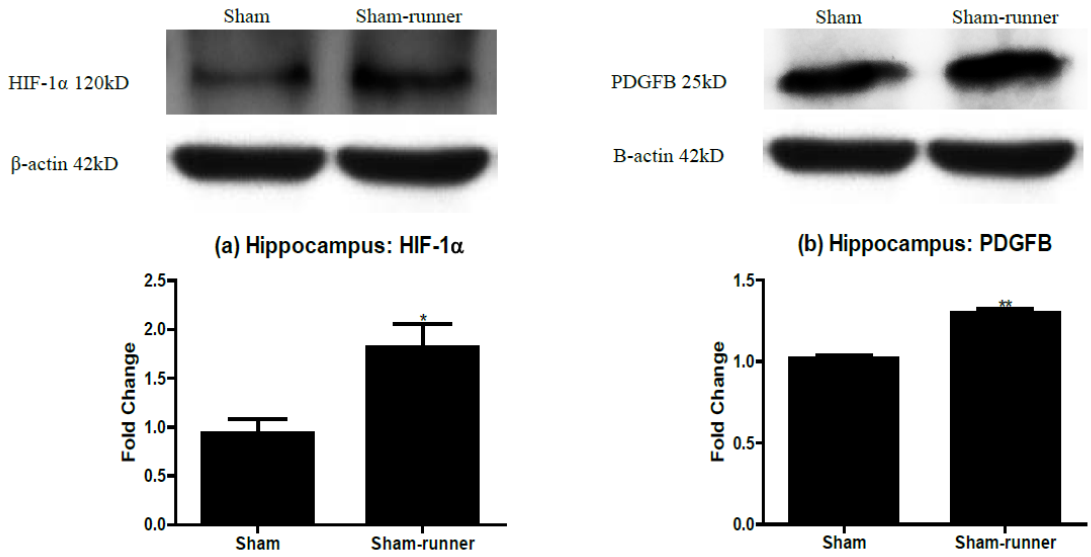

Fig. 26. HIF-1α and PDGFB protein expressions in the hippocampus. The HIF-1α and PDGFB antibodies detect the band at 120kD and 25kD respectively with *β*-actin at 42kD as the housekeeping protein. Changes in HIF-1α (a) and PDGFB (b) protein levels were recorded with statistically significant increase at 1.82 ± 0.24 and 1.30 ± 0.03 fold respectively in the sham-runner rats when compared with the sham rats. All data were analysed using unpaired t-test with *p-value<0.05 and **p-value<0.01.

3.2.8 Angiogenic factors and angiogenesis in cortex

All animals assigned to either exercise or sedentary groups were sacrificed at ten weeks post-surgery (include the total time allocated for trainings and eight weeks of actual exercise regime for the runner groups), with two days wash-out period after the last run, with or without MCAo.

3.2.8.1 Effects of exercise on angiogenic factors' mRNA and protein expression

The whole ipsilateral hemispheres of the cerebral cortices were used for the analysis of mRNA and protein expressions in all groups with additional examination of whole contralateral hemispheres for both MCAo and MCAo-runner rats. As shown in Fig. 27a, HIF-1α mRNA expressions showed a slight upward trend following eight weeks of forced treadmill exercise in the sham-runner rats (1.23 ± 0.08 fold) as compared with the sham rats. HIF-1α mRNA expression recorded a significant downward trend in both ipsilateral and contralateral cortices of the MCAo rats (0.46 ± 0.02 and 0.50 ± 0.05 fold respectively) in contrast to the sham rats, p-value<0.01. Eight weeks of post-ischemic forced treadmill exercise did not yield significant change to the HIF-1α mRNA expression which remained comparable with MCAo rats.

Fig. 27b illustrated that neither prolonged forced exercise nor brain ischemia had any significant effect on VEGF mRNA expression. VEGF mRNAs were calculated at 0.91 ± 0.04 fold in the sham-runner rats and were worked out at 1.00 ± 0.28 and 0.88 ± 0.09 fold

in both ipsilateral and contralateral cortices of the MCAo rats respectively. These results from both groups were not statistically significant when compared with the sham rats. Following eight weeks of post-ischemic forced treadmill exercise, VEGF mRNA expressions in both ipsilateral and contralateral cortices of the MCAo-runner rats were evaluated at 0.61 ± 0.10 and 0.99 ± 0.17 fold respectively which were comparable to the MCAo rats. Even though there was marginal down-regulation seen in the ipsilateral cortices, the change was not statistically significant.

VEGFR2 mRNA expressions (Fig. 27c) were calculated at 1.77 ± 0.35 fold following eight weeks of forced treadmill exercise in the sham-runner rats, and were recorded at 1.06 ± 0.01 and 1.16 ± 0.003 fold in both ipsilateral and contralateral cortices of the MCAo rats respectively, however these observations were not statistically significant when compared with the sham rats. Subsequent to eight weeks of post-ischemic forced treadmill exercise, VEGFR2 mRNA expressions in both ipsilateral and contralateral cortices of the MCAo-runner rats were determined at 1.03 ± 0.14 and 1.05 ± 0.12 fold respectively which were comparable with the MCAo rats.

PDGFB mRNA expressions were significantly increased by 1.46 ± 0.10 fold following eight weeks of forced treadmill exercise in the sham-runner rats as compared with the sham rats, p-value<0.01 (Fig. 27d). In the MCAo rats, PDGFB mRNA expression were evaluated at 1.59 ± 0.08 and 1.51 ± 0.06 fold in both ipsilateral and contralateral cortices respectively when compared with the sham rats, p-value<0.01. PDGFB mRNA

expression, following eight weeks of post-ischemic forced treadmill exercise, in both ipsilateral and contralateral cortices of the MCAo-runner rats were determined at 0.79 ± 0.09 and 1.19 ± 0.02 fold. Notably, PDGFB mRNA expression in the ipsilateral cortices of the MCAo-runner rats were decreased when compared with the same cortices in the MCAo rats with p-value<0.01.

Fig. 27e showed that PDGFRB mRNA expressions were calculated at 0.79 ± 0.11 fold following eight weeks of forced treadmill exercise in the sham-runner rats as compared with the sham rats. PDGFRB mRNA expression under ischemia (MCAo rats) were recorded at 1.60 ± 0.15 and 1.75 ± 0.27 fold in both ipsilateral and contralateral cortices respectively as compared with the sham rats. Although changes were observed following either forced exercise or brain ischemia, these alterations were not statistically significant when compared with the sham rats. PDGFRB mRNA expression, following eight weeks of post-ischemic forced treadmill exercise, in the ipsilateral cortices of the MCAo-runner rats were further increased by 2.82 ± 0.75 fold but remained at 1.68 ± 0.21 fold in contralateral cortices of the MCAo-runner rats. However, the change in the ipsilateral cortices was not statistically significant in contrast with the MCAo rats.

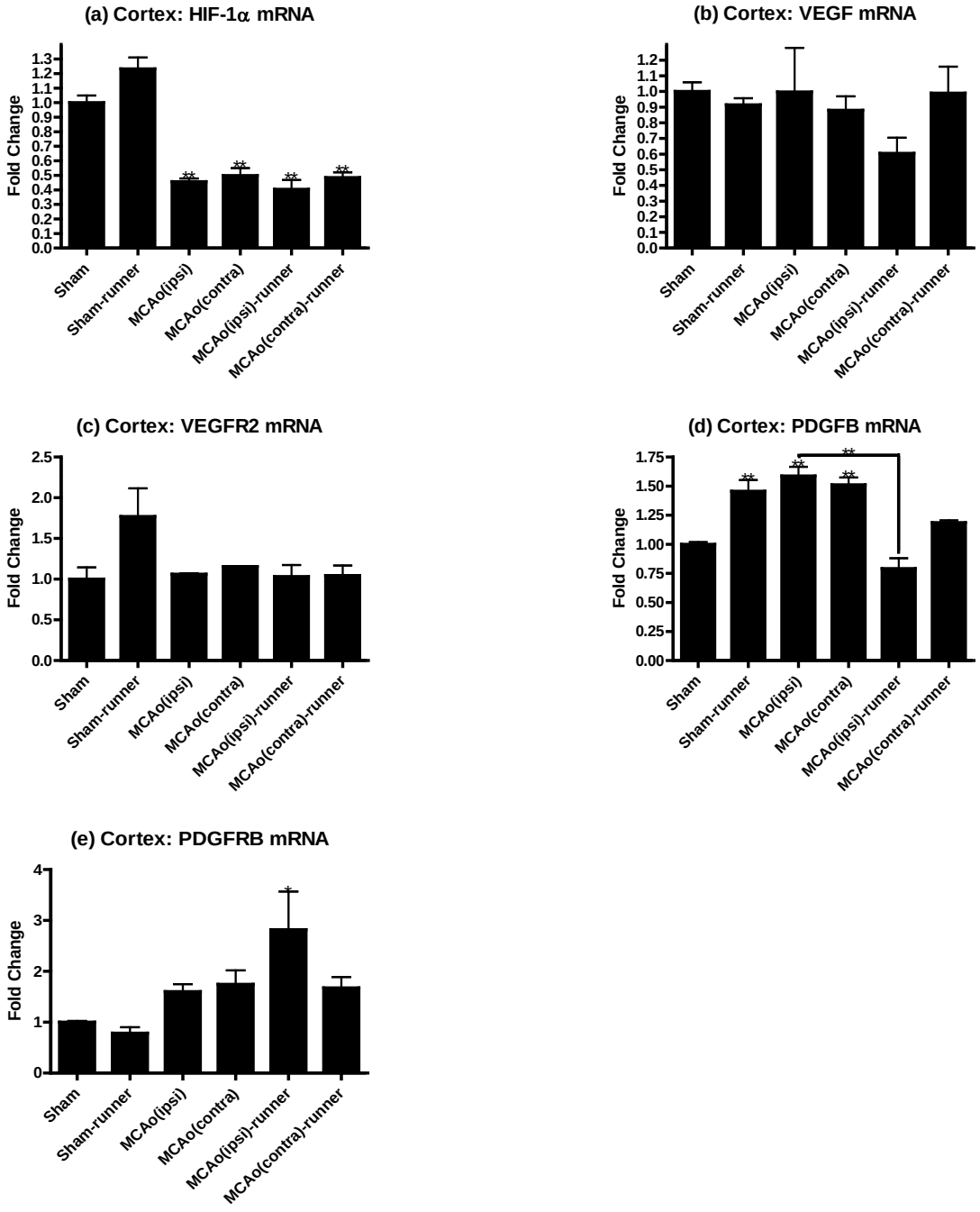

Fig. 27. mRNA expressions of HIF-1α and angiogenic factors in the cortex. Changes to mRNA levels in either whole ipsilateral or whole contralateral hemispheres of the cerebral cortices were evaluated by quantitative real-time PCR. (a) Long term forced exercise show increase HIF-1α mRNA expression in the sham-runner but the change is not statistically significant. Post-MCAo show that HIF-1α mRNA levels are down-regulated significantly by 0.46 ± 0.02 and 0.50 ± 0.05 fold in the ipsilateral and contralateral hemispheres respectively as compared to the sham. Post-ischemic exercise did not have any influence on the HIF-1α mRNA which remained at 0.40 ± 0.06 and 0.48 ± 0.04 fold in the ipsilateral and contralateral hemispheres respectively following

experimental ischemia. (b) The data showed that prolonged period of forced exercise did not have any effect on the expression of VEGF mRNA under both ischemic and non-ischemic conditions. (c) An upward trend was observed in the VEGFR2 mRNA expression following forced treadmill exercise (sham-runner) albeit non-significant. Experimental brain ischemia did not have any observable effect on the VEGFR2 mRNA and remained at post-MCAo's level in the MCAo-runner rats. (d) Expression of PDGFB mRNA was up-regulated significantly after subjected to prolonged period of increased physical activities by 1.46 ± 0.10 fold and permanent ischemia by 1.59 ± 0.08 and 1.51 ± 0.06 fold in both ipsilateral and contralateral hemispheres respectively. Post-ischemic exercise brought down the PDGFB mRNA levels in the ipsilateral cortices significantly to 0.79 ± 0.09 fold as compared to the same cortices of the MCAo rats. (e) Upward trend of PDGFRB mRNA levels observed in the MCAo rats was not statistically significant. However PDGFRB mRNA expressions were further increased after post-ischemic exercise and the increase was statistically significant. Post-ischemic exercise did not produce any significant increase in PDGFRB mRNA expression. All data were analysed with One way ANOVA, Tukey's Multiple Comparison Test with *p-value<0.05 and **p-value<0.01.

Illustrated in Fig. 28a, HIF-1α protein expressions following eight weeks of forced treadmill exercise in the sham-runner rats were calculated at 1.17 ± 0.05 fold which was not statistically significant as compared with the sham rats. Ipsilateral cortices of the MCAo rats worked out a considerable up-regulation of HIF-1α protein expression recorded at 1.51 ± 0.09 fold and with p-value<0.01 when compared with the sham rats. Though the contralateral cortices of the MCAo rats were determined at 1.22 ± 0.05 fold, the changes were not statistically significant in contrast with the sham rats. Following eight weeks of post-ischemic forced treadmill exercise, HIF-1α protein expression in both ipsilateral and contralateral cortices of the MCAo-runner rats were measured at 1.55 ± 0.08 and 0.90 ± 0.11 fold respectively which was not statistically significant when compared with the MCAo rats.

In Fig. 28b, PDGFB protein expressions following eight weeks of forced treadmill exercise in the sham-runner rats were worked out at 1.20 ± 0.07 fold and this alteration was not statistically significant in contrast to the sham rats. PDGFB protein expressions in both ipsilateral and contralateral cortices of the MCAo rats were calculated at 0.77 ± 0.09 and 1.17 ± 0.09 respectively was also not statistically significant when compared with the sham rats. PDGFB protein expressions, following eight weeks of post-ischemic forced treadmill exercise, in the ipsilateral cortices of the MCAo-runner rats were recorded with a significant increase by 1.43 ± 0.11 fold, while the contralateral cortices of the MCAo-runner rats were documented at 1.30 ± 0.12 fold. Interestingly, PDGFB protein expressions in the ipsilateral cortices of the MCAo-runner rats were increased when

compared with the same cortices in the MCAo rats, p-value<0.01. All data were analyzed with One way ANOVA, Tukey's Multiple Comparison Test.

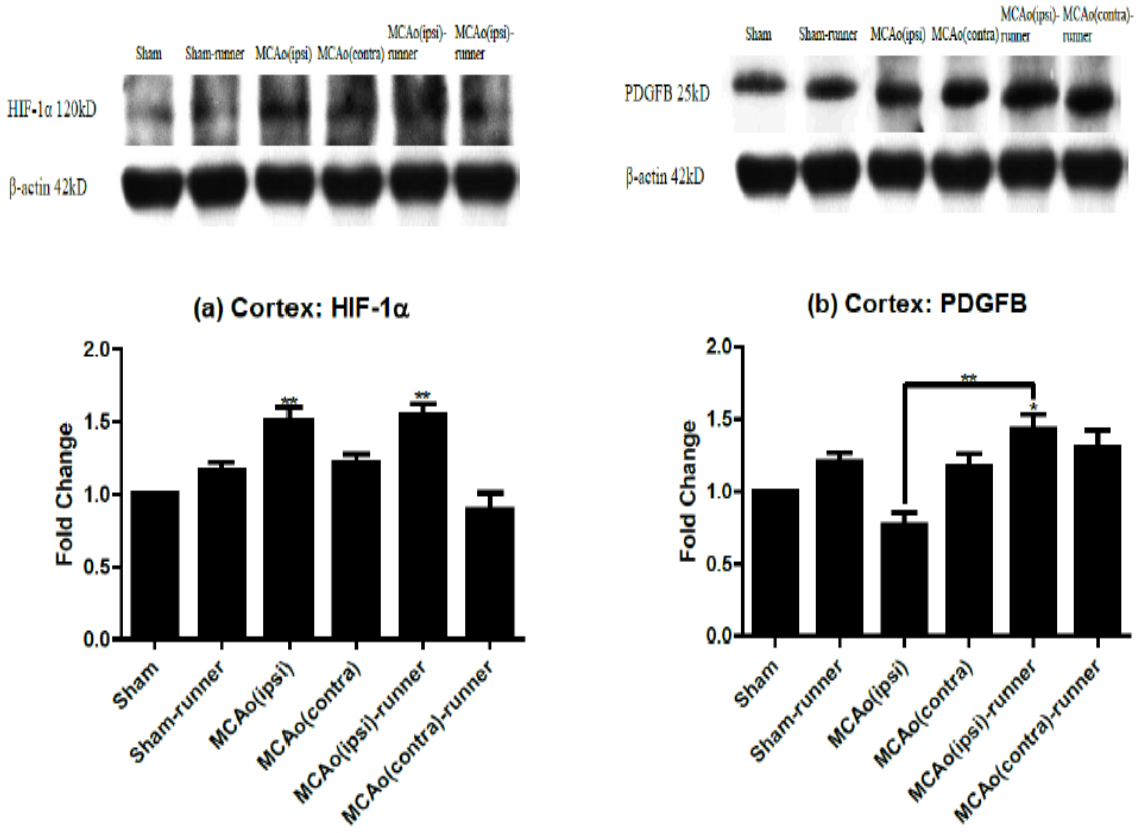

Fig. 28. HIF-1α and PDGFB protein expressions in the cortex. The HIF-1α and PDGFB antibodies detect the band at 120kD and 25kD respectively with housekeeping β-actin at 42kD. Changes to protein levels in either whole ipsilateral or whole contralateral hemispheres of the cerebral cortices were semi-quantified using Western blot. (a) An upward trend of the HIF-1α protein expression is documented in the sham-runner but the change is non-significant. Considerable increase in the level of HIF-1α protein expression is determined in the ipsilateral cortices of MCAo rats at 1.51 ± 0.09 fold, and post-ischemic exercise did not alter this elevation which remained at 1.55 ± 0.08 fold. (b) PDGFB protein level is increased significantly to 1.43 ± 0.11 fold in the ipsilateral cortices in the MCAo-runner rats when compared with ipsilateral cortices of the MCAo rats. All data were analysed with One way ANOVA, Tukey's Multiple Comparison Test with *p-value<0.05 and ** p-value<0.01.

3.2.8.2 Effects of forced treadmill exercise and brain ischemia on Pecam-1 expression

These confocal images in Fig. 29 depicted the parietal cortex (bregma -2.0 to -5.0mm ± 0.5mm) under different experimental conditions. The tissues were double stained with Pecam-1 (green) and DAPI (blue). Sham rats are displayed in Fig. 29A to C and sham-runner rats are presented in Fig. 29D to F. The ipsilateral and contralateral cortices of MCAo rats are shown in Fig. 29G to I and Fig. 29J to L respectively. The ipsilateral and contralateral cortices of MCAo-runner rats are exhibited in Fig. 29M to O and Fig. 29P to R respectively.

Basal level of Pecam-1 was observed in sham rats (Fig. 29A to C). In comparison with the sedentary group, sham-runner rats displayed a striking increase in Pecam-1 expressions (Fig. 29D to F). Following prolonged ischemic insult, Pecam-1 was observed in both cortices of the MCAo rats (Fig. 29G to I and Fig. 29J to L) comparable to the basal level seen in sham rats. An increase of Pecam-1 expression was noted in both cortices of the MCAo-runner rats (Fig. 29M to O and in Fig. 29P to R) over the sedentary rats with brain ischemia.

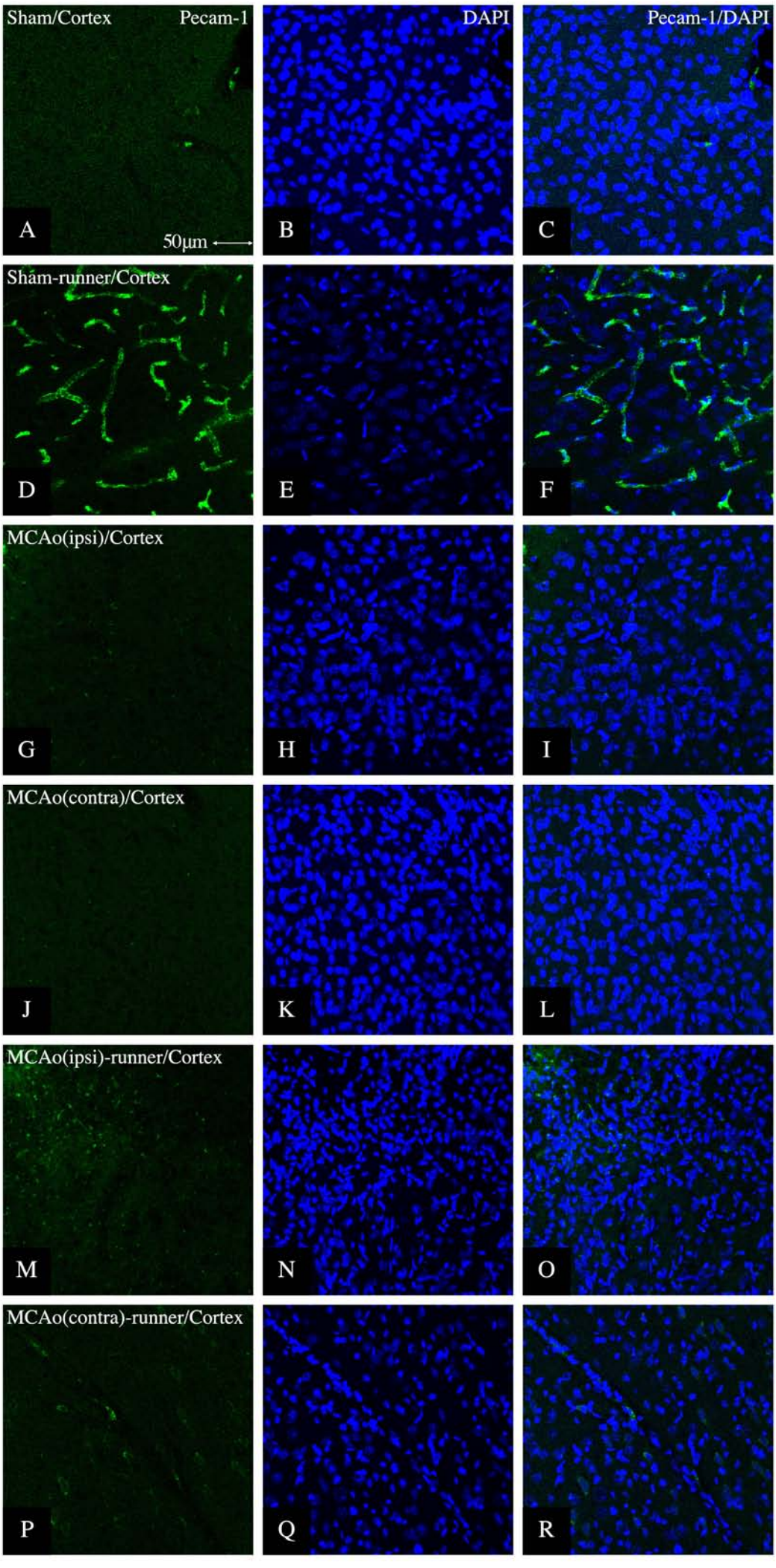
Sham/Cortex
Pecam-1
DAPI
Pecam-1/DAPI
A
50μm
B
C
Sham-runner/Cortex
D
E
F
MCAo(ipsi)/Cortex
G
H
I
MCAo(contra)/Cortex
J
K
L
MCAo(ipsi)-runner/Cortex
M
N
O
MCAo(contra)-runner/Cortex
P
Q
R

Fig. 29. Double staining of Pecam-1 and DAPI in cortex. The brain sections are prepared from either sham-operated or MCAo rats following eight weeks with or without forced treadmill exercise. These confocal images depict the parietal cortex at bregma -2.0 to -5.0mm ± 0.5mm under different experimental conditions. The tissues were double stained with Pecam-1 (green) and DAPI (blue). In the sham-runner rats, Pecam-1 staining profile is very prominent as compared with the basal activity in the sham rats. Post-ischemic exercise is able to modestly increase the staining intensity in both ipsilateral and contralateral cortices of MCAo-runner rats when compared with the MCAo rats.

3.2.9 Erythropoietic factors in hippocampus

All animals were sacrificed at ten weeks (includes trainings and eight weeks of actual exercise regime) with two days wash-out period after the last run.

3.2.9.1 Effects of exercise on erythropoietic factor's protein expression

Eight weeks of forced treadmill exercise (sham-runner rats) up-regulated EPO protein expression by 1.97 ± 0.30 fold as compared with the sham rats, p-value<0.05 (Fig. 30a).

As illustrated in Fig. 30b, EPOR protein expression was increased by 1.63 ± 0.19 fold following eight weeks of forced treadmill exercise in the sham-runner rats in contrast to the sham rats, p-value<0.05. All data were analyzed with unpaired t-test.

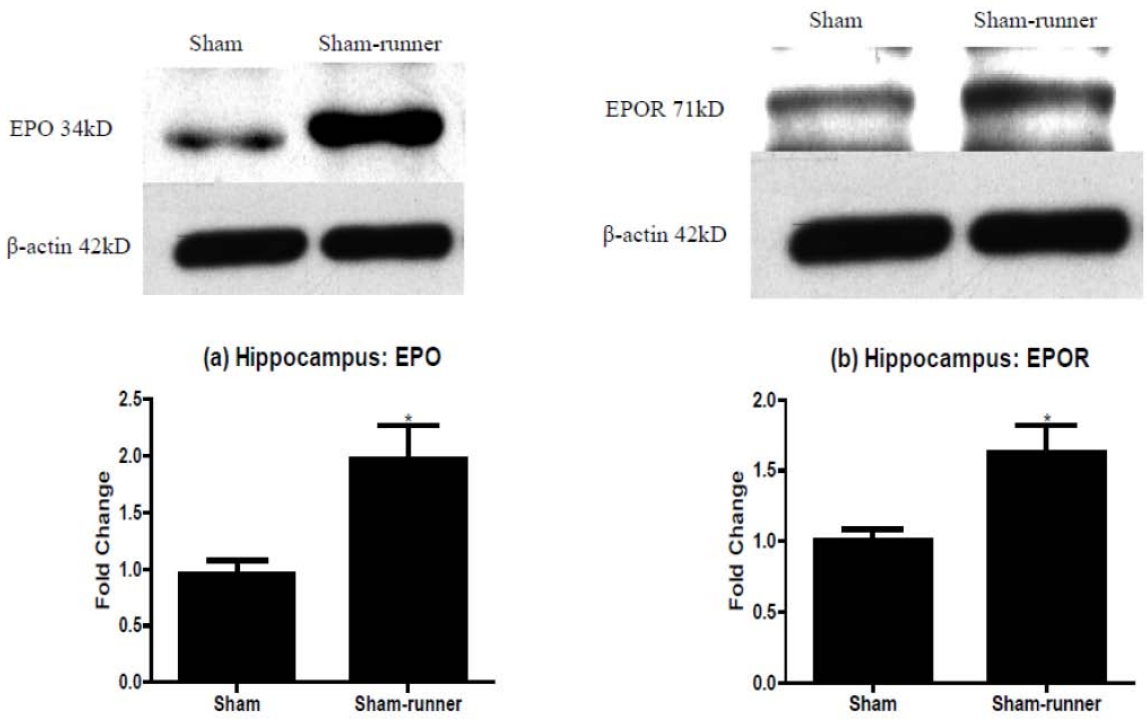

Fig. 30. EPO and EPOR protein expressions in the hippocampus. The EPO and EPOR antibodies detect the bands at 34kD and 71kD respectively with housekeeping β-actin at 42kD. (a) EPO protein levels are up-regulated by 1.97 ± 0.30 fold and (b) EPOR protein expressions are significantly increased by 1.63 ± 0.19 fold in the sham-runner rats when compared with sham rats. All data are analysed using unpaired t-test with *p-value<0.05.

3.2.9.2 Effects of exercise and ischemia on staining profile of erythropoietin (EPO) in the CA1 region

These confocal images in Fig. 31 depicted the CA1 region (bregma -2.0 to -5.0mm ± 0.5mm) under different experimental conditions. In the sham rats (Fig. 31A to C), there was hardly any EPO expression observed in the CA1 region. Following prolonged moderate exercise regime, punctated staining pattern of EPO was detected with some being co-localised with neurons (NeuN) in sham-runner rats' CA1 region (Fig. 31D to F).

Following the footsteps of sham-runner rats, EPO expressions of the MCAo rats were also fashioned in punctated patterns and were observed in some neurons (NeuN) residing in the CA1 region from the ipsilateral hippocampus (Fig. 31G to I). EPO staining in the ipsilateral CA1 region of the MCAo-runner rats (Fig. 31M to O) appeared to be increased both in number and intensity as compared with the ipsilateral region of the MCAo rats.

In the contralateral hippocampi of the MCAo and MCAo-runner rats (Fig. 31J to L and Fig. 31P to R), punctated staining pattern of the EPO were markedly increased in the CA1 and also extensively expressed in the oriens layer and stratum radiatum. Resembling the ipsilateral hippocampi of the MCAo rats, the contralateral CA1s of the MCAo-runner rats appeared to be further enhanced.

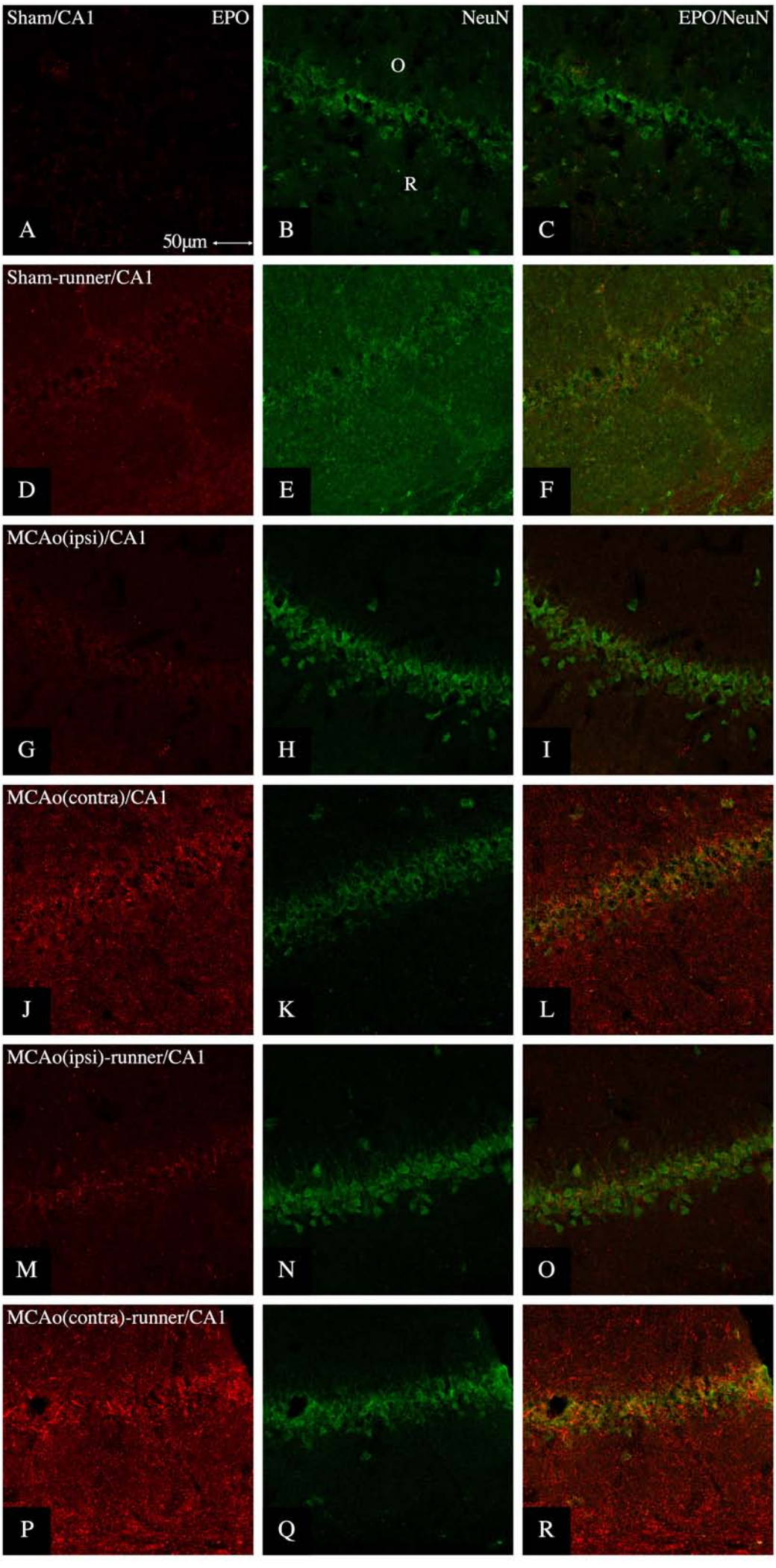
Sham/CA1
EPO
A
50μm
NeuN
O
R
B
EPO/NeuN
C
Sham-runner/CA1
D
E
F
MCAo(ipsi)/CA1
G
H
I
MCAo(contra)/CA1
J
K
L
MCAo(ipsi)-runner/CA1
M
N
O
MCAo(contra)-runner/CA1
P
Q
R

Fig. 31. Double staining of EPO and NeuN in CA1. These are brain sections from either sham-operated or MCAo rats following eight weeks with or without forced treadmill exercise. These confocal images depict CA1 region at bregma -2.0 to -5.0mm ± 0.5mm under different experimental conditions. The tissues were double stained with EPO (red) and NeuN (green). Sham rats' CA1s display basal level of EPO expressions which are seen increase in sham-runner rats. The ipsilateral CA1s of both MCAo and MCAo-runner rats show subdued increment in contrast with their contralateral CA1s where the EPO immunoreactivities are notably higher, in addition, some are co-localised with NeuN labeled neurons. O, oriens layer and R, stratum radiatum.

3.2.9.3 Effects of exercise and ischemia on staining profile of EPO receptor (EPOR) in the CA1 region

These confocal images in Fig. 32 depicted the CA1 (bregma -2.0 to -5.0mm ± 0.5mm) under different experimental conditions. In the sham rats (Fig. 32A to C), EPOR expressions were detected and with some being co-localised with CA1's NeuN labeled neurons. In addition, EPOR expression was also detected in the oriens layer and stratum radiatum. Comparable stainings were seen in the sham-runner rats (Fig. 32D to F).

In both sides of the MCAo rats' hippocampus (Fig. 32G to I), EPOR immunoreactivity appeared to be reduced. EPOR staining in the CA1 region of the MCAo-runner rats (Fig. 32M to O and Fig. 32P to R) was marginally higher when compared with the CA1 region of the MCAo rats. In the contralateral hippocampi of both MCAo and MCAo-runner rats (Fig. 32J to L and), punctated staining pattern of the EPOR were detected in the CA1 neurons and expressed in the oriens layer and stratum radiatum.

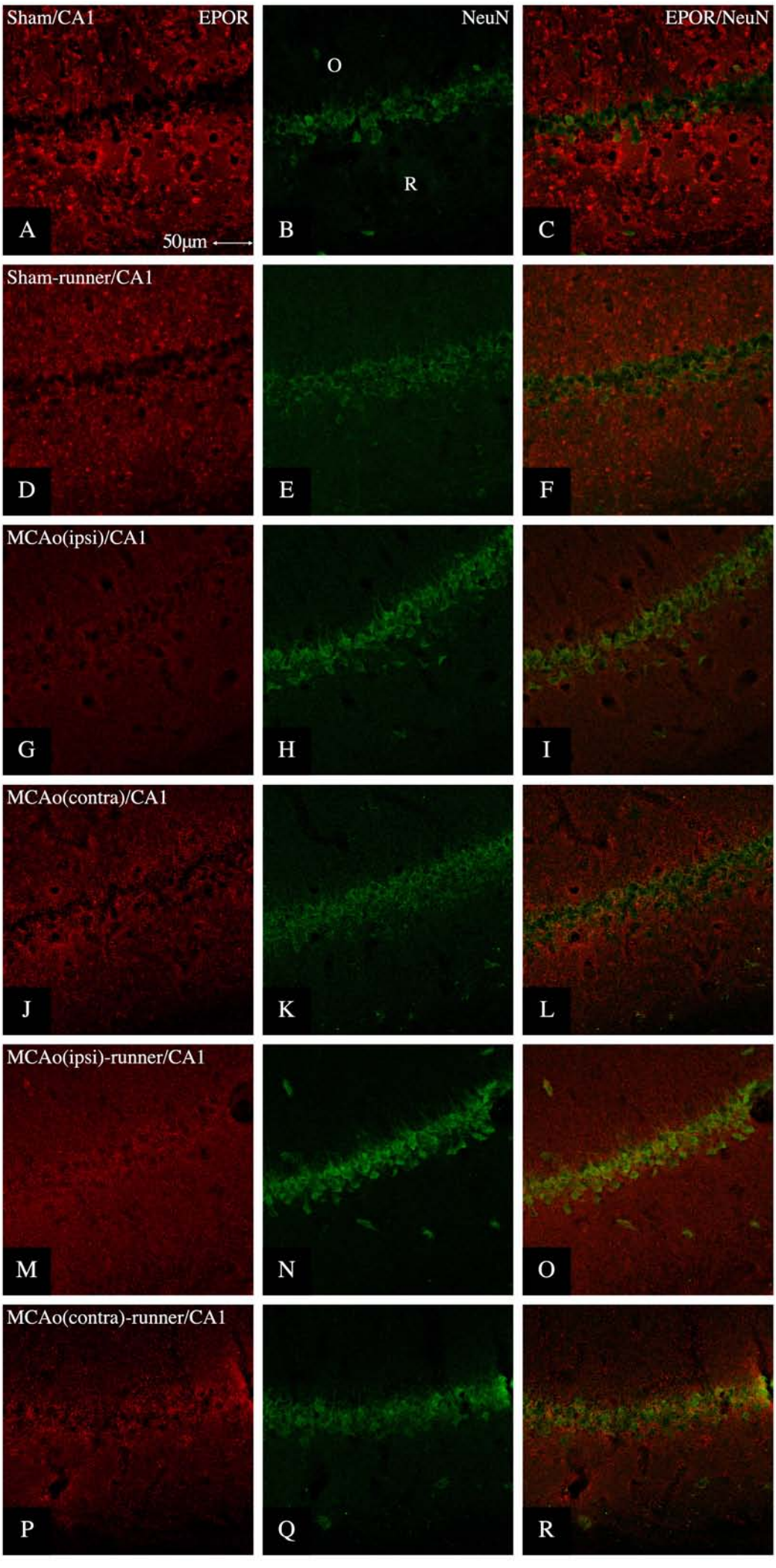
Sham/CA1
EPOR
NeuN
O
R
EPOR/NeuN
A
50μm
B
C
Sham-runner/CA1
D
E
F
MCAo(ipsi)/CA1
G
H
I
MCAo(contra)/CA1
J
K
L
MCAo(ipsi)-runner/CA1
M
N
O
MCAo(contra)-runner/CA1
P
Q
R

Fig. 32. Double staining of EPOR and NeuN in CA1. Brain tissues are sectioned from either sham or MCAo rats following eight weeks with or without forced treadmill exercise. These confocal images depict CA1 region at bregma -2.0 to -5.0mm ± 0.5mm under different experimental conditions. The tissues were double stained with EPOR (red) and NeuN (green). EPOR expressions are comparable between sham and sham-runner rats. EPOR expressions appear to be down-regulated in both ipsilateral and contralateral CA1s of the MCAo rats. Forced running following ischemia seems to up-regulate the EPOR expression in both sides of the CA1s. O, oriens layer and R, stratum radiatum.

3.2.9.4 Effects of exercise and ischemia on staining profile of EPO in the DG

These confocal images in Fig. 33 depicted the DG (bregma -2.0 to -5.0mm ± 0.5mm) under different experimental conditions. EPO expression was hardly detected in the DGs of the sham rats (Fig. 33A to C). However, subsequent to forced treadmill exercise, punctated expressions of EPO were unambiguously observed in the sham-runner rats' DGs (Fig. 33D to F).

In both ipsilateral and contralateral hippocampi of the MCAo and MCAo-runner rats (Fig. 33G to I, Fig. 33J to L, Fig. 33M to O and Fig. 33P to R), instantly recognizable punctated staining pattern of EPO was spotted in a similar fashion as examined in the sham-runner rats. Interestingly, EPO was strongly expressed in the NeuN positive neurons in the ipsilateral DGs of MCAo-runner rats (Fig. 33O).

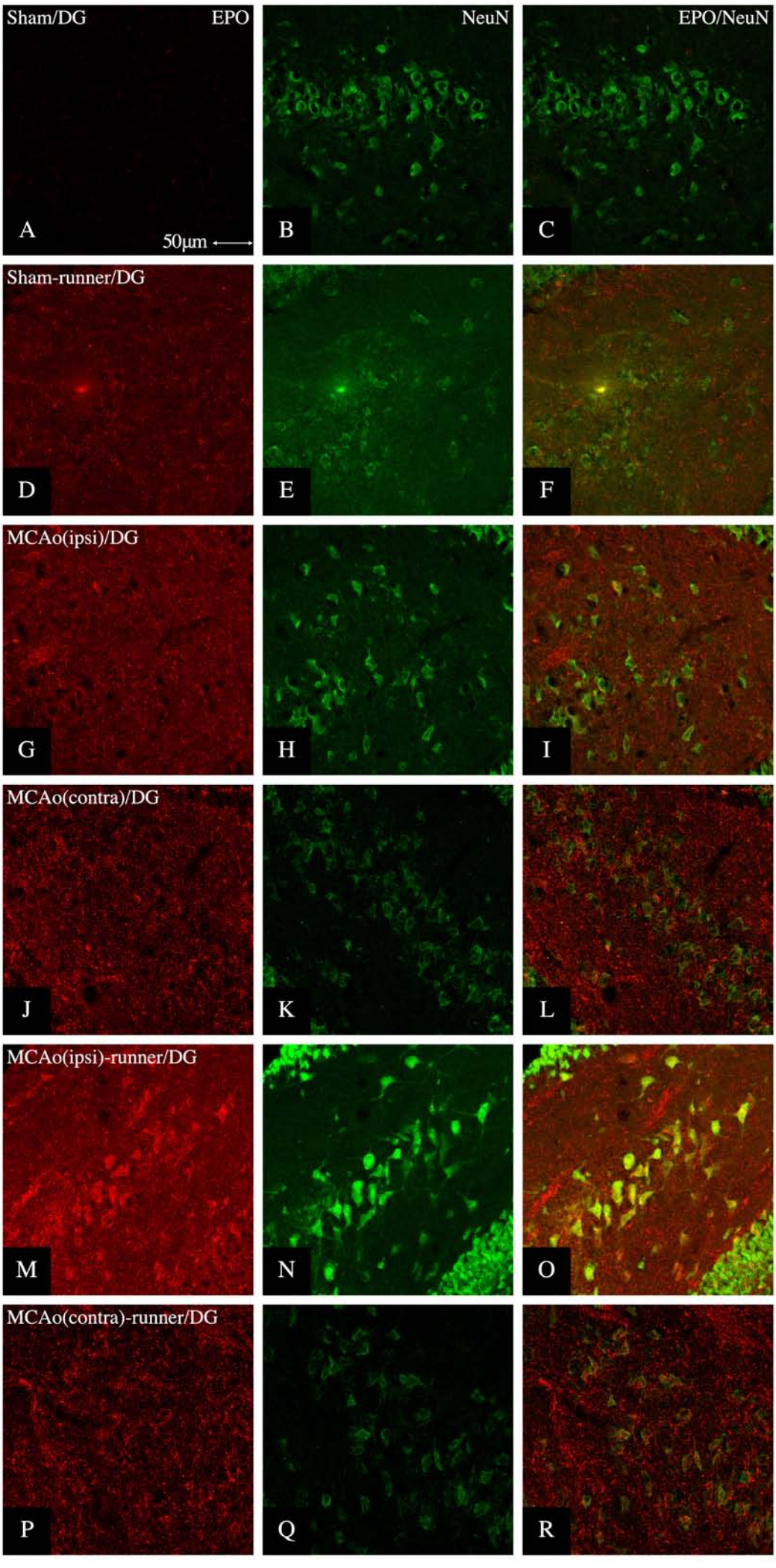
Sham/DG
EPO
A
50μm
NeuN
B
EPO/NeuN
C
Sham-runner/DG
D
E
F
MCAo(ipsi)/DG
G
H
I
MCAo(contra)/DG
J
K
L
MCAo(ipsi)-runner/DG
M
N
O
MCAo(contra)-runner/DG
P
Q
R

Fig. 33. Double staining of EPO and NeuN in DG. Brain sections are taken from either sham-operated or MCAo rats following eight weeks with or without forced treadmill exercise. These confocal images depict the DG at bregma -2.0 to -5.0mm ± 0.5mm under different experimental conditions. The tissues were double stained with EPO (red) and NeuN (green). EPO expression appear to be absent in the sham rats. The EPO expression is increased following both exercise and brain ischemia independently or in combination. EPO are prominently expressed in neurons of the ipsilateral DGs following forced exercise.

3.2.9.5 Effects of exercise and ischemia on staining profile of EPOR in the DG

These confocal images in Fig. 34 depicted the DG (bregma -2.0 to -5.0mm ± 0.5mm) under different experimental conditions. In the sham rats (Fig. 34A to C), EPOR expression was detected in the DG with some being co-localised with NeuN positive neurons. Eight weeks of regimented treadmill exercise appeared to marginally reduced EPOR immunoreactivities in DG of the sham-runner rats (Fig. 34D to F).

Insulted ipsilateral side from MCAo (Fig. 34G to I) and MCAo-runner (Fig. 34M to O) rats demonstrated mild EPOR immunoreactivities in their DGs. Control contralateral side of the MCAo (Fig. 34J to L) and MCAo-runner DGs (Fig. 34P to R) showed marginally higher immunoreactivities of EPOR when compared to the ischemic side.

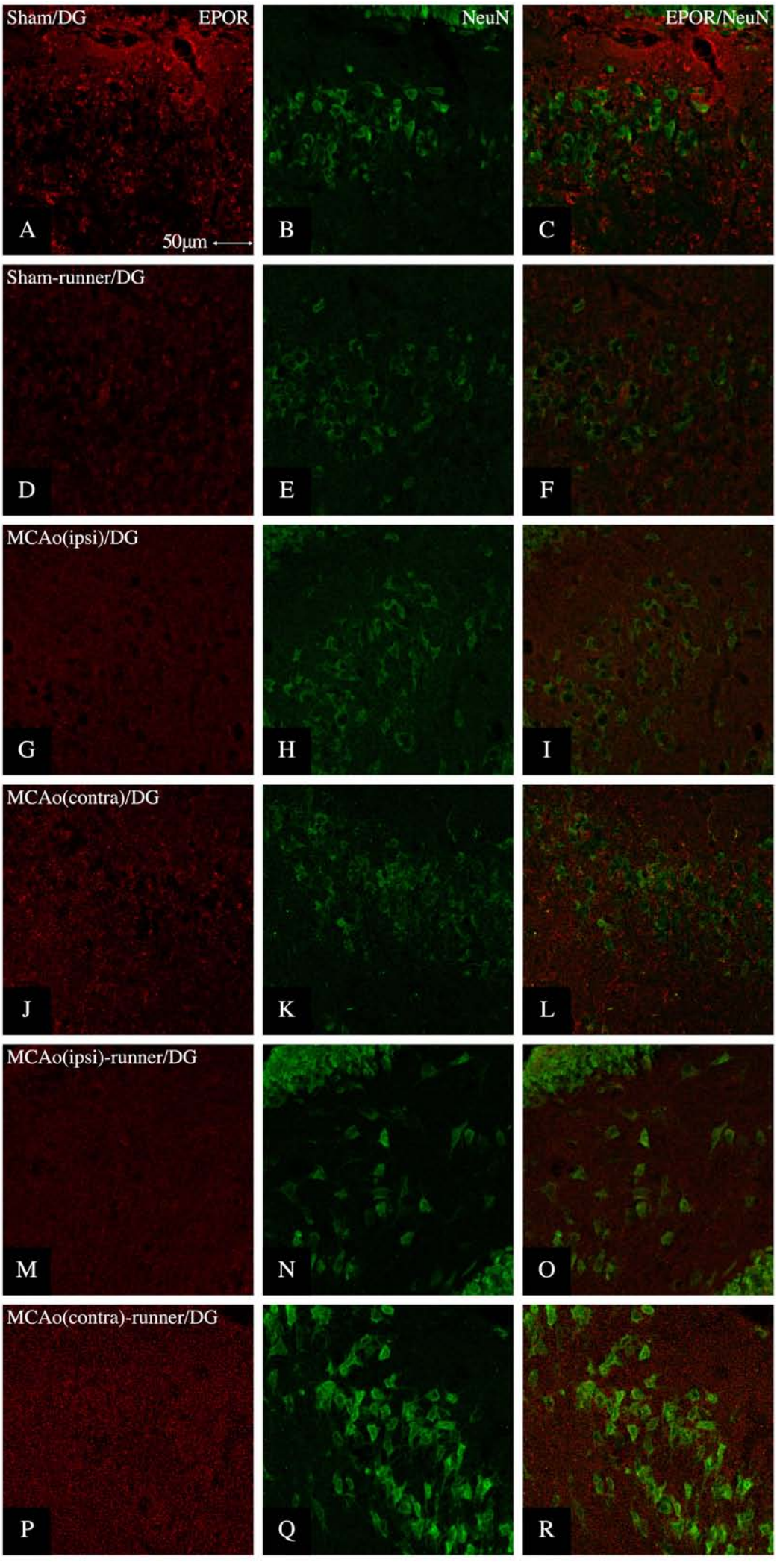
Sham/DG
EPOR
NeuN
EPOR/NeuN
A
50μm
B
C
Sham-runner/DG
D
E
F
MCAo(ipsi)/DG
G
H
I
MCAo(contra)/DG
J
K
L
MCAo(ipsi)-runner/DG
M
N
O
MCAo(contra)-runner/DG
P
Q
R

Fig. 34. Double staining of EPOR and NeuN in DG. Brain samples are sectioned from either sham or MCAo rats following eight weeks with or without forced treadmill exercise. These confocal images depict the DG at bregma -2.0 to -5.0mm ± 0.5mm under different experimental conditions. The tissues are double stained with EPOR (red) and NeuN (green). Expression of EPOR appears to be reduced following forced exercise. The EPOR expressions are seen to be higher in the contralateral than the ipsilateral DGs of both MCAo and MCAo-runner rats.

3.2.10 Erythropoietic factors in cortex

All animals assigned to either exercise or sedentary groups were sacrificed at ten weeks post-surgery (includes the total time allocated for trainings and eight weeks of actual exercise regime for the runner groups), with two days wash-out period after the last run, with or without MCAo .

3.2.10.1 Effects of exercise on erythropoietic factor's protein expression

Eight weeks of forced treadmill exercise produced a significant up-regulation of EPO protein expression in the cortices of sham-runner rats (1.42 ± 0.04 fold) as compared with the sham rats, p-value<0.05 (Fig. 35a).

Ipsilateral cortices of the MCAo rats similarly recorded a significant increase in EPO protein expression by 1.36 ± 0.05 fold (p-value<0.05) in contrast to the sham rats. The alteration to the EPO protein levels was not statistically significant in contralateral cortices of MCAo rats which were calculated at 1.13 ± 0.08 fold when compared with the sham rats.

Subsequent to eight weeks of post-ischemic forced treadmill exercise, EPO protein expression in both ipsilateral and contralateral cortices of the MCAo-runner rats were further increased by 1.76 ± 0.08 and 1.57 ± 0.11 fold respectively. However, only the

EPO protein expressions in the ipsilateral cortices of the MCAo-runner rats were significantly enhanced when compared with the same cortices in the MCAo rats with p-value<0.05.

EPOR protein expression depicted in Fig. 35b, showed a significant increment following eight weeks of forced treadmill exercise in the sham-runner rats (1.28 ± 0.04 fold) as compared with the sham rats, p-value<0.05.

Ensuing experimental brain ischemia, EPOR protein level was affected and calculated at 1.21 ± 0.04 fold in the ipsilateral cortices of the MCAo rats however the differences were not statistically significant. On the other hand, the changes to the EPOR expression level in contralateral cortices of the MCAo rats registered a statistically significant 1.49 ± 0.04 fold with p-value<0.01 when compared with the sham rats.

Following eight weeks of post-ischemic forced treadmill exercise, EPOR protein level in ipsilateral cortices of the MCAo-runner rats displayed a statistically significant further increment by 2.19 ± 0.06 fold (p-value<0.01) and remained elevated in the contralateral cortices at 2.00 ± 0.11 fold in contrast to the MCAo rats.

All data were analyzed with One way ANOVA, Tukey's Multiple Comparison Test.

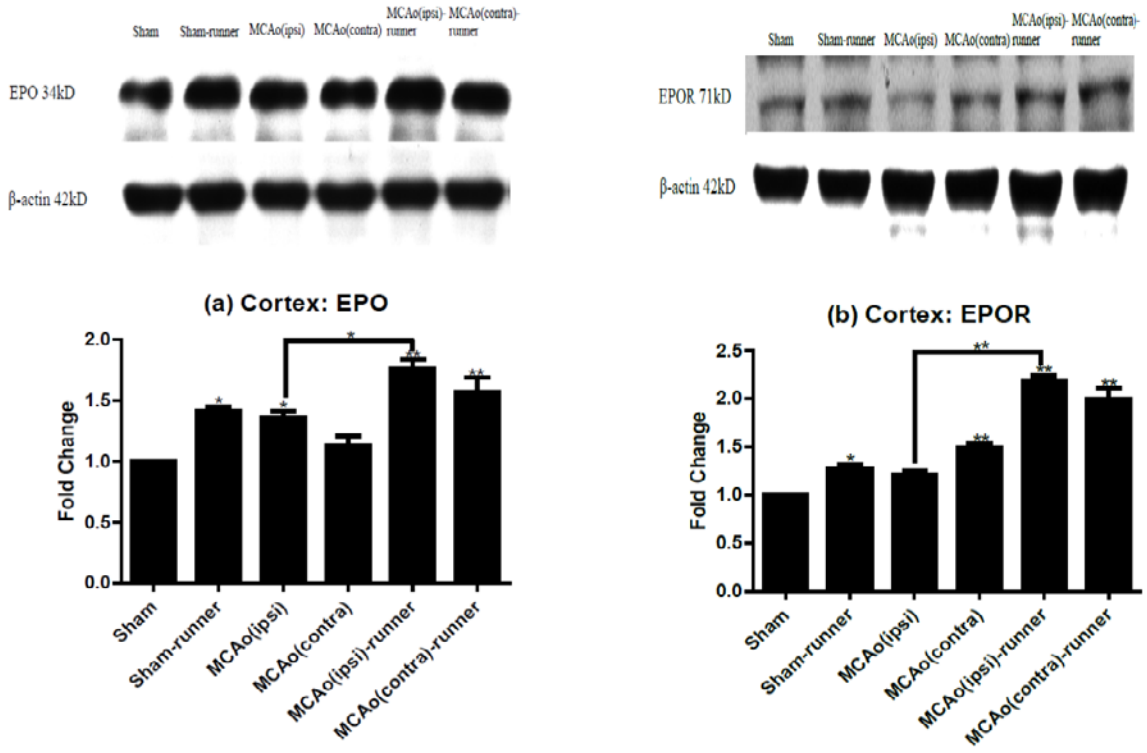

Fig. 35. EPO and EPOR protein expressions in the cortex. The EPO and EPOR antibodies detect the band at 34kD and 71kD with housekeeping β-actin at 42kD. Changes to protein levels in either whole ipsilateral or whole contralateral hemispheres of the cerebral cortices were semi-quantified using Western blot. (a) EPO protein level was significantly increased in the sham-runner rats by 1.42 ± 0.04 fold when compared with the sham rats. Experimental brain ischemia up-regulated the EPO level, only in the MCAo(ipsi), by 1.36 ± 0.05 fold. Post-ischemic exercise can further enhance the expression of EPO by 1.76 ± 0.08 fold in the ipsilateral cortices in contrast with the same cortices from MCAo rats. (b) EPOR protein expression was augmented significantly in the sham-runner and MCAo(contra) by 1.28 ± 0.04 and 1.49 ± 0.04 fold respectively when comparing with the sedentary rats. Post-ischemic exercise further increased the EPOR level significantly in the ipsilateral cortices of MCAo-runner rats by 2.19 ± 0.06 fold. All data were analysed with One way ANOVA, Tukey's Multiple Comparison Test with *p-value<0.05 and **p-value<0.01.

3.2.10.2 Effects of exercise and ischemia on staining profile of EPO

These confocal images in Fig. 36 depicted the parietal cortex (bregma -2.0 to -5.0mm ± 0.5mm) under different experimental conditions. The tissues were double stained with EPO (red) and NeuN (green). Sham rats are displayed in Fig. 36A to C and sham-runner rats are presented in Fig. 36D to F. The ipsilateral and contralateral cortices of MCAo rats are shown in Fig. 36G to I and Fig. 36J to L respectively. The ipsilateral and contralateral cortices of MCAo-runner rats are exhibited in Fig. 36M to O and Fig. 36P to R respectively.

Fine punctated EPO immunoreactive stainings were evenly distributed over the cortex of the sham-operated rats (Fig. 36A to C). Subsequent to eight weeks of regimented treadmill exercise in the sham-runner rats, the EPO expression appeared to be marginally increased (Fig. 36D to F). Some degrees of co-localisation with NeuN neurons were also observed.

Induced stroke caused increased in coarse granules of EPO immunoreactive products interspersed between fine immunoreactive specks, in both MCAo (Fig. 36G to I) and MCAo-runner (Fig. 36M to O) rats. Co-localisation of EPO in NeuN neurons appear more prominent in the MCAo (Fig. 36I and O) rats. In the contralateral cortices of the MCAo (Fig. 36J) and MCAo-runner (Fig. 36P) rats, EPO immunoreactivity was comparable to the sham-runner rats (Fig. 36D).

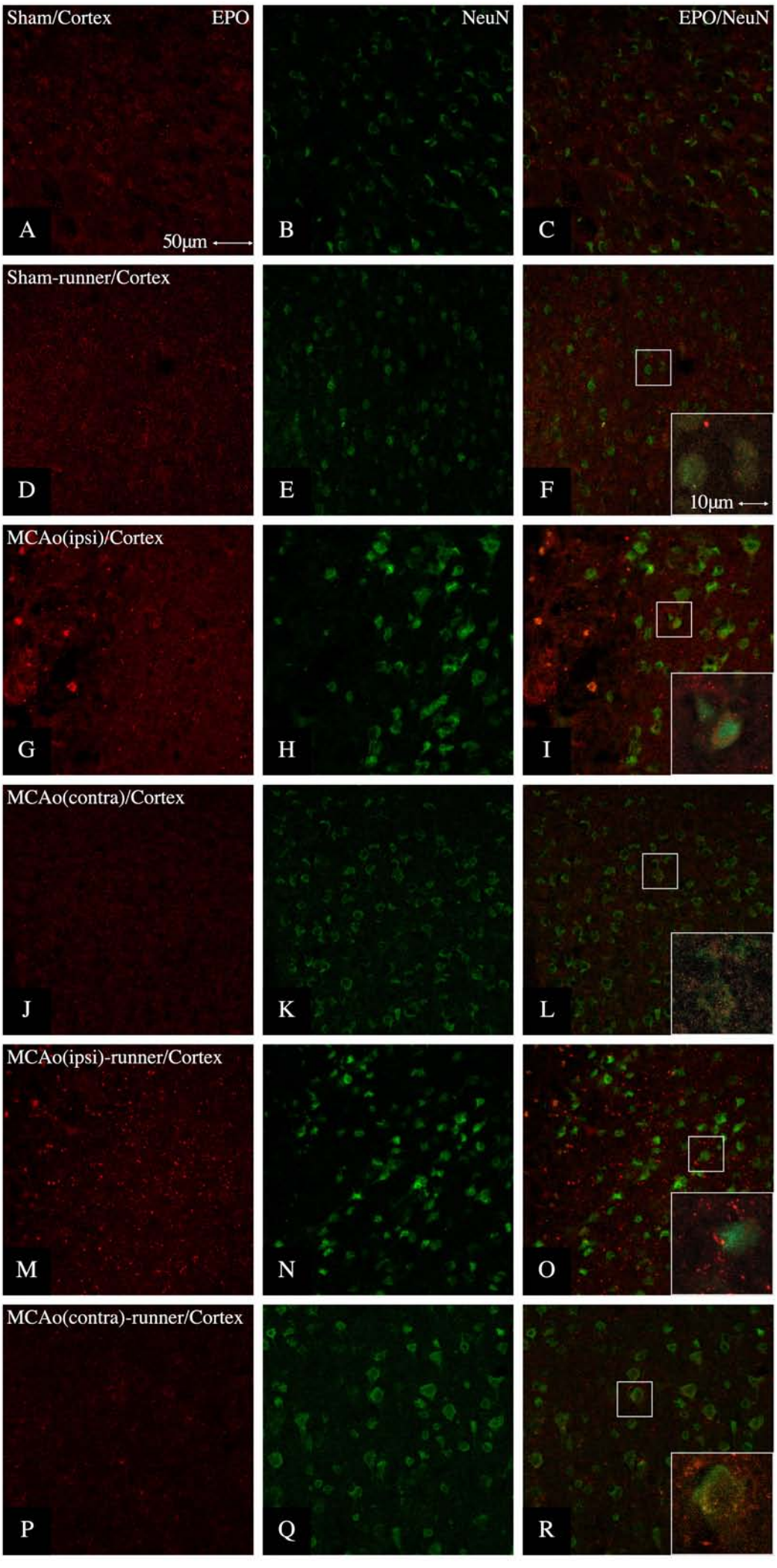
Sham/Cortex
EPO
NeuN
EPO/NeuN
A
50μm
B
C
Sham-runner/Cortex
D
E
F
10μm
MCAo(ipsi)/Cortex
G
H
I
MCAo(contra)/Cortex
J
K
L
MCAo(ipsi)-runner/Cortex
M
N
O
MCAo(contra)-runner/Cortex
P
Q
R

Fig. 36. Double staining of EPO and NeuN in cortex. These brain sections are prepared from either sham-operated or MCAo rats following eight weeks with or without forced treadmill exercise. These confocal images depict the parietal cortex at bregma -2.0 to -5.0mm ± 0.5mm under different experimental conditions. The tissues were double stained with EPO (red) and NeuN (green). EPO staining intensity appears to increase marginally in sham-runner rats as compared with the sham rats. Experimental brain ischemia, with or without forced exercise, enhanced the EPO staining in the appearance of coarse granules interspersed between fine immunoreactive specks in the ipsilateral cortices and only moderately intensified the EPO staining in the opposite sides.

3.2.10.3 Effects of exercise and ischemia on staining profile of EPOR

These confocal images in Fig. 37 depicted the parietal cortex (bregma -2.0 to -5.0mm ± 0.5mm) under different experimental conditions. The tissues were double stained with EPOR (red) and NeuN (green). Sham rats are displayed in Fig. 37A to C and sham-runner rats are presented in Fig. 37D to F. The ipsilateral and contralateral cortices of MCAo rats are shown in Fig. 37G to I and Fig. 37J to L respectively. The ipsilateral and contralateral cortices of MCAo-runner rats are exhibited in Fig. 37M to O and Fig. 37P to R respectively.

EPOR expressions in punctated staining pattern were observed in sham rats (Fig. 37A to C). The EPOR expression pattern in the sham-runner rats (Fig. 37D to F) remained comparable to sham rats albeit higher in quantity.

In the ipsilateral cortices of the MCAo (Fig. 37G to I) and MCAo-runner rats (Fig. 37M to O), EPOR-immunoreactivity was highly expressed in the periphery of the primary infarct zone. Though some EPOR was co-localised in NeuN neurons, much of them appeared to be localised in other cell types with astrocytic like processes. Running following MCAo, appeared to reduce the intensity as well as distribution of EPOR-immunoreactive products. The contralateral cortices of the MCAo rats (Fig. 37J to L) shared similar staining patterns with the sham rats, but the contralateral cortices of the

MCAo-runner rats (Fig. 37P to R) appeared to display a stronger staining signal than the sedentary rats.

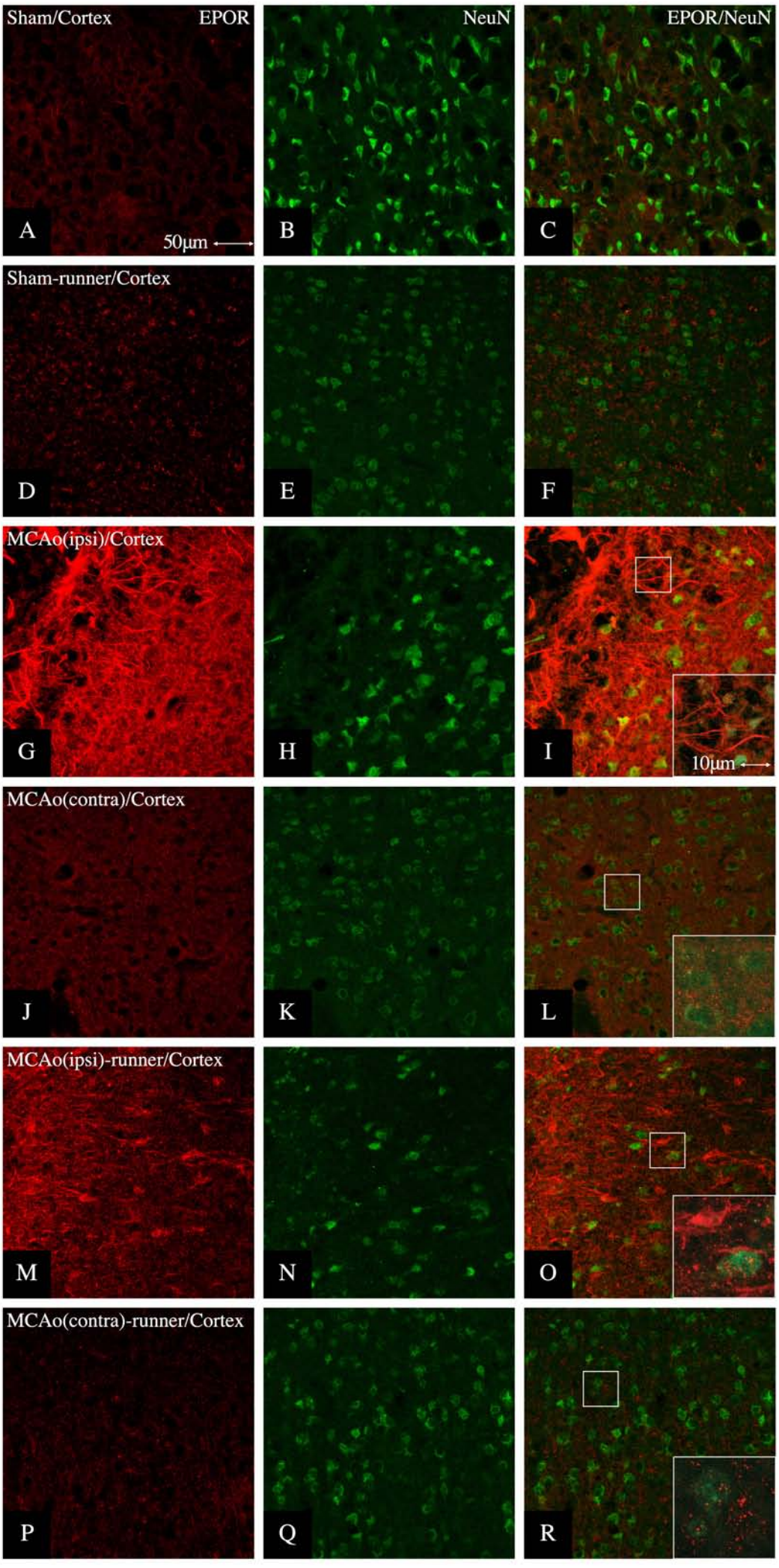
Sham/Cortex
EPOR
NeuN
EPOR/NeuN
A
50μm
B
C
Sham-runner/Cortex
D
E
F
MCAo(ipsi)/Cortex
G
H
I
10μm
MCAo(contra)/Cortex
J
K
L
MCAo(ipsi)-runner/Cortex
M
N
O
MCAo(contra)-runner/Cortex
P
Q
R

Fig. 37. Double staining of EPOR and NeuN in cortex. Sections of the brain are prepared from either sham or MCAo rats following eight weeks with or without forced treadmill exercise. These confocal images depict the parietal cortex at bregma -2.0 to -5.0mm ± 0.5mm under different experimental conditions. The tissues were double stained with EPOR (red) and NeuN (green). Sham-runner share similar EPOR staining patterns as compared with sham. EPOR staining in the ipsilateral cortices of MCAo rats [MCAo(ipsi)] and MCAo-runner rats [MCAo(ipsi)-runner] outlined astrocytic-like processes at the periphery of infarct zone. Post-ischemic exercise appear to increase EPOR expressions in the contralateral cortices of MCAo-runner rats [MCAo(contra)-runner] as compared with the MCAo rats [MCAo(contra)].

3.2.11 Antioxidants' profile in hippocampus following forced treadmill exercise

All animals were sacrificed at ten weeks (includes trainings and eight weeks of actual exercise regime) with two days wash-out period after the last run.

3.2.11.1 Effects of exercise on antioxidants' protein expression

Eight weeks of forced treadmill exercise did not have any effect on the Cu/ZnSOD protein expressions in the sham-runner rats which were calculated at 1.00 ± 0.04 fold which was not statistically significant when compared with the sham rats (Fig. 38a).

Catalase protein expressions in the sham-runner rats were determined at 1.05 ± 0.05 fold following eight weeks of forced treadmill exercise which was not statistically significant when compared with the sham rats (Fig. 38b).

GPx1 protein expressions were increased by 1.26 ± 0.02 fold following eight weeks of forced treadmill exercise in the sham-runner rats in contrast to the sham rats, $p\text{-value}<0.01$ (Fig. 38c). All data were analyzed with unpaired t-test.

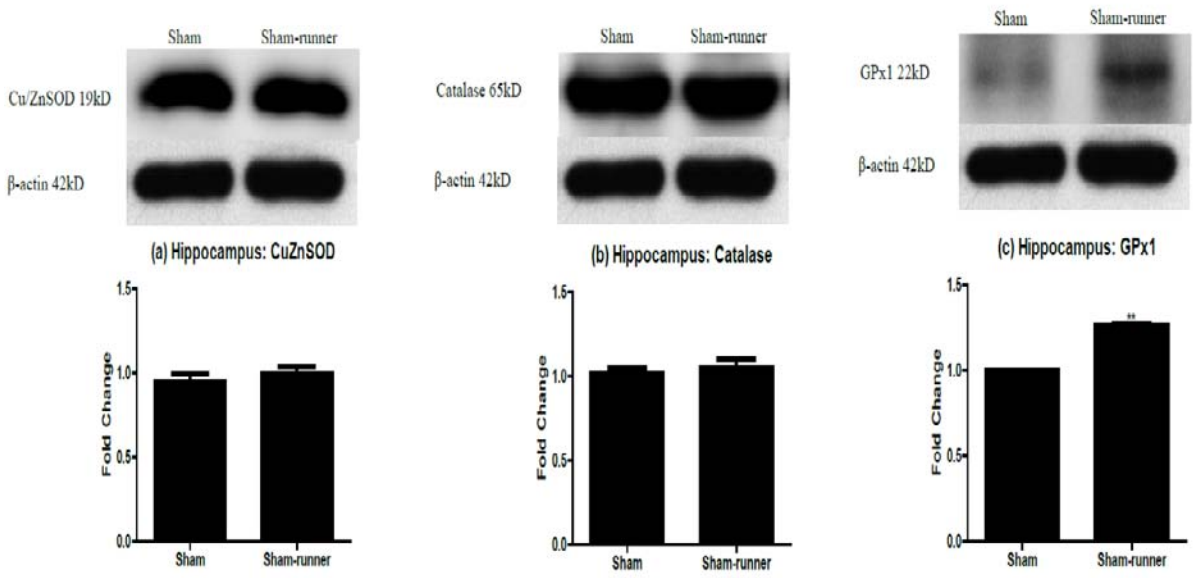

Fig. 38. Protein expressions of antioxidants in the hippocampus. The Cu/ZnSOD**,** catalase and GPx1 antibodies detect the bands at 19kD, 65kD and 22kD with housekeeping *β*-actin at 42kD. Increased physical activity did not give any boost to the hippocampal (a) Cu/ZnSOD and (b) catalase protein expressions in the sham-runner as compared with the sham rats. (c) Hippocampal GPx1 protein level was the only significantly up-regulated protein expression by 1.26 ± 0.02 fold in the sham-runner in contrast with the sham. All data were analysed using unpaired t-test with **p-value<0.01.

3.2.12 Antioxidants' profile in cortex following forced treadmill exercise and brain ischemia

All animals assigned to either exercise or sedentary groups were sacrificed at ten weeks post-surgery (includes the total time allocated for trainings and eight weeks of actual exercise regime for the runner groups), with two days wash-out period after the last run, with or without MCAo .

3.2.12.1 Effects of exercise on antioxidants' protein expression

The whole ipsilateral hemispheres of the cerebral cortices were used for the analysis of protein expressions in all groups with additional examination of whole contralateral hemispheres for both MCAo and MCAo-runner rats. Cu/ZnSOD protein expression in the sham-runner rats showed up-regulation calculated at 1.19 ± 0.07 fold but was not statistically significant when compared with the sham rats (Fig. 39a). Conversely, rats that was exposed to brain ischemia, Cu/ZnSOD protein expressions recorded significant increment in both ipsilateral and contralateral cortices of the MCAo rats (1.65 ± 0.03 and 1.76 ± 0.05 fold respectively) in contrast to the sham rats, p-value<0.01. Cu/ZnSOD protein expression, following eight weeks of post-ischemic forced treadmill exercise, in both ipsilateral and contralateral cortices of the MCAo-runner rats, comparable to MCAo rats, remained elevated at 1.53 ± 0.06 and 1.36 ± 0.03 fold respectively.

Compared with the sham rats, eight weeks of forced treadmill exercise showed significant increase of catalase protein expression in the sham-runner rats by 1.32 ± 0.06 fold, p-value<0.05 (Fig. 39b). Similar to sham-runner rats, catalase protein expression recorded a considerable increase in the contralateral cortices of the MCAo rats at 1.32 ± 0.11 fold as compared with the sham rats, p-value<0.05. However, the ipsilateral cortices of the MCAo rats were determined only at 1.06 ± 0.08 fold which was not statistically significant as compared with the sham rats. Catalase protein expression, following eight weeks of post-ischemic forced treadmill exercise, in both ipsilateral and contralateral cortices of the MCAo-runner rats were documented at 1.19 ± 0.04 and 1.16 ± 0.01 fold respectively which were flat when compared with the MCAo rats.

Shown in Fig. 39c, GPx1 protein expressions showed significant up-regulation in the sham-runner, both ipsilateral and contralateral cortices of the MCAo rats by 1.38 ± 0.03, 2.87 ± 0.06 and 2.75 ± 0.08 fold respectively with p-value<0.01 when compared with the sham rats. GPx1 protein expression, following eight weeks of post-ischemic forced treadmill exercise, in both ipsilateral and contralateral cortices of the MCAo-runner rats were determined at 1.36 ± 0.02 and 1.33 ± 0.07 fold respectively. Interestingly, GPx1 protein expressions in the ipsilateral cortices of the MCAo-runner rats were reduced when compared with the same cortices in the MCAo rats with p-value<0.01.

All data were analyzed with One way ANOVA, Tukey's Multiple Comparison Test.

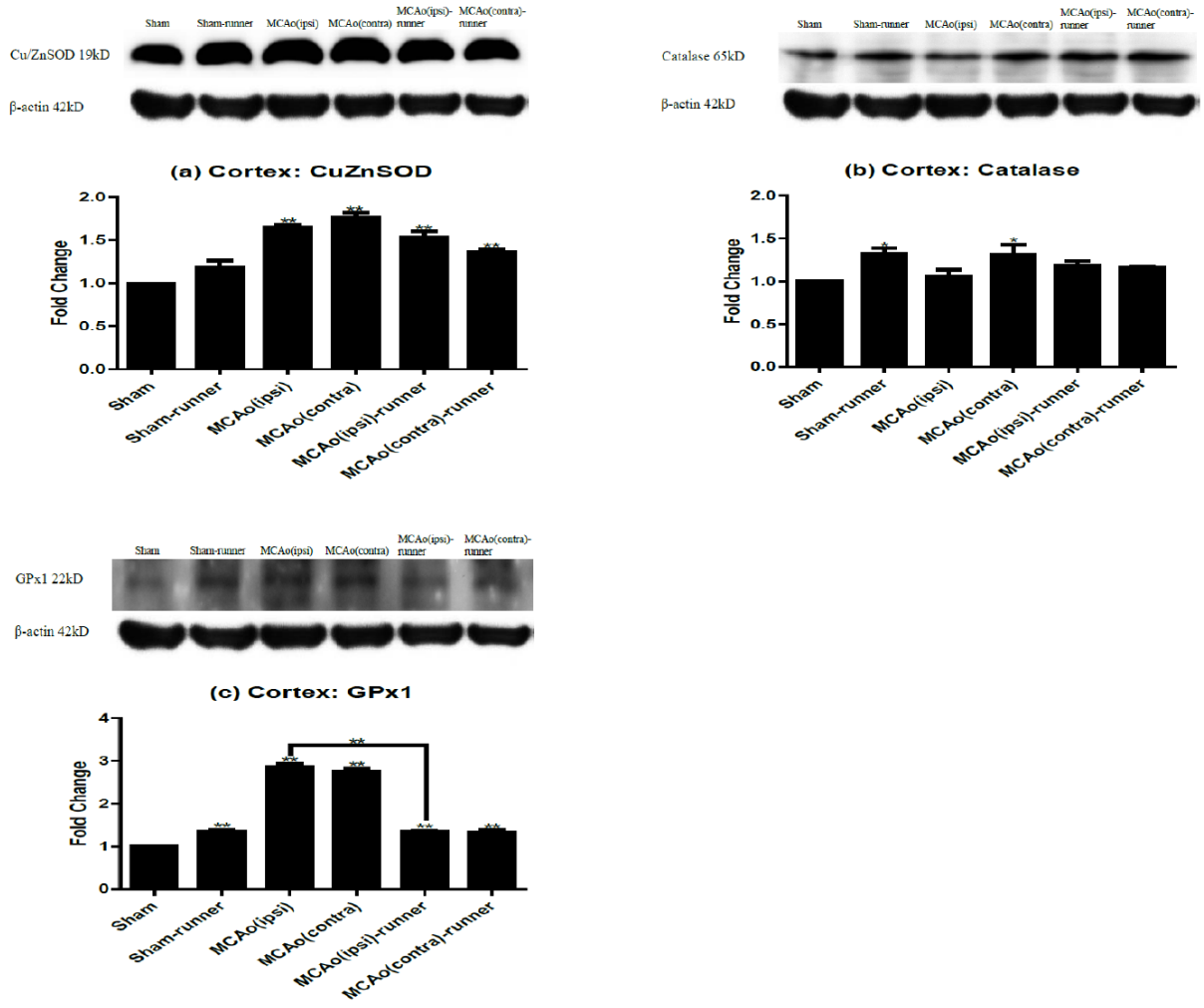

Fig. 39. Protein expressions of antioxidants in the cortex. The Cu/ZnSOD**,** catalase and GPx1 antibodies detect the bands at 19kD, 65kD and 22kD with housekeeping *β*-actin at 42kD. Changes to protein levels in either whole ipsilateral or whole contralateral hemispheres of the cerebral cortices were semi-quantified using Western blot. (a) Cu/ZnSOD protein expressions of the MCAo rats were significantly increased by 1.65 ± 0.03 and 1.76 ± 0.05 fold in ipsilateral and contralateral hemispheres respectively. MCAo-runner rats are comparable to the sendentary rats with brain ischemia. (b) Forced treadmill exercise significantly increased catalase protein expression in the sham-runner by 1.32 ± 0.06 fold and experimental brain ischemia significantly enhanced catalase protein level in the contralateral cortex [MCAo(contra)] by 1.32 ± 0.11 fold when compared with sham. (c) Increased in physical activity and experimental brain ischemia can increase GPx1 protein level by 1.38 ± 0.03, 2.87 ± 0.06 and 2.75 ± 0.08 fold for sham-runner rats, MCAo(ipsi) and MCAo(contra) respectively in comparison with sham rats. Post-ischemic exercise significantly down-regulate GPx1 expression in MCAo(ipsi)-runner to 1.36 ± 0.02 fold as compared with the MCAo(ipsi). All data are analysed with One way ANOVA, Tukey's Multiple Comparison Test with *p-value<0.05 and **p-value<0.01.

DISCUSSION

CHAPTER FOUR

4.1 Effects of single modality and combined treatment on infarct volume and intracellular ATP level in acute phase following MCAo

In the event of stroke, effective management of brain ischemia in the acute phase is usually achieved by pharmacological interventions with therapeutic windows shown clinically to be below three hours following ischemic onset (Clark and Madden, 2009). At present, only rt-PA for thrombolytic treatment and antiplatelet therapy are approved intravenous medications for the goals of arterial thrombus degradation and restoration of vessel patency and blood flow to achieve improved clinical prognosis. However, the treatment program fall short in offering direct help to the affected cells of the nervous system which is vulnerable and susceptible to cell damage and death when the blood flow rate fall under certain threshold.

Cell death modes via apoptosis and necrosis have been shown to occur following MCAo, a focal cerebral ischemic model. They have long been recognized and documented as two distinct forms of cell death, either biochemically or morphologically, where apoptosis is an energy requiring programmed process and necrosis is presumably an unregulated mode (Wyllie et al., 1980). However, a body of evidence has shown that apoptosis and necrosis may not be mutually exclusive pathways, but may share some common events in the earlier cell death process, intracellular ATP level, and the downstream controller, which is the primary determinant for the switch between apoptosis and necrosis (Eguchi et al., 1997). In the present study, single modality treatment with both the pan-caspase

and PARP inhibitors, z-VAD-fmk and 3-AB respectively, have shown infarct size reduction following MCAo. Thus, the present data confirmed that both apoptosis and necrosis can occur together in the pronecrotic settings of ischemic model. This could also imply that the two cell death mode may be initiated by the same stimuli (Lee et al., 1999).

Since the two neuroprotectants work via different pathways, it seems logical to administer them concurrently in treating a multi-cell-death-pathways ischemic injury. In the combined inhibitors treatment, the present data showed that it has reduced the infarct size further when administered with the same pharmacological intervention time course as in the single modality experiment. Though studies have shown that both apoptosis and necrosis can occur in a cell initiated by common stimuli (Bonfoco et al., 1995; Shimizu et al., 1996; Formigli et al., 2000; Papucci et al., 2004), the present data hinted that both apoptotic and necrotic outcomes can be regulated by different checkpoints as suggestive evidence has shown that combined inhibitors treatment can yield better outcome as compared to single inhibitor treatment. Although there is no data to suggest a general correlation between the infarct size and the intracellular ATP level, it has been observed that the intracellular ATP level of the animals which received the combined inhibitors treatment was kept above 4.52×10^{-3}moles/mg tissue. This might imply that higher intracellular ATP level play an important role in maintaining the cell's well being in the ischemic brain. Also in the present combined inhibitors experiment, we have shown that the longer the time taken for pharmacological intervention, the smaller the infarct size reduction. PARP activity has been shown in other studies to peak at the first 30 minutes

(LaPlaca, 1999), while initiator caspase-8 activation begins only at the sixth hour and executioner caspase-3 was observed 24hr following permanent MCAo (Velier et al., 1999; Harrison et al., 2001). Therefore, this difference is mainly due to the peak PARP activity and not caspase activation. Interestingly, in the Western blot analysis, there was PARP cleavage independent of caspase-3 activation. This phenomenon was also noted in another study by Cole and Perez-Polo (2002). This might be due to the intracellular ATP level not being high enough for the cells to complete the apoptotic process.

It has been suggested that intensity and duration, but not the type of insults, and intracellular ATP level can determine the switch between the two cell death modes (Bonfoco et al., 1995; Leist et al., 1997). Western blot analysis of the cleaved caspase-3 and PARP revealed that there was caspase-3 activation and PARP cleavage at 30mg/kg and 50mg/kg 3-AB, but not in 10mg/kg 3-AB. The possible explanation is that the dosage of 10mg/kg 3-AB was not effective in handling the over-activated PARP which led to an inclination for necrotic death mode, and 30mg/kg 3-AB is the minimum dosage required, in the current study, to preserve the ATP pool (this is in agreement with data in the ATP level experiment in Fig. 8a). 1mg/kg z-VAD-fmk showed caspase-3 activation and PARP cleavage but not 3mg/kg and 5mg/kg z-VAD-fmk. In the present study, this could be explained that the minimum of 3mg/kg z-VAD-fmk is required to prevent apoptosis, but not ischemic damage via other cell death pathways. Although treatments with either 3mg/kg or 5mg/kg z-VAD-fmk can effectively prevent executioner caspase activation, 5mg/kg z-VAD-fmk treatment group showed higher intracellular ATP level with lower

yield of infarct size reduction. The higher intracellular ATP level for the 5mg/kg z-VAD-fmk treatment may be due the inhibition of the energy-requiring apoptotic pathway which reduces the utilization of the intracellular ATP. In recent years, more evidences have shown that caspases are not only important in apoptosis but they may have opposing roles in cellular survival (Los et al., 2001) and neuronal plasticity (Gulyaeva et al., 2003). Therefore, the 5mg/kg z-VAD-fmk treatment which yielded a lower infarct size reduction as compared to the 3mg/kg z-VAD-fmk treatment despite a higher intracellular ATP level may suggest the other possible role of caspases as an endogenous neuroprotecting factor following an ischemic insult. The data also demonstrate that z-VAD-fmk and 3-AB are not able to prevent cell death fully, and they switched the mode of cell death (Wallisser and Thies 1999; Los et al., 2002; Prabhakaran et al., 2004).

The data show that there are clear distinction between the sham-operated brain tissue intracellular ATP level ($1.01\times10^{-2} \pm 9.87\times10^{-4}$moles/mg) and the untreated control brain tissue intracellular ATP level ($3.36\times10^{-3} \pm 2.09\times10^{-4}$moles/mg). Interestingly, the intracellular ATP level measured in the brain tissues of the animals under the single modality treatment showed that the 30mg/kg 3-AB treated animals have higher intracellular ATP level as compared to the 3mg/kg z-VAD-fmk treated animals, even though they have comparative infarct size reduction (26.98% ± 2.22% versus 24.13% ± 3.89% respectively, $p>0.05$). This can be explained mechanistically, that the two neuroprotectants work differently to inhibit cell death. z-VAD-fmk inhibited the caspase

family and prevent the progression of apoptotic program, while allowing PARP to utilize the ATP pool to resynthesize NAD^+ (Prabhakaran et al., 2004). 3-AB, on the other hand, binds to PARP and preserves the ATP level by preventing the PARP (over-activation) from utilizing the ATP (Coppola et al., 1995). Although in vitro studies have shown that intracellular ATP level increment is positively correlated with cell survival (Izyumov et al., 2004), the present data have shown that there is no implied correlation between intracellular ATP level and infarct size. However in the 3-AB treated group, there appeared to be a trend that suggested higher intracellular ATP level is correlated with lower infarct size, and this fashion is not present in the other treatment groups. This comparison demonstrates that infarct size following ischemia could be either dependent or independent of the intracellular ATP level, depending on the conditions, and for this study on the types of inhibitors administered. Therefore, use of the intracellular ATP level as an indication for the severity of infarct following ischemia may have to be considered carefully.

In conclusion, the study has shown that combined inhibitors treatment with z-VAD-fmk and 3-AB can achieve better infarct size reduction as compared to single modality treatment using the same chemical compounds. Though the combined inhibitors treatment can also further reduce infarct size with pharmacological intervention at 24hr post MCAo, it is the earlier intervention that gave the largest reduction in infarct size. Although there is no general correlation between intracellular ATP level and infarct size (as a consequence of the possible dual roles of caspases which complicate the results in the

pan-caspase treatment), in the case of the treatment with PARP inhibitors, there is a trend which showed that intracellular ATP level is inversely related to the size of infarct. More studies will be required to confirm the possible relationship between the intracellular ATP level and the infarct size following an ischemic insult which will have an important implication in clinical settings.

4.2 Brain ischemia and exercise affect changes in body weight and neurological score

As any form of surgical procedures is considered invasive, the weights of all rats were measured at 24hr post surgery. The measurements were compared in percentage, as opposed to absolute units of weight, because the present animal cohort was grouped by age and thus vary in sizes and weights. A universal decline in weights was observed across all groups following surgery. Interestingly, weight lost of animals either in MCAo or MCAo-runner rats, which were subjected to actual occlusion, exhibited a reduction approximately 2.5 fold more than the drop that had been seen in both sham or sham-runner rats with $p\text{-value}<0.05$. Therefore, the rats with insulted brain showed bigger weight reduction as compared with sham-operated rats. Generally, weight loss is not uncommon with human stroke patient which indicates poor nutritional status (Jönsson et al., 2008). The rats were then weighed again at tenth week post-surgery prior to sacrifice to ascertain if exercise or brain pathology may have any effect on weight gain. Without exception, all the rats registered weight gain across-the-board. However, notably, the

gained weight in either sham or MCAo rats, which were not placed on the forced treadmill exercise, acquired larger weight gain approximately 2.5 fold more than the gained mass seen in the rats that were subjected to forced treadmill exercise with p-value<0.05. Interestingly, there was no difference in regaining body weight seen between sham-operated rats and rats with actual occlusion. Therefore the results showed that the rats were able to gain weight and possibly maintained healthy nutritional status regardless of the status of brain pathology. In addition, perhaps expectedly, the prolonged exercise regime was able to have an effect on body weight in all conditions set in the present study.

Sham-operated rats recovered quickly from the surgical procedures without any reported neurological deficits and accounted death. On the other hand, 30% mortality rate was accounted for in rats with actual experimental MCAO, thus suggested that the death was due to the ischemic brain insults and not the surgical procedures. Rats with experimental brain ischemia that survived were subjected to neurological evaluation for a total of ten weeks. These rats showed some signs of paralysis which included abnormal posture, hemiplegia and a reduction in spontaneous movements. Typically, these symptoms were maximal during the first week, and then gradually improved over the following nine weeks with or without any forced exercise. Both MCAo and MCAo-runner rats showed indications of improving gait functions during the first week of resting period (resting period was set at one week and served as the buffering phase that allowed animals to heal wounds sustained from the invasive surgical procedures). However, from the fourth week

onwards (i.e. two weeks of post-ischemic forced treadmill exercise), MCAo-runner rats began to show slightly better functional recovery, as reflected by lower score achieved in the neurological examination, as compared to MCAo rats. And at the end of tenth week, rats that were subjected to forced treadmill running showed distinct functional recovery in contrast with sedentary rats. Running distances covered in the present study were considered as moderate regime reported to be effective for enhancing expressions of some key gene products believed to mediate favorable effects of exercise on the brain. Therefore, eight weeks of moderate forced treadmill exercise following MCAo was able to assist stroked rats to regain neurological outcomes earlier and better, which may have been linked to up-regulation of some key advantageous gene products, in comparison to sedentary animals with MCAo (Shen et al., 2001).

4.3 Long term chronic exercise influences apoptosis in both sham-operated and ischemic brain with reference to caspase-3 activation and TUNEL

As the recovery from stroke requires an extended duration therefore a long term management plan must be put in place to improve clinical outcomes. Physiotherapy has often been prescribed as a complementary therapeutic program on top of pharmacological means. Lee and coworkers (2006) have shown that under ischemic conditions, increased physical exercises can reduce expression of activated caspase-3. Moreover, various studies have shown that increased physical activities can up-regulate endogenous neurotrophic factors with effects that have been known to be able to decrease caspase-3

activation (Wu et al., 2008; Nguyen et al., 2009; Stranahan et al., 2009). Primarily, caspases are synthesized as proenzymes activated by proteolytic cleavage at Asp-X sites which contain a conserved pentapeptide QACXG sequence, and have been implicated in the progression of apoptotic activity (Cohen, 1997; Nicholson and Thornberry, 1997). Among the family of capases, caspase-3 holds a pivotal position as the executioner caspase in the downstream of the cascade pathway, and is activated via the proteolytic processing of its inactive zymogen into activated p17 and p12 subunits. Activated caspase-3 can cause breaks in DNA strand which is one of the hallmarks of apoptosis. The ailing cells with broken DNA strands then respond by activating their Poly (ADP-ribose) polymerase (PARP) which is a DNA repair enzyme. However, PARP being a substrate of caspase-3 can be cleaved and rendered inactive by activated caspase-3 during apoptosis (Soldani and Scovassi, 2002).

It was demonstrated in the present study that long term forced treadmill exercise, under sham-operated condition did not affect the level of both caspase-3 activation and PARP cleavage in the hippocampus and cortex. These observations suggested that the regimented exercise program designed for the study did not bring about any stress that may produce caspase-dependent apoptotic event under sham-operated condition. At the same time, TUNEL staining in the brains were also negative for the sham-runner rats.

As the middle cerebral artery do not branch into the hippocampus, this section mainly cover on the effects of brain ischemia in the cerebral cortices which bear direct

implications following experimental MCAo. In the current permanent MCAo model, executioner caspase, caspase-3, was shown to be persistently elevated by 2.84 ± 0.27 fold in the ipsilateral cortices of the MCAo rats when compared to the sham rats. This relentless elevation of caspase-3 activation in the current animal model suggested occurrence of continuing evolvement of brain ischemic pathology even at the chronic phase. And the ongoing ischemic episodes were backed by positive TUNEL staining being detected in the ipsilateral cortices. This observation of increased activated caspase-3 was not repeated in the contralateral cortices within the same MCAo rats thus showed that the effect of surgery was localized to specific cortex.

The cleavage of substrate PARP, has been shown to be cleaved *in vitro* by almost all caspases, while *in vivo* it is the targeted substrate of caspase-3 and -7 (Germain et al., 1997), was shown to be increased in both ipsilateral and contralateral cortices by 1.50 ± 0.09 and 1.44 ± 0.13 fold respectively in the MCAo rats. These observations suggested that the cleavage of PARP seen in the contralateral cortices was independent of caspase-3 activation. This phenomenon of PARP cleavage in the absence of caspase-3 has also been documented in earlier publications by other laboratories (J¨anicke et al., 1998; Woo et al., 1998; Slee et al., 2001). As seen in the acute phase experiments, the demise of the cells may occur via apoptosis or other non-apoptotic pathways (Yap et al., 2006). The PARP cleavage observed in the contralateral cortices may be an effort of the body to prevent over-activation of PARP which will lead to depletion of intracellular ATP and subsequent cell death due to bio-energetic crisis.

Subsequent to ischemic insults, MCAo-runner rats were allowed to rest for one week before the initiation of one week familiarization and training on the treadmill (with a shorter distance) and eight weeks of moderate exercise regime (for a distance of 892m in each run). A “dose-response” correlation between exercise duration/intensity and beneficial effects has been reported, whereby the best outcomes were associated with moderate exercise. Running distances covered in the present study were well above the threshold level of 500m/day, was considered as moderate regime, reported to be needed for up-regulation of some key gene products believed to mediate valuable effects of exercise on the brain (Shen et al., 2001).

In the present experiment, it was demonstrated that the long term post-ischemic exercise could decrease the caspase-3 activation remarkably from 2.84 ± 0.27 fold (seen in the MCAo rats) to 0.94 ± 0.04 fold in the insulted ipsilateral cortices of the MCAo-runner rats, indicating activated caspase activities at pathological stratum returning back to normal level (with reference to the sham rats), when compared with the same cortices of the MCAo rats. The caspase-3 activation in the contralateral cortices within the MCAo-runner rats was not influenced in any degree after subjected to post-ischemic exercise contrasting with MCAo rats. These observations showed that post-ischemic exercise alone could effectively reduced the pathological expression of activated caspase-3 in the affected region. Contrary to the level of caspase activity, TUNEL staining was paradoxically increased in the ipsilateral cortices MCAo-runner rats following post-ischemic exercise as compared to the same cortices in the MCAo rats.

This observation seemed to put forward an idea that post-ischemic exercise exacerbated cell death in the ischemia insulted cortex, but this contradiction upon further consideration of various cell death modes in an inevitable cell death circumstance, suggested that the increased in TUNEL staining seen in the MCAo-runner rats may ironically be beneficial to the ischemic milieu of the nervous system as apoptosis has been considered as "less messy" cell death mode which precludes subsequent inflammatory response (Patel et al., 2009). Moreover, expression of activated capase-3 that is inversely correlated with positive TUNEL staining had also been reported in earlier studies which showed DNA breakage independent of caspase-3 activation (Liang et al., 2008; Madeo et al., 2009).

Post-ischemic exercise did not show any significant effect on PARP cleavage in the ipsilateral cortices as PARP cleavage was only observed with a marginal drop. However, the PARP cleavage in the MCAo-runner rats, in contrast with the MCAo rats, was reduced significantly to 0.73 ± 0.03 fold in the contralateral cortices. These observations showed that post-ischemic exercise program in the present study could down-regulate PARP cleavage in the contralateral cortices more effectively as opposed to PARP cleavage reduction in the ipsilateral cortices, therefore suggested the disparity may be due the continuing evolvement of the ischemic cortices. As PARP participates in the modulation of chromatin architecture, maintenance of genomic stability, regulation of transcriptional processes, and the regulation of DNA repair (Lindahl et al., 1995), the

reduction in PARP cleavage, in any degree, after post-ischemic exercise may suggest a neuroprotective and neuroregenerative role of exercise following ischemic brain insults.

In conclusion, the study has shown that eight weeks of forced treadmill exercise under sham-operated condition did not change the level of caspase-3 activation, PARP cleavage and TUNEL both in the hippocampus and cortex. Eight weeks of post-ischemic exercise were able to lower the level of caspase-3 activation effectively but not PARP cleavage (which play pivotal role in caspase-dependent apoptosis) in the ipsilateral cortices from the MCAo-runner rats. The paradoxical increase of positive TUNEL staining seen in the MCAo-runner rats' ipsilateral cortices may possibly serve to better manage unpreventable cell death. Future studies will be required to study the mechanisms involved in reduction of activated caspase-3 following post-ischemic exercise, together with combinatorial treatment, and quantify the infarct size using magnetic resonance tools which will have an important implication to further exploit physiotherapy in clinical settings.

4.4 Correlation of apoptosis and TGF-β signaling pathway in both sham-operated and ischemic brains with or without exercise

TGF-β1 is a member of super-family of multifunctional cytokines that orchestrates various critical physiological processes, including proliferation, differentiation, growth inhibition, and apoptosis (Schuster and Krieglstein, 2002). In another word, TGF-β1 plays a critical role in the maintenance of homeostasis between cell survival and mortality.

TGF-β is produced by neurons, astrocytes and microglia in the CNS, and contributes to the regulation of neuronal survival (Prehn et al., 1994). Each member of the TGF-β superfamily binds characteristically with different receptor configuration where the combination of ALK-5 (TGFBR-I) and TGFBR-II is most common for TGF-β1. Smads are divided into three classifications such as receptor-activated smads (R-smads including smad2 and smad3), common-partner smad (Co-smad including smad4) and inhibitory smad (I-smad including smad6 and smad7). TGF-β1 primarily activates both smad2 and smad3 where smad2 and smad3 will form a heterotrimeric complex with smad4 and translocate into the nucleus to regulate key target gene transcription cascade (Shi and Massague, 2003; ten Dijke and Hill, 2004). The TGF-β1 signaling can be inhibited by smad7 but not by smad6 (Shi and Massague, 2003). Smad7 inhibits TGF-β1 signaling either by preventing the interaction between smad2 and smad3 with ALK receptor, or by inducing the ubiquitination or proteosomal degradation of ALK receptor (Bonni et al., 2001).

Long term forced treadmill exercise following sham-operation illustrated in the present study showed increased expressions of both TGF-b1 mRNA and TGF-β1 protein by 1.40 ± 0.06 and 1.38 ± 0.05 fold respectively in the sham-operated hippocampus. Unlike in the hippocampus, cortices of sham-runner rats did not show any increase in neither TGF-b1 mRNA nor TGF-β1 protein subsequent to the forced treadmill exercise program which remained at 1.07 ± 0.15 fold and 1.05 ± 0.05 fold respectively. On the other hand, both hippocampal and cortical TGFBR-II mRNA did not show any significant change

following the forced treadmill exercise. The disproportion of TGF-β1 expression seen in the cortex and hippocampus subsequent to exercise suggested that the profile of TGF-β1 expression may depend on distinct anatomical structures and their functions within these structures. Take for example, the immunofluorescence data showed that sham rats' TGF-β1 expressions in both CA1 and DG were detected but did not co-localise with NeuN positive neurons. TGF-β1 expression has been shown to be an impediment for neurogenic activities which happen in the DG of the hippocampus (Buckwalter et al., 2006). Interestingly, succeeding forced treadmill exercise, the sham-runner rats showed that TGF-β1 expressions were localised with some NeuN labeled neurons in the CA1 region and also detected in a diffused pattern in both oriens layer and stratum radiatum. The TGF-β1 expression in the DG, on the other hand, was substantially reduced. With TGF-β1 assuming various roles, it is crucial to note that high level of endogenous TGF-β1 has been shown to be inhibitive on neurogenesis (Buckwalter et al., 2006). Therefore observations made in the DG, associated with zone of neurogenesis supporting learning and memory function, provided possible evidences that suggested forced treadmill exercise could assist in preventing inhibition of neurogenesis with reduced TGF-β1 expression and its anti-neurogenic properties especially in DG of hippocampus. All in all, results from both Western blots and immunofluorescence experiments showed that increased TGF-β1 expression in the hippocampus was accounted for in the CA1 which may benefit neuronal survivability (Prehn et al., 1994). The TGF-β1 expression in the cortices of the sham-runner rats, shared a similar staining pattern seen in the CA1, with more being localised with NeuN positive neurons subsequent to forced treadmill

exercise in comparison with sham rats. As TGF-β1 has been shown to play a neuroprotective role in pathological CNS (Dhandapani and Brann, 2003), these observations suggested that forced treadmill exercise regime in the current sham-operation setting may produce exercise-induced effects comparable to those seen in ischemic preconditioning as reported by earlier studies (Boche et al., 2003; Ding et al., 2006), provide neuroprotection to ensuing brain ischemia by virtue of being localised to neuronal cells. At the same time, some TGF-β1 immunoreactive structures that resembled vasculatures suggested TGF-β1 being a possible component of angiogenesis that too offer protection when responding to subsequent ischemic attack (Roethy et al., 2001).

Smad2 mRNA level was not increased with prolonged forced treadmill exercise, but both smad7 mRNA and protein level was up-regulated significantly by 2.30 ± 0.45 fold and 1.54 ± 0.07 fold respectively in the hippocampi of sham-runner rats. As in the case of the hippocampus, forced treadmill exercise did not induce any significant increase in cortical smad2 mRNA level. Conversely, cortical expression of both smad7 mRNA and protein, differing from the hippocampus, did not register any significant increase following the exercise program. Smad7 is an inhibitory smad which interrupts the downstream signaling pathway of TGF-β1, therefore its concomitant increase expression alongside with up-regulated TGF-β1 level in the hippocampus may play an essential role in regulating TGF-β1 signals. The sham rats' immunofluorescence data showed that smad7 expression was detected in the oriens layer, stratum radiatum and DG. The sham-runner rats seemed to have more smad7 being expressed by NeuN positive neurons in both CA1

and DG. These observations suggested that the localisation of smad7 to CA1's neurons may be due to the concomitant increase in TGF-β1 expression to moderate TGF-β1 signaling in sham-runner rats' CA1's neurons. Although TGF-β1 staining profile may have been reduced in the DG, the detection of smad7 in neurons resided in the DG were possibly regulated by factors found in other pathways that also has been noted with the same capacity to illicit TGF-β1 signaling (Ulloa et al., 1999; Bitzer et al., 2000). And this detection of smad7 in the DG may further suppressed the already reduced TGF-β1's action and accentuate its condition for neurogenesis. Sharing a similar staining pattern as the hippocampus, the smad7 expressions in the cortices of the sham-runner rats appeared to be localised more with the NeuN labeled neurons after forced treadmill exercise in comparison with the sham rats. This staining pattern of smad7 when mirrored that of the cortical TGF-β1 staining profile suggested co-expression of smad7 and TGF-β1 in neurons may indicate likelihood of moderated TGF-β1 signaling subsequent to forced treadmill exercise.

MCAo rats' cortical TGF-b1 and TGFBR-II mRNAs expressions did not register any significant change following prolonged permanent MCAo in both ipsilateral and contralateral cortices. The cortical TGF-β1 protein expression was observed at 1.28 ± 0.05 fold in the ipsilateral cortices but the marginal change was also not statistically significant when compared with the sham rats. The contralateral cortices, on the other hand, registered a significant up-regulation of the cortical TGF-β1 protein expression which was calculated at 1.71 ± 0.08 fold. The reasons for the differences seen in the

TGF-b1 mRNA and TGF-β1 protein levels in the contralateral cortices may be attributed to the involvement of ill defined post-transcriptional mechanisms and in vivo half lives (Greenbaum et al., 2003). TGF-β1 protein expression in earlier studies have been shown to be up-regulated in the acute phase subsequent to brain ischemia and asserted neuroprotective functions (Ata et al., 1999; Boche et al., 2003). In the present study, TGF-β1 protein expressions in the chronic phase were considerably up-regulated only within the contralateral cortices. With reference to the expression profile of activated caspase-3 at 2.84 ± 0.27 and the detected positive TUNEL, the marginal increase of TGF-β1 protein in the ipsilateral cortices was not sufficient to reduce activation of the executioner caspase and subsequent caspase-3 dependent apoptosis, therefore showing that TGF-β1 protein expression were not able to retain its expression level that could provide effective neuroprotective threshold in the chronic phase of experimental MCAo. At the other end of the spectrum, persistent elevation seen in its contralateral cortices may be accountable for ischemic preconditioning (Boche et al., 2003; Ding et al., 2006). The immunofluorescence data of the MCAo rats showed that cortical TGF-β1 proteins were highly immunostained and appeared to be more localised with NeuN positive neurons in both ipsilateral and contralateral cortices analogous to the observations made in the CA1s. TGF-β1 has been reported to have neuroprotective functions and thus these observations seen in the MCAo rats suggested that the localisation of TGF-β1 to neurons in the immediate periphery of injury may prevent neuronal cell damage and assist cellular repair (Ata et al., 1999; Boche et al., 2003). However the present TUNEL data showed some cortical neurons with positive TUNEL staining thus suggested that neuroprotection via

the TGF-β1 was possible to protect but not able to prevent the entire population of neurons from imminent (apoptotic) cell death when cross referenced with the activated caspase-3 protein level in the ipsilateral cortices. The detection of TGF-β1 protein, in both NeuN labeled neurons and other cell structures, further away from the injury site suggested that non-neuronal type cells also produced TGF-β1 protein following ischemic insults and contributed to the extracellular level of TGF-β1 spotted in the interstitium of the cortex and hippocampus (Prehn et al., 1994).

Cortical smad2 and smad7 mRNAs, following experimental brain ischemia, were not significantly altered in both ipsilateral and contralateral cortices of MCAo rats. However, cortical smad7 protein expressions were increased significantly in both cortices of the MCAo rats at 1.50 ± 0.09 fold (ipsilateral cortices) and 1.43 ± 0.10 (contralateral cortices) fold. These differences seen in the smad7 mRNA and protein levels, like in the case of TGF-β1, may be attributed to the involvement of ill defined post-transcriptional mechanisms and in vivo half lives (Greenbaum et al., 2003). Smad7 expression increases in response to both TGF-β1 and factors regulating TGF-β1 (Ulloa et al., 1999; Bitzer et al., 2000), however the increased in smad7 protein expression in the ipsilateral cortices may further undermined the marginal elevation of TGF-β1 proteins for neuroprotective functions thus exacerbating the harsh ischemic pathology. The immunofluorescence data showed that cortical smad7 proteins of the MCAo rats were expressed in both NeuN labeled neurons and other cell structures in the two cortices. Therefore the observed increment and co-localisation of smad7 to neurons, in addition to the expressions of

TGF-β1, in the ailing ipsilateral cortices suggested that neuroprotective domain of TGF-β1 activities, not only were unsustainable, but were further challenged and handicapped by inhibitory smad during the chronic phase of experimental MCAo (Park, 2005; Hong et al., 2007). With reference to the TUNEL data, the neurons of the ipsilateral cortices with positive TUNEL staining reiterated that TGF-β1 signals, which can be moderated by inhibitory smads, were compromised for neuroprotection following prolonged experimental brain ischemia. In the same experimental group, hippocampal smad7 proteins appeared to be marginally increased and were co-localised with the neurons and other cell structures in both CA1s and DGs of ipsilateral and contralateral hippocampi when compared with the sham rats. These observations made on smad7 staining patterns in the MCAo rats suggested that the inhibitory smad may follow the staining patterns of the TGF-β1 in an attempt to moderate actions of TGF-β1 signaling. However, since TGF-β1 has been shown to suppress neurogenesis, the presence of smad7, which inhibited TGF-β1 activity, in neurons located in the DGs perhaps could be regarded as a favorable response to regain learning and memory functions (Buckwalter et al., 2006).

MCAo-runner rats' cortical TGF-b1 mRNA levels in the ipsilateral cortices were further increased when compared with the sedentary MCAo rats and were considered significantly increased following post-ischemic exercise when compared with the sham rats. On the other hand, the cortical TGF-b1 mRNA level in the contralateral cortices of the same experimental group remained up-regulated as was in the MCAo rats. The

cortical TGF-β1 protein expressions of the MCAo-runner rats were recorded with statistically significant increase of 1.55 ± 0.05 fold in ipsilateral cortices while the TGF-β1 protein in contralateral cortices remained at an elevated level as compared with the MCAo rats at 1.73 ± 0.12 fold. Cortical TGFBR-II mRNA registered a significant down-regulation in the ipsilateral cortices of the MCAo-runner rats by 0.59 ± 0.06 fold, and the cortical TGFBR-II mRNA in the contralateral cortices remained comparable to the level similar with sham rats. With up-regulated TGF-β1 protein level in the ipsilateral cortices, these changes in the TGFBR-II mRNA did not influence the reduction of activated caspase-3. In comparison with the MCAo rats, post-ischemic exercise was able to elevate the TGF-β1 protein to a significant level which was effective and correlated with considerable reduction in the activation of executioner caspases (Zhu et al., 2001). TUNEL stainings on the other hand showed a conflicting trend of increased apoptosis in neurons (with more positive TUNEL immunoreactivities) in the ipsilateral cortices following post ischemic exercise, even when the immunofluorescence data of the MCAo-runner rats showed that cortical TGF-β1 proteins in the ipsilateral cortices were localised to both NeuN labeled neurons and other cells. In the contralateral cortices of the MCAo-runner rats, cortical TGF-β1 proteins were expressed mainly in non-neuronal cells. These observations in the MCAo-runner rats showed that post-ischemic exercise in the present study was able to further increase the cortical TGF-β1 protein level in the ischemia-insulted ipsilateral cortices. Following post-ischemic exercise, TGF-β1 proteins were localised with more non-NeuN positive cells than NeuN labeled neurons in both cortices suggested that TGF-β1 protein production under such circumstances involved

more non-neuronal type of cells, and TGF-β1 localised to neurons in the ipsilateral cortices may imply cellular protection for the vulnerable neurons or merely swaying the cell death mode to less “messy” apoptotic course. Therefore, the increase in TUNEL detection in the ipsilateral cortices following post-ischemic running may not necessarily be taken as a failed attempt in improving the outcome after experimental stroke. In the same experimental group, the hippocampal TGF-β1 protein in the CA1 region was localised to both NeuN labeled neurons and other cell structures in both ipsilateral and contralateral hippocampi. Sharing a similar trend seen in the sham-runner rats, the hippocampal TGF-β1 staining patterns in the DG were substantially reduced in intensity subsequent to post-ischemic exercise. The detection of persistent expression of TGF-β1 protein in the CA1 region and the lowered staining TGF-β1 intensity in the DG suggested that the beneficial effects of post-ischemic exercise may be moderated for neuroprotection in the CA1 region and neuroregenerative potential in the DG.

MCAo-runner rats, as compared with the MCAo rats, registered slight drop in cortical smad2 mRNA level at 1.24 ± 0.14 and 1.10 ± 0.04 fold and smad7 mRNA level at 0.73 ± 0.04 and 1.01 ± 0.10 fold in both ipsilateral and contralateral cortices respectively albeit not statistically significant following post-ischemic exercise when compared with the sedentary MCAo rats. Cortical smad7 protein expression in the ipsilateral cortices was significantly brought down to 1.03 ± 0.07 fold in the MCAo-runner rats, comparable to sham rats, in contrast with the same cortices of the MCAo rats. On the other hand, no alteration to the cortical smad7 protein expression was observed in the contralateral

cortices following post-ischemic exercise which remained at 1.36 ± 0.08 fold when compared with MCAo rats. This significant reduction in the smad7 protein, in addition to increased TGF-β1 polypeptide, presented permissive conditions in the ipsilateral cortices which were correlated with down-regulation of activated caspase-3 therefore reinforced the neuroprotective role of TGF-β1 signaling following post-ischemic exercise. Even with the background of paradoxical increased apoptosis in neurons depicted in the TUNEL data, the outcome may not necessary be viewed with negative connotation and instead offered a more favorable condition for the body to manage inevitable cellular death by going down a route which will less likely to induce inflammatory responses. The immunofluorescence data of MCAo-runner rats showed that cortical smad7 protein expressions were restricted to neurons in the ipsilateral cortices and highlighted the influence of smad7 within NeuN neurons being more widespread following post-ischemic exercise, reversing the hopes hinged on the anti-apoptotic functions of TGF-β1. The staining patterns of the cortical smad7 protein in the contralateral cortices of the MCAo-runner rats did not differ much as compared to the same cortices of the MCAo rats. Even with smad7 protein level being greatly reduced in the ipsilateral cortices, the localisation of smad7 to neurons may still have an inhibitive grip on the TGF-β1's neuroprotective function to a certain degree therefore impeded the prevention of cell death to individual neurons. Several studies had been conducted and showed up-regulation of TGF-β1 in other types of tissue following exercise (Hering et al., 2002; Heinemeier et al., 2003); however this is the first study to document the beneficial effects of forced exercise and post-ischemic exercise on TGF-β1 expression profile in (rat) brain

tissues. In ipsilateral hippocampi of the same experimental group, the hippocampal smad7 protein expressions at both CA1 region and DG were detected with lower staining intensity subsequent to post-ischemic exercise. Following the same discussion thread earlier, the reduced intensity of smad7 may enhance the neuroprotective role of TGF-β1 in the CA1 region, but on the other hand, may undermined neuroregenerative potential in the DG. The hippocampal smad7 protein expression at both CA1 region and DG in the contralateral hippocampi of the MCAo-runner rats did not show any contrasting difference in the staining profile as compared with the MCAo rats.

In conclusion, the study has shown that eight weeks of forced treadmill exercise may be able to induce preconditioning-like effects and enhance neurogenic potential via TGF-β signaling in hippocampus, but not cortex, with increased TGF-β1 and smad7 under non-ischemic condition. And eight weeks of post-ischemic exercise were reported to be able to bring about neuroprotection via enhanced TGF-β signaling (cross reference to the reduction in activated caspase-3) with elevated TGF-β1 and down-regulated smad7 protein expressions. More studies will be needed to study the effects of exercise, together with combinatorial treatment, on regulation TGF-β signaling in permanent focal brain ischemia at different phases of the insults which will bear an important implication in clinical settings.

4.5 Impact of exercise on angiogenesis in brain with or without ischemia in reference to PDGFB level

Hypoxia-inducible factor 1 (HIF-1) is a wide spectrum transcription factor that encodes for various proteins that mediate molecular responses to reduced oxygen availability (Stroka et al., 2001; Shao et al., 2005). During hypoxia, HIF-1α subunit is protected from ubiquitination and proteasomal degradation thus allowing accumulation of HIF-1α subunit which is then translocated into the nucleus from the cytoplasm to form heterodimerization of the HIF-1α and HIF-1β subunits (Semenza, 1999; Wenger, 2000). This complex, together with its transcriptional co-activators, will then bind to the hypoxia response elements of various HIF-1 target genes such as VEGF and PDGF (Fandrey et al., 2006; Yoshida et al., 2006) to elicit an appropriate response. Vascular endothelial growth factor (VEGF) is a major family of angiogenic growth factor that induces vascularisation (Carmeliet and Storkebaum, 2002). VEGF ligand binds to the vascular endothelial growth factor receptors (VEGFR), a tyrosine kinase receptor, other than to induce vascularisation, also elicit several intracellular signaling pathways to promotes cell proliferation and induce cell survival (Takahashi et al. 1999; Kilic et al. 2006). VEGFR are dichotomized into VEGFR-1 and VEGFR-2 with VEGFR-2 being the primary transducer of VEGF signals. VEGF expression level is increased following a variety of brain insults. On top of its angiogenic property, VEGF signals have been documented to play a neuroprotective and neurotrophic roles (Carmeliet and Storkebaum 2002) and exert direct effects on different cell types such as neurons, astrocytes, and microglia. Under

hypoxia, VEGFR-2 expression was found to co-localise with the endothelial cells of blood vessels, astrocytes, and neurons (Kovacs et al., 1996; Kilic et al., 2006) at 48hr post-stroke and persist up to ten days. Platelet-derived growth factor (PDGF) is expressed as an inactive monomeric form is then activated proteolytically to form homodimeric or heterodimeric complexes. Active PDGF ligands interact with two distinct, but structurally related, membrane bound receptor tyrosine kinases, PDGF receptor-A (PDGFRA) and PDGF receptor-B (PDGFRB) (Fredriksson et al., 2004; Reigstad et al., 2005). Each PDGFR has been shown to have different affinity with different PDGF ligands (Heldin and Westermark, 1999; Li et al., 2000; Bergsten et al., 2001; LaRochelle et al., 2001), where PDGF-BB has a greater binding affinity for PDGFRB. In congruence of VEGF and VEGFR roles in vascularisation, PDGFB and its receptor PDGFRB displayed a complementary role in the maturation process (Folkman and D'Amore, 1996; Lindahl et al., 1997; Yancopoulos et al., 2000). In the CNS, PDGFB and its receptor PDGFRB were found to be expressed strongly in neurons (Sasahara et al., 1991; Smits et al., 1991). Following cerebral ischemia, expression of the ligand has been up-regulated in neurons and macrophages, and expression of its receptor has been observed in neurons, astrocytes and macrophages which suggest possibly neuroprotective function in addition to the role of angiogenic maturation (Iihara et al., 1994; Cheng and Mattson, 1995; Iihara et al., 1996; Krupinski et al., 1997; Kaneko et al., 1998).

In the present study, it was demonstrated that hippocampal HIF-1α protein was increased significantly by 1.82 ± 0.24 fold subsequent to long term forced treadmill exercise. The

hippocampal HIF-1α mRNA on the other hand was also evaluated with an upward trend at 1.67 ± 0.42 fold albeit not statistically significant. Both hippocampal VEGF mRNA and hippocampal VEGFR2 mRNA were observed with up-regulation at 1.38 ± 0.38 and 2.07 ± 0.91 folds respectively following forced treadmill exercise but were not statistically significant due to wide ranging standard error. The VEGF protein expression level in an earlier work had shown that VEGF was up-regulated significantly following long term exercise (Ding et al., 2004). And this increase in the VEGF protein level may have been influenced by the exercise induced up-regulation of HIF-1α proteins, transcription factor of VEGF, seen in the hippocampus in the current study (Fandrey et al., 2006). Both hippocampal PDGFB mRNA and hippocampal PDGFRB mRNA were significantly increased by 1.53 ± 0.16 and 2.58 ± 0.35 folds respectively following forced treadmill exercise. Accordingly, the PDGFB protein level was also calculated with a significant increment at 1.30 ± 0.03 fold after forced treadmill exercise. The increase in PDGFB, like in the case of VEGF, may have been influenced by the exercise induced up-regulation of HIF-1α which is also a transcription factor of PDGF (Yoshida et al., 2006). Studies have shown that hypoxic preconditioning can enhance ischemic tolerance and prevent exacerbation of neurodegeneration via increase in HIF-1α (Baranova et al., 2007; Gu et al., 2008; Peng et al., 2008). And in separate studies, exercise preconditioning has been described to emulate hypoxic preconditioning in ameliorating neurodegeneration (Ding et al., 2005; Ding et al., 2006). The present study is the first report to show up-regulation of hippocampal HIF-1α following eight weeks of forced treadmill exercise. Thus, apart from regulating the angiogenic factors, this increased in

hippocampal HIF-1α may also contribute directly to the neuroprotective properties seen in studies looking at preconditioning effects. Studies using animal model have also reported that increased physical exercise can induce neurogenesis and improve spatial memory (Clark et al., 2008; Naylor et al., 2008). PGDFB, has been implicated in the maturation process of neo-vascularisation in earlier studies, was shown to be increased in the hippocampi after forced treadmill exercise under sham-operated condition in the current settings (Folkman and D'Amore, 1996; Lindahl et al., 1997; Yancopoulos et al., 2000). Similarly, up-regulation of PGDFB, like VEGF, may have been under the influenced of increased level of HIF-1α. Taken together with increased VEGF following exercise shown in earlier studies, the PDGF/VEGF system may play an important role of stabilizing angiogenesis in support of the neurogenesis and enhanced learning and memory properties seen in other studies (Clark et al., 2008; Naylor et al., 2008).

The cortices presented different expressional profiles as compared with the hippocampi, the study demonstrated that both cortical HIF-1α mRNA and cortical HIF-1α protein were increased marginally by 1.23 ± 0.08 and 1.17 ± 0.05 folds respectively subsequent to long term forced treadmill exercise, but the changes were not statistically significant in contrast to the sham rats. The cortical VEGF mRNA did not register any significant difference after forced treadmill exercise. Although the cortical VEGFR2 mRNA was observed with up-regulation at 1.77 ± 0.35 fold following forced treadmill exercise, the change was also not statistically significant due to wide standard error. However, the up-regulation of cortical VEGF recorded in earlier exercise studies, in contrast with the

absence of concomitant increase in HIF-1α observed in the present study, suggested that regulation of VEGF protein level may involve other transcription factors in brain cortices thus different means of regulations may be used in various brain regions (Ding et al., 2004; Birk et al., 2008). While the cortical PGDFB mRNA level was increased significantly by 1.46 ± 0.10 fold after forced treadmill exercise, the cortical PGDFB protein and PDGFRB mRNA did not show any significant alteration when compared with the sham rats. In contrast with the hippocampal region, the cortical expressions of both HIF-1α and PGDFB protein were noted with increment that was not significant. Although the increment of PDGFB in this group was marginal, angiogenesis as represented by Pecam-1 was detected in the cortices. These observations suggested that even marginal increase in PDGFB, together with the expected VEGF increment shown in earlier studies, played a maintenance role important for sustaining the integrity of new vascular structure produced following long term forced treadmill exercise (Ding et al., 2004). These new blood vessels formed would be able to meet the demand of increased brain metabolism and its presence also offered physical evidence to support preconditioning-like effects. Taken together, the data from both hippocampus and cortex showed a consistent correlative trend between HIF-1α and PGDFB which highlighted the possibility that HIF-1α play a major role in regulating PGDFB's expressions in sham-operated brain.

The MCAo rats' cortical HIF-1α proteins were significantly up-regulated by 1.51 ± 0.09 fold in the ipsilateral cortices but not in the contralateral cortices which was evaluated at 1.22 ± 0.05 fold in contrast with the sham rats. These results implied that the ischemic

brain pathology was still evolving at the chronic phase following experimental MCAo and the ipsilateral cortices of the MCAo rats were able to adapt to the unremitting ischemic insult by increasing the cortical HIF-1α protein appreciably. This increase in HIF-1α protein also reflected the tissue's localised adaptation to ischemic insults (Ratan et al., 2007). However, the cortical HIF-1α mRNA registered an opposite expression profile with a significant down-regulation in both ipsilateral and contralateral cortices at 0.46 ± 0.02 and 0.50 ± 0.05 respectively. Although both cortical VEGF mRNA and cortical VEGFR2 mRNA in the two cortices were not observed with any significant change in the chronic phase of experimental brain ischemia, increased VEGF protein expression was reported in earlier study during chronic phase of brain ischemia (Zhang et al., 2002). On the other hand, both ipsilateral and contralateral cortices of the MCAo rats recorded significant increase of cortical PGDFB mRNA recorded at 1.59 ± 0.08 and 1.51 ± 0.06 fold respectively. However this significant genomic expression did not translate into similar protein profile. The cortical PGDFB proteins in the two cortices were not noted with any significant change. At the same time, cortical PDGFRB mRNA expressions managed apparent but not statistically significant upward trends in both ipsilateral and contralateral cortices recorded at 1.60 ± 0.15 and 1.75 ± 0.27 respectively. The reasons for the contradicting phenomenon seen in mRNA and protein levels of the ischemic cortices during the chronic phase of experimental MCAo may be attributed to the involvement of under defined post-transcriptional mechanisms and in vivo half lives (Greenbaum et al., 2003). As HIF-1α is one of the various transcription factors for PGDF, it was surprising to see absence of reciprocal increment of cortical PGDFB protein in

tangent with the increased HIF-1α protein in the ipsilateral cortices of the MCAo rats (Yoshida et al., 2006). This phenomenon of PGDFB protein repression in chronic phase of hypoxia/ischemia had also been reported by Ullerås and coworkers who suggested the involvement of a biphasic regulation of PGDFB **(**Ullerås et al., 2001). This repression of PDGFB in the late phase of chronic experimental stroke was correlated with compromised angiogenesis depicted by Pecam-1 immunoreactivities, thus PDGFB may have been highlighted for its importance in maintenance of stable neo-vasculature following brain ischemia.

Similarly with MCAo rats, cortical HIF-1α proteins in the MCAo-runner rats were significantly up-regulated in the ipsilateral cortices but not in the contralateral cortices. And the cortical HIF-1α mRNAs remained in the opposite expressional profiles noted with significant down-regulation in both cortices. Taken together with the sham-runner rats, these results showed that long term forced treadmill exercise did not have any effect on HIF-1α protein expressions in the cortical regions under both sham-operated and ischemic conditions. Both cortical VEGF and VEGFR2 mRNAs, in the two cortices of MCAo-runner rats similar to MCAo rats, were also not observed with significant change in the late phase of experimental brain ischemia. Subsequent to post-ischemic exercise, cortical PGDFB mRNA levels in the ipsilateral cortices of the MCAo-runner rats were significantly down-regulated to 0.79 ± 0.09 fold as compared with the same cortices of the MCAo rats at 1.59 ± 0.08 fold. Although the cortical PGDFB mRNA levels in the contralateral cortices were also observed with reduction following post-ischemic exercise

when compared with the MCAo rats, the change was not statistically significant. Interestingly, the cortical PGDFB proteins in the ipsilateral cortices of the MCAo-runner rats, showed an opposite trend to its genomic profile, were significantly up-regulated to 1.43 ± 0.11 fold as compared with the same cortices of the MCAo rats (and also sham-operated rats). PGDFB proteins in the contralateral cortices of the MCAo-runner rats also showed increment by 1.30 ± 0.12 fold albeit not statistically significant in contrast to the MCAo rats. At the same time, cortical PDGFRB mRNA in the ipsilateral was significantly increased by 2.82 ± 0.75 fold following post-ischemic exercise when compared with the sham rats but not the MCAo rats. The strong up-regulation of the cortical PGDFB proteins, following post-ischemic exercise, observed in the ipsilateral cortices of MCAo-runner rats were not accompanied by any further change in HIF-1α expressions, suggested that increased cortical PGDFB protein under ischemic condition was not due to HIF-1α alone but may involved other transcription factors and regulation as well (Dirks and Bloemers, 1996). The further increase of PGDFB protein seen in the MCAo-runner rats, in comparison with the sham-runner rats, suggested that ischemic insults and exercise could be regarded as two separate factors which allowed mutual potentiation in regulating the expressions of angiogenic factors. The increased of Pecam-1 staining intensity noted in MCAo-runner rats as compared to that of MCAo rats suggested that enhanced expressions of PDGFB protein following post-ischemic exercise were able to reverse compromised angiogenesis by a limited degree as angiogenic potential could have been thwarted by the harsh ischemic milieu. And cross referencing to the data on cleaved caspase-3 protein expression, post-ischemic exercise mediated increase in

PDGFB, other than in angiogenesis, was also correlated to the reduced activation of executioner caspase thus possibly serving neuroprotective function in addition to maturation of neo-vasculature.

In conclusion, the study has shown that eight weeks of forced treadmill exercise may induce preconditioning-like effects and enhance maturation of angiogenesis with marginal increase of HIF-1α and PDGFB under sham-operated condition. And eight weeks of post-ischemic exercise has shown to be able to up-regulate HIF-1α and especially PDGFB, as compared with sedentary rats with experimental brain ischemia, thus contributed to neuroprotection and maturation of newly formed blood vessels under ischemic condition. Future studies will be required to study the effects of exercise together with combinatorial treatment on HIF-1α and PDGFB in permanent MCAo at varying temporal profile which will have an important implication in clinical settings.

4.6 Effects of exercise on erythropoietic factors in brain under either sham-operation or ischemia

EPO is produced mainly in the adult kidney and the foetal liver (Fisher, 2003). However, both EPO and its receptor (EPOR) are also expressed in the CNS (Bernaudin et al., 1999; Bernaudin et al., 2000; Sirén et al., 2001b). As EPO is a target gene of transcription factor HIF-1α, during hypoxia and ischemia, expressions of erythropoietin (EPO) and its receptor (EPOR) are enhanced as a result of HIF-1α accumulation (Semenza and Wang,

1992; Wenger, 2000). In several *in vitro* and *in vivo* experiments, endogenous EPO has shown neuroprotective effects against neurological injury (Grasso et al., 2001; Junk et al., 2002) and neurotrophic effects to support neurogenesis (Shingo et al., 2001), in addition to its role in erythropoiesis (Yamaji et al., 1996). Treatment with rHuEPO in hypoxic and ischemic animal experiments have shown significant reduction in delayed neuronal cell death in the CA1 area of the hippocampus and prevented cognition impairment in the passive avoidance test (Sakanaka et al., 1998; Catania et al., 2002; Zhang et al., 2006). Taken together, EPO can exert both direct and indirect effects to improve sensory, cognitive and endocrine functions of the CNS following brain insults. The direct effects of EPO are independent of erythropoiesis but acting as a neurotrophic or neuroprotective factor (Marti et al., 2000). EPO prevents hypoxia- and glutamate-induced neuronal cell death by activation of calcium channels, increasing the activity of antioxidant enzymes in neurons, modulation of angiogenesis in the ischemic brain, and by anti-apoptotic effects via the activation of janus kinase-2 (JAK2) and nuclear factor κB (NF-κB) signaling pathways (Digicaylioglu and Lipton, 2001; Chong et al., 2002). Whereas indirectly, the EPO act through its erythropoiesis-stimulating effect to increase the oxygen supply to the brain thus counteracts the detrimental effects of hypoxia on neurons (Marti and Risau, 1999).

In the present study, the hippocampal EPO and EPOR proteins were demonstrated to increase significantly by 1.97 ± 0.30 and 1.63 ± 0.19 folds respectively subsequent to long term forced treadmill exercise. This statistically significant up-regulation of EPO

and EPOR proteins were repeated in the cortex at 1.42 ± 0.04 and 1.28 ± 0.04 folds respectively in the sham-runner rats in contrast with the sham rats. In the immunofluorescence experiment, EPO proteins were hardly detected in the CA1s and DGs but were mildly detected in the cortices of the sham rats. Subsequent to forced treadmill exercise, EPO proteins not only were detected but were also co-localised with the NeuN labeled neurons in all the three regions stated above. As DG has been regarded as the high plasticity region in adult brain, the detection of EPO in the DGs may suggest plausible neurotrophic role in inducing neurogenesis leading to improved learning and memory properties with moderate exercise (Marti et al., 2000; Zhang et al., 2006). EPOR proteins on the other hand were constitutively expressed in the CA1s, DGs and cortices. While the staining intensities of EPOR proteins remained relatively similar following forced treadmill exercise in the CA1s and cortices, the EPOR immunoreactivity in the DGs seemed to be slightly reduced. These results showed that exercise under sham-operated condition not only increased but also redistributed the EPO protein mainly to the neurons found in CA1s, DGs and cortices. Because EPO can exert both direct and indirect effects, the localisation of EPO to neurons after exercise suggested that the exercise regime used for the present experiment could bring about the direct effects of EPO possibly with a neuroprotective and neurotrophic functions (Grasso et al., 2001; Shingo et al., 2001; Junk et al., 2002). EPOR had been shown in other study to play an essential role in neurogenesis, therefore the elevation of EPOR protein measured in the present study suggested that long term forced exercise may permit EPO-EPOR mediated neuroprotection and neurogenesis (Tsai et al., 2006). Although earlier studies had

reported EPO production could be induced by increased physical activity, this is the first work to show the effects of forced treadmill exercise enhancing expression of EPO together with its receptor in the CNS that may form one of the underlying mechanism for preconditioning-like effects as well as improved learning and memory properties following exercise seen in other studies (Robert and Smith, 1999; Marti et al., 2000; Schobersberger et al., 2000; Ding et al., 2005; Zhang et al., 2006).

In the MCAo rats, cortical EPO proteins were registered with a statistically significant increase of 1.36 ± 0.05 fold in the ipsilateral cortices. However, the cortical EPOR protein was up-regulated significantly by 1.49 ± 0.04 fold only in the contralateral cortices. Although EPOR protein in the ipsilateral cortices was also increased by 1.21 ± 0.04 fold, the adjustment was not statistically significant. In the immunofluorescence experiment, subsequent to prolonged ischemic insult in the MCAo rats, cortical EPO and EPOR proteins were localised to both neurons and other cells in both cortices. Interestingly, in the immediate periphery of the injury site, resembling astrocytic-like processes were distinctively outlined by strong EPOR immunoreactivities where EPOR was shown to be expressed by neurons, astrocytes and endothelial cells, especially astrocytic processes surrounding the capillaries (Yamaji et al., 1996; Bernaudin et al., 1999; Bernaudin et al., 2000; Brines et al., 2000; Sirén et al., 2001b). Therefore, this phenomenon in the present study showed that the astrocytic-like processes could be the astrocytes cells that were expressing EPOR to receive EPO ligands to modulate angiogenesis (via the EPO-EPOR system) or barriergenesis in the penumbra responding to compromised neurovasculature

following ischemic insult (Wu et al, 1999; Kertesz et al, 2004; Lee et al., 2009a). However, with reference to the present data on cortical caspase-3 activation in the ipsilateral cortices of the MCAo rats, the increased endogenous cortical EPO following ischemic insult may not have been sufficient to moderate the apoptotic process. In CA1s, EPO and EPOR proteins in the ipsilateral hippocampi were localised mainly to neurons, with EPOR being seen with a reduced staining intensity. Hippocampal EPO and EPOR proteins in the contralateral CA1s, in addition to neuronal cells, were also detected in the oriens layer and stratum radiatum. In DGs, hippocampal EPO and EPOR proteins were co-localised with NeuN positive neurons and other cells, with EPOR again seen in mildly reduced staining intensity. The MCAo rats involved other cells for the production of EPO protein in both DG and cortex (Masuda et al., 1994). The data from the rats with experimental MCAo showed that EPO and EPOR proteins in the ipsilateral CA1s were expressed in neurons following brain ischemia possibly fulfilling neuroprotective function, while the expression of EPO and EPOR proteins in the DG involved both NeuN positive neurons and non NeuN labeled cells which may serve to mediate neuroregeneration in addition to neuroprotection as discussed earlier (Shingo et al., 2001).

In the MCAo-runner rats, cortical EPO protein was recorded with a statistically significant increment at 1.76 ± 0.08 fold in ipsilateral cortices and 1.57 ± 0.11 fold in contralateral cortices following post-ischemic exercise when compared with the sham rats (and additionally, ipsilateral cortices of MCAo rats). Cortical EPOR proteins in the MCAo-runner rats were also registered with statistically significant increase by 2.19 ±

0.06 fold and 2.00 ± 0.11 fold in the ipsilateral cortices and contralateral cortices respectively after post-ischemic exercise in contrast to the sham rats (again additionally, ipsilateral cortices of MCAo rats). At the same time, In contrast with the sham-runner rats, the further increase in the expression of EPO and EPOR proteins for the MCAo-runner rats showed that ischemic insults (Wen et al., 2004; Gu et al., 2008) and exercise (Robert and Smith, 1999; Schobersberger et al., 2000) could be regarded as two separate realms which allowed mutual potentiation in regulating the expression of erythropoietic factors. With reference to the data on reduced cortical cleaved caspase-3 protein expression seen in the ipsilateral cortices of the MCAo-runner rats, post-ischemic exercise mediated increase in EPO and EPOR signaling may be correlated with reduced apoptotic process. In the immunofluorescence experiment, MCAo-runner rats displayed immunoreactivities of cortical EPO proteins in the two cortices that were comparable to the distribution trend seen in the MCAo rats where the EPO proteins were localised to both NeuN positive neurons and other cells. The cortical EPOR staining profiles in the ipsilateral cortices of MCAo-runner rats shared similar but slightly less intense staining for the astrocytic-like processes as compared with the MCAo rats. Taken together, post-ischemic exercise increased overall expression (based on Western blot analysis) but did not alter the distribution of cortical EPO and EPOR proteins under ischemic conditions. In the CA1s of the MCAo-runner rats, higher staining intensity of both hippocampal EPO and EPOR proteins were observed in the ipsilateral hippocampi's neurons when compared with the MCAo rats. In the DGs, similar staining profiles of hippocampal EPOR proteins were observed between the MCAo-runner rats and MCAo

rats but hippocampal EPO proteins were more prominent following post-ischemic exercise. The localisation of EPO and EPOR proteins to neurons following either ischemic insult or exercise suggested that both events could act separately or come together in triggering neuroprotection of the neurons.

In conclusion, the study has shown that eight weeks of forced treadmill exercise were able to enhance neuroprotection and erythropoietic potential in both hippocampus and cortex, with increased EPO and EPOR under sham-operated condition. And eight weeks of post-ischemic exercise has shown to be able to up-regulate EPO and EPOR further, as compared with sedentary rats with experimental MCAo, thus provided support possibly for both neuroprotection and anigiogenesis/barriergenesis. More studies are needed at different temporal profile to study the effects of exercise, together with combinatorial treatment, on EPO and EPOR in permanent MCAo.

4.7 Changes in antioxidants' profile for both sham-operated and ischemic brain with or without exercise

Reactive oxygen species (ROS) or free radicals, e.g. superoxide and hydrogen peroxide, are generated physiologically via aerobic metabolism, although with short half-life, when produced in excess ROS will lead to oxidative stress which are implicated in the pathophysiology of many neurologic disorders and brain dysfunctions such as stroke (Kontos, 1985; Siesjö et al., 1989; Chan, 1994). This malice against the individual cell by

the ROS are capable of damaging lipids, proteins and DNA, and are scavenged and mediated by a variety of antioxidant enzymes such as superoxide dismutase (SOD), catalase and glutathione peroxidase (GPx) (Crack et al., 2003). Superoxide anions can be readily dismuted enzymatically from superoxide to hydrogen peroxide by SOD, which is subsequently converted to water by GPx or neutralized to water and oxygen by catalase (Fujimura et al., 2005). Expressions of endogenous antioxidants are up-regulated following ischemic attack, however can be insufficient when the brain ischemia episode proved too challenging (Fukui et al., 2002). Although studies have shown that increased physical activities can enhance antioxidants enzyme activities in the brain, most of the studies used normal animals in the experimental settings (Somani et al., 1995; Devi et al., 2004; Cechetti et al., 2007; Cechetti et al., 2008; Lappalainen et al., 2009). Currently, this is the first experiment that attempted to study the effects of long term forced treadmill exercise in modulation of antioxidants enzyme activities under sham-operated and ischemic conditions.

In the present study, it was demonstrated that both cortical and hippocampal GPx1 proteins were increased significantly by 1.38 ± 0.03 and 1.26 ± 0.02 folds respectively subsequent to long term forced treadmill exercise. This up-regulation seen in the current experiment reaffirmed observations made in earlier study which used older rats (at 14 weeks) (Lappalainen et al., 2009). As superoxide is the key constituent of oxidative stress, up-regulation of SOD will play a critical role in antioxidation. However, the exercise regime in the current study did induce any significant change to the enzyme

activity of the Cu/ZnSOD in both cortex and hippocampus (Lappalainen et al., 2009). This could be attributed to the Cu/ZnSOD's short half lives of about six to ten minutes and also the enzyme's activity being already in abundance in neural tissues rendering the current exercise regime not able to effect further changes (Fujimura et al., 2005). Interestingly, expression of catalase was only up-regulated significantly in the cortex but not in the hippocampus under sham-operated condition. This observation suggested that catalase's enzymatic activity may be dependent on the anatomical location in the brain subsequent to long term forced treadmill exercise. All in all, the changes to various antioxidant enzymes evaluated in the study suggested that the current exercise program was able to induce adaptation to possibly increased oxygen consumption in the brain (Somani et al., 1994; Servais et al., 2003). The results also suggested that both "second line" of antioxidants, GPx1 and catalase, were essential for adapting to changes in increased metabolism. However, the effect of forced treadmill exercise on enzymatic activity level of Cu/ZnSOD may have to be relooked upon at an earlier timing due to its short half lives.

In the MCAo rats, cortical GPx1 enzyme activities were significantly increased in the ipsilateral and contralateral cortices by 2.87 ± 0.06 and 2.75 ± 0.08 folds respectively following ischemic insults. In the same group, Cu/ZnSOD enzyme activities were also significantly increased in the ipsilateral and contralateral cortices by 1.65 ± 0.03 and 1.76 ± 0.05 folds respectively following ischemic insults. These observations suggested that Cu/ZnSOD were constantly expressed under the evolving ischemic milieu, otherwise

detection of its increase would be difficult to accomplish due to its short half lives. Overexpression of Cu/ZnSOD has been shown to reduce ischemic damage only in transient focal cerebral ischemia (Kinouchi et al., 1991; Yang et al., 1994; Kondo et al., 1997), but neither Cu/ZnSOD overexpression nor Cu/ZnSOD targeted deletion has shown any beneficial effect in permanent focal ischemia, thus pointing out Cu/ZnSOD's requirement for reperfusion to happen in order to serve its function (Chan et al., 1993; Fujimura et al., 2001). Although the present study employed a permanent MCAo model, the up-regulation in Cu/ZnSOD enzymatic activities could be relevant when collateral arteries were formed. However, catalase expression level was only elevated significantly by 1.32 ± 0.11 fold in the contralateral cortices. These results showed that the level of enzymatic activities of both GPx1 and Cu/ZnSOD, except catalase, remained up-regulated in the ipsilateral cortices thus suggested their importance in a continuously evolving pathology in the chronic phase following brain ischemia.

In the MCAo-runner rats, post-ischemic exercise significantly down-regulated cortical GPx1 enzyme activity to 1.36 ± 0.02 and 1.33 ± 0.07 folds in both ipsilateral and contralateral cortices respectively as compared with the MCAo rats. However, the GPx1 enzyme activity remained significantly elevated when compared with the sham rats. These downward trends were also noted for Cu/ZnSOD with a smaller margin to 1.53 ± 0.06 and 1.36 ± 0.03 folds in both ipsilateral and contralateral cortices respectively as compared with the MCAo rats. However, the enzymatic activities of cortical Cu/ZnSOD, similar with GPx1, were also significantly higher than the sham rats. Catalase enzyme

activity in the contralateral cortices was reduced to 1.19 ± 0.04 fold following post-ischemic exercise which rendered its activity level comparable to the sham rats. So far, there has been no data reporting the effect of post-ischemic exercise on enzymatic activities of antioxidants. Taken together, the multi-level of enzymatic activities of the three antioxidants posted a drop following post-ischemic exercise. Thus with much consideration, the present data may suggest long term moderate post-ischemic exercise were able to alleviate ischemic damages thus lowering the requirements of antioxidative defense. However, enzyme activity level of both GPx1 and Cu/ZnSOD remained elevated and relevant in evolving brain ischemia following post-ischemic exercise.

In conclusion, the study has shown that eight weeks of forced treadmill exercise were able to enhance the enzyme activities of GPx1 and catalase, and chronic phase of permanent MCAo has shown to be able to increase the enzyme activities of GPx1 and Cu/ZnSOD, thus outlining the varying repertoire of antioxidants used in different conditions. And in general, eight weeks of post-ischemic exercise has shown to down-regulate the enzyme activities of the three antioxidants which may suggest changes to an ischemic condition that has lower requirement for antioxidative defense and improved oxidative stress status. Future studies are recommended to study the effects of exercise, together with combinatorial treatment, on the enzyme activities of antioxidants at varying temporal profile following permanent MCAo.

CONCLUSION

CHAPTER FIVE

Stroke can be temporally classified into hyper-acute phase, acute phase, sub-acute phase and chronic phase for brain ischemia, where pharmacological intervention plays an important mediating role in the early phase while physiotherapy in addition to medication are proven clinical approach for managing the late phases of brain ischemia. The present study in the acute phase has shown that treatment with combined inhibitors using z-VAD-fmk and 3-AB can achieve better infarct size reduction as compared to single modality treatment with the same chemical compounds when delivered at the same timing. Though the combined inhibitors treatment can also further reduce infarct size with pharmacological intervention at 24hr post MCAo, it is the earlier intervention that gave the largest reduction in infarct size. Although intracellular ATP level was not correlated to infarct size, treatment with PARP inhibitor showed that intracellular ATP level was inversely related to the size of infarct. This limited observation in the PARP inhibitor treatment group may be consistent with the prevention of energy utilization by the PARP.

Earlier studies have shown that exercise, prior to ischemic insult, can induce neurotrophic factors that are beneficial to the brain. Physiotherapy, in the form of forced physical activities, prescribed as a complementary therapeutic program in addition to pharmacological intervention happen after stroke. The present study looked at the effects of forced exercise following experimental brain ischemia and showed that eight weeks post-ischemic exercise were able to lower the level of caspase-3 activation and PARP cleavage in the ipsilateral cortices from the MCAo-runner rats. In addition, present study showed that eight weeks of forced treadmill exercise under sham-operated condition did

not change the level of caspase-3 activation and PARP cleavage both in the hippocampus and cortex, and also did not induce any DNA damage or apoptosis. Although, the present study showed the paradoxical increase of positive TUNEL staining in the MCAo-runner rats, this may be a caspase independent apoptosis in which the body positioned to better manage the unpreventable cell death.

TGF-β1 is a cytokine which orchestrates various critical physiological processes, including proliferation, differentiation, growth inhibition, and apoptosis. Eight weeks of forced treadmill exercise increased TGF-β signaling in hippocampus with increased TGF-β1 and smad7 under sham-operated condition which may account for preconditioning-like effects and enhance neurogenic potential seen in earlier studies. The moderate increase in TGF-β1 accompanied by significant increase in smad7 was correlated to persistent high expression of caspase-3 activation and PARP cleavage in the ipsilateral cortices of the sedentary rats with MCAo. This high level of caspase activation was turned around with elevated TGF-β1 expression and down-regulated smad7 level following post-ischemic exercise, thus suggesting an anti-caspase-dependent-apoptosis property of TGF-β1's role in neuroprotection.

In addition to neuroprotection, neuroregeneration after ischemic insults is pivotal for a more favorable prognosis. In order for neuroregeneration to happen, it is necessary for complementing increase in angiogenic and erythropoietic activities to form new and effective oxygen delivery vascular structures. HIF-1 is a wide spectrum transcription

factor that encodes for various proteins (such as EPO and PDGFB) that mediate molecular responses to reduced oxygen availability. In the sham-operated hippocampus, eight weeks of forced treadmill exercise increased HIF-1α level which may have led to the up-regulation of both EPO and PDGFB. At the same time, expression of EPOR was also increased following prolonged exercise. Similarly in the sham-operated cortex, long term forced exercise was able to bring about an upward trend in both HIF-1α and PDGFB expression, albeit not significant. Fortunately, EPO and EPOR were significantly increased, thus these observations suggested that exercise could induce the angiogenic and erythropoeitic potential to condition the brain to be less susceptible to subsequent ischemia via formation of new blood vessels as illustrated by the Pecam-1 expression.

PDGFB seem to have a significant bearing on the Pecam-1 expression, as neo-vasculature was not evident in the cortices of MCAo rats even when HIF-1α was significantly up-regulated. As a consolation, both EPO and EPOR were increased by varying degree in the ipsilateral cortices of the MCAo rats. These observations suggested that brain ischemia could induce angiogenesis; however, lacking in concomitant increase of PDGFB may impede the maturation process of neo-vascularisation resulting in poorly formed blood vessels. Post-ischemic exercise was able to further increase the HIF-1α, EPO and EPOR expression in the MCAo-runner when compared with MCAo rats. Moreover, exercise under permanent ischemia was also able to build up PDGFB level. However, even in the presence of increased PDGFB, neo-vascularisation was unimpressive. Thus suggested that brain ischemia may produce or remove another unidentified factor that

may form either inhibitive or necessary conditions for the angiogenic property of PDGFB to work. These observations postulated that post-ischemic exercise although was able to increase endogenous neuroprotective and angiogenic activities in the MCAo-runner rats, but the increment was incapable of fully overcoming the limitation set by the ischemic milieu.

In the late phase of brain ischemia, collateral arteries may be formed to resupply oxygen and glucose to the insulted region. During these times, reperfusion to the affected area may result in oxidative stress thus generate changes in the antioxidants profile. The study has shown that eight weeks of forced treadmill exercise under sham-operated condition were able to enhance the enzyme activities of GPx1 and catalase, and chronic phase of permanent MCAo has shown to be able to increase the enzyme activities of GPx1 and Cu/ZnSOD, thus outlining the varying repertoire of antioxidants used in different conditions. And in general, eight weeks of post-ischemic exercise has shown to down-regulate the enzyme activities of the three antioxidants which suggest changes to an ischemic condition that has lower requirement for antioxidative defense and may be a reflection of the oxidative stress status. Therefore, the present chronic phase study showed that eight weeks of moderate forced treadmill post-ischemic exercise may be able to reduce secondary damages, and achieve better clinical outcome following brain ischemia via multi-modal neuroprotective and angiogenic (in supporting of neuroregeneration) mechanisms.

In conclusion, treatment of stroke requires understanding of its molecular mechanisms at different temporal profiles. While waiting for the conditions to stabilize, during the acute phase of stroke, primary goals of achieving arterial thrombus degradation and restoration of vessel patency and blood flow may also need to involve neuroprotective compounds that can minimize tissue damage to further improve clinical prognosis. Due to the complexity nature of progression in cellular damage after ischemia, combinatorial treatment has offered a glimpse of how it can work better than single modality approach in the acute phase experiment. Together with strategies to minimize tissue damaged during the acute phase of stroke and along with the principle of poly-sequences cellular damage, prolonged moderate forced treadmill exercises following experimental stroke have shown to induce the body to endogenously respond to challenges posed by ischemic insults via neuroprotective and angiogenic potentials improving gait functions and overall outcomes. Further experiments will be needed to look at the studying both acute and chronic phases together as a single model. Philosophically, these observations can be compared to city planning where formation of new blood vessels are likened to laying down new infrastructures such as roads and railway tracks. These neo-vasculature formed will enhance transport of neuroprotective and neuroregenerative factors more efficiently to the affected regions to restore devastations done and achieve improved clinical outcomes. Or in the case of city planner: Achieving sustainable living.

REFERENCES

Adibhatla RM, Hatcher JF (2006) Phospholipase $A_{2,}$ reactive oxygen species, and lipid peroxidation in cerebral ischemia. Free Radic Biol Med. 40: 376–87.

Ang ET, Wong PT, Moochhala S, Ng YK (2004) Cytokine changes in the horizontal diagonal band of broca in the septum after running and stroke: a correlation to glial activation, Neuroscience 129: 337–347.

Ang ET, Wong PTH, Moochhala S, Ng YK (2003) Neuroprotection associated with running: is it a result of increased endogenous neurotrophic factors Neurosci 118: 335–345.

Astrup J, Siesjö BK, Symon L (1981) Thresholds in cerebral ischemia—the ischemic penumbra. Stroke 12: 723–725.

Ata KA, Lennmyr F, Funa K, Olsson Y, Terent A (1999) Expression of transforming growth factor-beta1, 2, 3 isoforms and type I and II receptors in acute focal cerebral ischemia: an immunohistochemical study in rat after transient and permanent occlusion of middle cerebral artery. Acta Neuropathol (Berl). 97: 447–455.

Ata KA, Lennmyr F, Funa K, Olsson Y, Terént A (1999) Expression of transforming growth factor-beta1, 2, 3 isoforms and type I and II receptors in acute focal cerebral ischemia: an immunohistochemical study in rat after transient and permanent occlusion of middle cerebral artery. Acta Neuropathol. 97: 447–455.

Avendano C, Roda JM, Carceller F, Dieztejedor E (1995) Morphometric study of focal cerebral ischemia in rats: a stereological evaluation. Brain Res. 673: 83–92.

Back T, Zhao W, Ginsberg (1995) MD Three-dimensional image analysis of brain glucose metabolism-blood flow uncoupling and its electrophysiological correlates in the acute ischemic penumbra following middle cerebral artery occlusion. J. Cereb. Blood Flow Metab. 15: 566–577.

Bader MK, Palmer S (2006) What's the "hyper" in hyperacute stroke? Strategies to improve outcomes in ischemic stroke patients presenting within 6 hours. AACN Adv Crit Care. 17: 194–214.

Baranova O, Miranda LF, Pichiule P, Dragatsis I, Johnson RS, Chavez JC (2007) Neuron-specific inactivation of the hypoxia inducible factor 1 alpha increases brain injury in a mouse model of transient focal cerebral ischemia. J Neurosci. 27: 6320–6332.

Baud O, Greene AE, Li J, Wang H, Volpe JJ, Rosenberg PA (2004) Glutathione peroxidase-catalase cooperativity is required for resistance to hydrogen peroxide by mature rat oligodendrocytes. J Neurosci 24: 1531–1540.

Belayev L, Alonso OF, Busto R, Zhao W, Ginsberg MD. (1996) Middle cerebral artery occlusion in the rat by intraluminal suture. Neurological and pathological evaluation of an improved model. Stroke 27: 1616–622.

Belayev L, Zhao W, Busto R, Ginsberg MD (1997) Transient middle cerebral artery occlusion by intraluminal suture. I. Three-dimensional autoradiographic image analysis of local cerebral glucose metabolism-blood flow interrelationships during ischemia and early recirculation. J. Cereb. Blood Flow Metab. 17: 1266–1280.

Berger S J, Sudar DC, Berger NA (1986) Metabolic consequences of DNA damage: DNA damage induces alterations in glucose metabolism by activation of poly (ADP-ribose) polymerase. Biochem. Biophys. Res. Commun. 134: 227–232.

Bergsten E, Uutela M, Li X, Pietras K, Ostman A, Heldin CH, Alitalo K, Eriksson U (2001) PDGF-D is a specific, protease-activated ligand for the PDGF β-receptor. Nature Cell Biol. 3: 512–516.

Bernaudin M, Bellail A, Marti HH, Yvon A, Vivien D, Duchatelle I, MacKenzie ET, Petit E (2000) Neurons and astrocytes express EPO mRNA: oxygen-sensing mechanisms that involve the redox-state of the brain. Glia 30: 271–278.

Bernaudin M, Marti HH, Roussel S, Divoux D, Nouvelot A, MacKenzie ET, Petit E (1999) A potential role for erythropoietin in focal permanent cerebral ischemia in mice. J. Cereb. Blood Flow Metab. 19: 643–651.

Birk DM, Barbato J, Mureebe L, Chaer RA (2008) Current insights on the biology and clinical aspects of VEGF regulation. Vasc Endovascular Surg. 42: 517–530.

Bitzer M, von Gersdorff G, Liang D, Dominguez-Rosales A, Beg AA, Rojkind M, Bottinger EP (2000) A mechanism of suppression of TGF-β/SMAD signaling by NF-κB/RelA. Genes Dev. 14: 187–197.

Boche D, Cunningham C, Gauldie J, Perry VH (2003) Transforming growth factor-beta 1-mediated neuroprotection against excitotoxic injury in vivo. J Cereb Blood Flow Metab. 23: 1174–1182.

Bolander HG, Persson L, Hillered L, Dargy R, Ponten U, Olsson Y (1989) Regional cerebral blood flow and histopathologic changes after middle cerebral artery occlusion in rats. Stroke 20: 930–937.

Bonfoco E, Kranic D, Ankarcrona M, Nicotera P, Lipton SA (1995) Apoptosis and necrosis: two distinct events induced respectively by mild and intense insults with NMDA or nitric oxide/superoxide in cortical cell cultures. Proc. Natl. Acad Sci. USA. 92: 7162–7166.

Bonni S, Wang HR, Causing CG, Kavsak P, Stroschein SL, Luo K, Wrana JL (2001) TGF-beta induces assembly of a Smad2-Smurf2 ubiquitin ligase complex that targets SnoN for degradation, Nat Cell Biol 3: 587–595.

Brigelius-Flohe R (1999) Tissue-specific functions of individual glutathione peroxidases. Free Rad Biol Med 27: 951–965.

Brint S, Jacewicz M, Kiessling M, Tanabe J, Pulsinelli WA (1988) Focal brain ischemia in rat: methods for reproducible neocortical infarction using tandem occlusion of the distal middle cerebral and ipsilateral common carotid arteries. J. Cereb. Blood Flow Metab. 8: 474–485.

Buchan A, Xue D, Slivka A (1992) A new model of temporary focal neocortical ischemia in the rat. Stroke 23: 273–279.

Buchan AM, Xue D, Huang ZG, Smith KH Lesiuk H (1991) Delayed AMPA receptor blockade reduces cerebral infarction induced by focal ischemia. Neuroreport 2: 473–476.

Buckwalter MS, Yamane M, Coleman BS, Ormerod BK, Chin JT, Palmer T, Wyss-Coray T (2006) Chronically increased transforming growth factor-beta1 strongly inhibits hippocampal neurogenesis in aged mice. Am J Pathol. 169: 154–164.

Caplan LR, Schoene WC (1978) Clinical features of subcortical arteriosclerotic encephalopathy (Binswanger disease). Neurology 12: 1206–15.

Carmeliet P, Storkebaum E (2002) Vascular and neuronal effects of VEGF in the nervous system: implications for neurological disorders. Semin. Cell Dev. Biol. 13: 39–53.

Catania MA, Marciano MC, Parisi A, Sturiale A, Buemi M, Grasso G, Squadrito F, Caputi AP, Calapai G (2002) Erythropoietin prevents cognition impairment induced by transient brain ischemia in gerbils. Eur J Pharmacol. 437: 147–50.

Cechetti F, Fochesatto C, Scopel D, Nardin P, Gonçalves CA, Netto CA, Siqueira IR (2008) Effect of a neuroprotective exercise protocol on oxidative state and BDNF levels in the rat hippocampus. Brain Res. 1188: 182–188.

Cechetti F, Rhod A, Simão F, Santin K, Salbego C, Netto CA, Siqueira IR (2007) Effect of treadmill exercise on cell damage in rat hippocampal slices submitted to oxygen and glucose deprivation. Brain Res. 1157: 121–125.

Chan PH (1994) Oxygen radicals in focal cerebral ischemia. Brain Pathol 4: 59–65.

Chan PH, Kamii H, Yang GY, Gafni J, Epstein CJ, Carlson E, Reola L (1993) Brain infarction is not reduced in SOD-1 transgenic mice after a permanent focal cerebral ischemia. NeuroReport 5: 293–296.

Chan PH, Kawase M, Murakami K, Chen SF, Li Y, Calagui B, Reola L, Carlson E, Epstein CJ (1998) Overexpression of SOD1 in transgenic rats protects vulnerable neurons against ischemic damage after global cerebral ischemia and reperfusion. J Neurosci 18: 8292–8299.

Chen ST, Hsu CY, Hogan EL, Maricq H, Balentine JD (1986) A model of focal ischemic stroke in the rat: reproducible extensive cortical infarction. Stroke. 17: 738–743.

Cheng B, Mattson MP (1995) PDGFs protect hippocampal neurons against energy deprivation and oxidative injury: evidence for induction of antioxidant pathways. J. Neurosci. 15: 7095–7104.

Cheng YD, Al-Khoury L, Zivin JA (2004) Neuroprotection for ischemic stroke: two decades of success and failure. NeuroRx 1:36–45.

Choi DW (1996) Ischemia-induced neuronal apoptosis. Curr. Opin. Neurobiol. 6: 667–672.

Chong ZZ, Kang JQ, Maiese K (2002) Hematopoietic factor erythropoietin fosters neuroprotection through novel signal transduction cascades. J. Cereb. Blood Flow Metab. 22: 503–514.

Chow J, Ogunshola O, Fan SY, Li Y, Ment LR, Madri JA (2001) Astrocyte-derived VEGF mediates survival and tube stabilization of hypoxic brain microvascular endothelial cells in vitro. Brain Res. 130: 123–132.

Clark PJ, Brzezinska WJ, Thomas MW, Ryzhenko NA, Toshkov SA, Rhodes JS (2008) Intact neurogenesis is required for benefits of exercise on spatial memory but not motor performance or contextual fear conditioning in C57BL/6J mice. Neuroscience. 155: 1048–1058.

Clark WM, Madden KP (2009) Keep the three hour TPA window: the lost study of Atlantis. J Stroke Cerebrovasc Dis. 18: 78–79.

Cohen GM (1997) Caspases: the executioners of apoptosis. Biochem. J. 326: 1–16.

Cole KK, Perez-Polo JR (2002) Poly (ADP-ribose) polymerase inhibition prevents both apoptotic-like delayed neuronal death and necrosis after H_2O_2 injury J. Neurochem. 82: 19–29.

Coppola S, Nosseri C, Maresca V, Ghibelli L (1995) Different basal NAD levels determine opposite effects of poly (ADP-ribose) polymerase inhibitors on H2O2-induced apoptosis. Exp. Cell Res. 221: 462–469.

Cotman CW, Berchtold NC, Christie LA (2007) Exercise builds brain health: key roles of growth factor cascades and inflammation, Trends in Neurosci. 30: 464–472.

Crack PJ, Taylor JM, Flentjar NJ, de Haan J, Hertzog P, Iannello RC, Kola I (2001) Increased infarct size and exacerbated apoptosis in the glutathione peroxidase-1 (Gpx-1) knockout mouse brain in response to ischemia/reperfusion injury. J Neurochem 78: 1389–1399.

Crack PJ, Taylor JM, de Haan JB, Kola I, Hertzog P, Iannello RC (2003) Glutathione peroxidase-1 contributes to the neuroprotection seen in the superoxide dismutase-1 transgenic mouse in response to ischemia/reperfusion injury. J Cereb Blood Flow Metab. 23: 19–22.

Croll SD, Goodman JH, Scharfman HE (2004a) Vascular endothelial growth factor (VEGF) in seizures: a double-edged sword. Adv Exp Med Biol 548: 57–68.

Croll SD, Ransohoff RM, Cai N, Zhang Q, Martin FJ, Wei T, Kasselman LJ, Kintner J,Murphy AJ, Yancopoulos GD,Wiegand SJ. (2004b) VEGF-mediated inflammation precedes angiogenesis in adult brain. Exp Neurol 187: 388–402.

Danial NN, Korsmeyer SJ (2004) Cell death: critical control points. Cell 116: 205–219.

De Haan JB, Bladier C, Griffiths P, Kelner M, O'Shea RD, Cheung NS, Bronson RT, Silvestro MJ, Wild S, Zheng SS, Beart PM, Hertzog PJ, Kola I (1998) Mice with a homozygous null mutation for the most abundant glutathione peroxidase, GPx1, show increased susceptibility to the oxidative stress-inducing agents paraquat and hydrogen peroxide. J Biol Chem 273: 22528–22536.

De Luca A, Weller M, Fontana A (1996) TGF-β1-induced apoptosis of cerebellar granule neurons is prevented by depolarization. J Neurosci 16: 4174–4185.

Devi SA, Kiran TR (2004) Regional responses in antioxidant system to exercise training and dietary vitamin E in aging rat brain. Neurobiol Aging 25: 501–508.

Dhandapani KM, Brann DW (2003) Transforming growth factor-beta: a neuroprotective factor in cerebral ischemia. Cell Biochem Biophys. 39: 13–22.

Digicaylioglu M, Lipton SA (2001) Erythropoietin mediated neuroprotection involves cross-talk between Jak2 and NF-kappaB signaling cascades. Nature 412: 641–647.

Ding Y, Zhou Y, Lai Q, Li J, Gordon V, Diaz FG (2001) Long-term neuroprotective effect of inhibiting poly(ADP-ribose) polymerase in rats with middle cerebral artery occlusion using a behavioral assessment. Brain Res. 915: 210–217.

Ding Y, Li J, Luan X, Ding YH, Lai Q, Rafols JA, Phillis JW, Clark JC, Diaz FG (2004) Exercise preconditioning reduces brain damage in ischemic rats that may be associated with regional angiogenesis and cellular overexpression of neurotrophin. Neuroscience. 124: 583–91.

Ding YH, Luan XD, Li J, Rafols JA, Guthinkonda M, Diaz FG, Ding Y (2004) Exercise-induced overexpression of angiogenic factors and reduction of ischemia/reperfusion injury in stroke. Curr Neurovasc Res. 1: 411–420.

Ding YH, Young CN, Luan X, Li J, Rafols JA, Clark JC, McAllister JP 2nd, Ding Y (2005) Exercise preconditioning ameliorates inflammatory injury in ischemic rats during reperfusion. Acta Neuropathol. 109: 237–246.

Ding YH, Mrizek M, Lai Q, Wu Y, Reyes R Jr, Li J, Davis WW, Ding Y (2006) Exercise preconditioning reduces brain damage and inhibits TNF-alpha receptor expression after hypoxia/reoxygenation: an in vivo and in vitro study. Curr Neurovasc Res. 3: 263–271.

Dirks RP, Bloemers HP (1995-1996) Signals controlling the expression of PDGF. Mol Biol Rep. 22: 1–24.

Dirnagl U, Iadecola C, Moskowitz MA (1999) Pathobiology of ischemic stroke: an integrated view. Trends Neurosci. 22: 391–397.

Dobkin BH (2004) Strategies for stroke rehabilitation. Lancet Neurol. 3: 528–536.

Dringen R (2000) Metabolism and functions of glutathione in brain. Prog Neurobiol. 62: 649–71.

Dringen R, Hamprecht B (1997) Involvement of glutathione peroxidise and catalase in the disposal of exogenous hydrogen peroxide by cultured astroglial cells. Brain Res 759: 67–75.

Dringen R, Kussmaul L, Gutterer JM, Hirrlinger J, Hamprecht B (1999) The glutathione system of peroxide detoxification is less efficient in neurons than in astroglial cells. J Neurochem 72: 2523–2530.

Eguchi Y, Shimizu S, Tsujimoto Y (1997) Intracellular ATP levels determine cell death fate by apoptosis or necrosis. Cancer Res. 57: 1835–1840.

Endres M, Namura S, Shimizu-Sasamata M, Waeber C, Zhang L, Gomez-Isla T, Hyman BT, Moskowitz MA (1998) Attenuation of delayed neuronal death after mild focal ischemia in mice by inhibition of the caspase family. J. Cereb. Blood Flow Metab. 18: 238–247.

Fandrey J, Gorr TA, Gassmann M (2006) Regulating cellular oxygen sensing by hydroxylation, Cardiovasc. Res. 71: 642–651.

Ferrer I, Planas AM (2003) Signaling of cell death and cell survival following focal cerebral ischemia: life and death struggle in the penumbra. J. Neuropathol. Exp. Neurol. 62: 329–339.

Fields WS (1986) Multi-infarct dementia. Neurol Clin. 2: 405-13.

Fisher JW (2003) Erythropoietin: physiology and pharmacology update. Exp. Biol. Med. 228: 1–14.

Flentjar NJ, Crack PJ, Boyd R, Malin M, de Haan JB, Hertzog P, Kola I, Iannello R (2002) Mice lacking glutathione peroxidase-1 activity show increased TUNEL staining and an accelerated inflammatory response in brain following a cold-induced injury. Exp Neurol 177: 9–20.

Folkman J, D'Amore PA (1996) Blood vessel formation: what is its molecular basis? Cell 87 1153–1155.

Formigli L, Papucci L, Tani A, Schiavone N, Tempestini A, Orlandini GE, Capaccioli S, Zecchi Orlandini S (2000) Aponecrosis: morphological and biochemical exploration of a syncretic process of cell death sharing apoptosis and necrosis. J. Cell Physiol. 182: 41–49.

Fredriksson L, Li H, Eriksson U (2004) The PDGF family: Four gene products form five dimeric isoforms. Cytokine Growth Factor Rev. 15: 197–204.

Fujimura M, Morita-Fujimura Y, Copin J, Yoshimoto T, Chan PH (2001) Reduction of copper,zinc-superoxide dismutase in knockout mice does not affect edema or infarction volumes and the early release of mitochondrial cytochrome c after permanent focal cerebral ischemia. Brain Res. 889: 208–213.

Fujimura M, Tominaga T, Chan PH (2005) Neuroprotective effect of an antioxidant in ischemic brain injury: involvement of neuronal apoptosis. Neurocrit Care 2: 59–66.

Garcia JH, Liu KF, Ho KL (1995) Neuronal necrosis after middle cerebral artery occlusion in Wistar rats progresses at different time intervals in the caudoputamen and the cortex. Stroke 26: 636–642.

Gebicke-Haerter PJ, Van Calker D, Norenberg W, Illes P (1996) Molecular mechanisms of microglial activation: A. Implications for regeneration and neurodegenerative diseases. Neurochem. Int. 29: 1–12.

Germain M, Affar EB, D'Amours D, Dixit VM, Salvesen GS, Poirier GG (1999) Cleavage of automodified poly(ADP-ribose) polymerase during apoptosis: Evidence for involvement of caspase-7. J Biol Chem 274: 28379–28384.

Ginsberg MD, Busto R (1989) Rodent models of cerebral ischemia. Stroke. 20: 1627–1642.

Giulian D (1987) Ameboid microglia as effectors of inflammation in the central nervous system. J. Neurosci. Res. 18: 155–171.

Gladstone DJ, Black SE, Hakim AM (2003) Heart and Stroke Foundation of Ontario Centre of Excellence in Stroke Recovery Toward wisdom from failure: lessons from neuroprotective stroke trials and new therapeutic directions. Stroke 33: 2123–2236.

Gonzalez-Scarano F, Baltuch G (1999) Microglia as mediators of inflammatory and degenerative diseases. Annu. Rev. Neurosci. 22: 219–40.

Grasso G, Buemi M, Alafaci C (2002) Beneficial effects of systemic administration of recombinant human erythropoietin in rabbits subjected to subarachnoid hemorrhage. Proc. Natl. Acad. Sci. USA 99: 5627–31.

Greenbaum D, Colangelo C, Williams K, Gerstein M (2003) Comparing protein abundance and mRNA expression levels on a genomic scale. Genome Biology 4: 117–125.

Greenberg JI, Shields DJ, Barillas SG, Acevedo LM, Murphy E, Huang J, Scheppke L, Stockmann C, Johnson RS, Angle N, Cheresh DA (2008) A role for VEGF as a negative regulator of pericyte function and vessel maturation. Nature 456: 809-13.

Gu GJ, Li YP, Peng ZY, Xu JJ, Kang ZM, Xu WG, Tao HY, Ostrowski RP, Zhang JH, Sun XJ (2008) Mechanism of ischemic tolerance induced by hyperbaric oxygen preconditioning involves upregulation of hypoxia-inducible factor-1alpha and erythropoietin in rats. J Appl Physiol. 104: 1185–1191.

Guegan C, Sola B (2000) Early and sequential recruitment of apoptotic effectors after focal permanent ischemia in mice. Brain Res. 856: 93–100.

Gulyaeva NV, Kudryashov IE, Kudryashova IV (2003) Caspase activity is essential for long-term potentiation. J. Neurosci. Res. 73: 853–864.

Ha HC, Snyder SH (1999) Poly(ADP-ribose)polymerase is a mediator of necrotic cell death by ATP depletion. Proc. Natl. Acad. Sci. USA 96: 13978–13982.

Harrison DC, Davis RP, Bond BC, Campbell CA, James MF, Parsons AA, Philpott KL (2001) Caspase mRNA expression in a rat model of focal cerebral ischemia. Mol. Brain Res. 89: 133–46.

Hayashi H, Abdollah S, Qiu Y, Cai J, Xu YY, Grinnell BW, Richardson MA, Topper JN, Gimbrone Jr. MA (1997) The Mad-related protein Smad7 associates with the TGFβ receptor and functions as an antagonist of TGFβ signaling. Cell 89: 1165–1173.

Heinemeier K, Langberg H, Kjaer M (2003) Exercise-induced changes in circulating levels of transforming growth factor-beta-1 in humans: methodological considerations. Eur J Appl Physiol. 90: 171–177.

Heiss WD (2000) Ischemic penumbra: evidence from functional imaging in man. J Cereb Blood Flow Metab 20: 1276–1293.

Heiss WD, Graf R, Wienhard K, Löttgen J, Saito R, Fujita T, Rosner G, Wagner R (1994) Dynamic penumbra demonstrated by sequential multi-tracer PET after middle cerebral artery occlusion in cats. J Cereb Blood Flow Metab. 14: 892–902.

Heldin CH, Westermark B (1999) Mechanism of action and in vivo role of platelet-derived growth factor. Physiol. Rev. 79: 1283–1316.

Hering S, Jost C, Schulz H, Hellmich B, Schatz H, Pfeiffer H (2002) Circulating transforming growth factor beta1 (TGFbeta1) is elevated by extensive exercise. Eur J Appl Physiol. 86: 406–410.

Ho YS, Magnenat JL, Bronson RT, Cao J, Gargano M, Sugawara M, Funk CD (1997) Mice deficient in cellular glutathione peroxidase develop normally and show no increased sensitivity to hyperoxia. J Biol Chem 272: 16644–16651.

Hong S, Lee C, Kim SJ (2007) Smad7 sensitizes tumor necrosis factor induced apoptosis through the inhibition of antiapoptotic gene expression by suppressing activation of the nuclear factor-kappaB pathway. Cancer Res.67: 9577–9583.

Hossmann KA (1994) Viability thresholds and the penumbra of focal ischemia. Ann Neurol 36: 557–565.

Huang LE, Gu J, Schau M, Bunn HF (1998) Regulation of hypoxiainducible factor 1alpha is mediated by an O2-dependent degradation domain via the ubiquitin-proteasome pathway. Proc Natl Acad Sci USA 95: 7987–7992.

Iihara K, Sasahara M, Hashimoto N, Uemura Y, Kikuchi H, Hazama F (1994) Ischemia induces the expression of the platelet-derived growth factor-B chain in neurons and brain macrophages in vivo. J. Cereb. Blood Flow Metab. 14: 818–824.

Iihara K, Sasahara M, Hashimoto N, Hazama F (1996) Induction of platelet-derived growth factor β-receptor in focal ischemia of rat brain. J. Cereb. Blood Flow Metab. 16: 941–949.

Ishibashi N, Prokopenko O, Weisbrot-Lefkowitz M, Reuhl KR, Mirochnitchenko O (2002) Glutathione peroxidase inhibits cell death and glial activation following experimental stroke. Brain Res Mol Brain Res. 109: 34–44.

Izyumov DS, Avetisyan AV, Pletjushkina OY, Sakharov DV, Wirtz KW, Chernyak BV, Vladimir P, Skulachev VP (2004) “Wages of fear”: transient threefold decrease in intracellular ATP level imposes apoptosis. Biochim. Biophys. Acta. 1658: 141–147.

J¨anicke RU, Ng P, Sprengart ML, Porter AG (1998) Caspase-3 is required for alpha-fodrin cleavage but dispensable for cleavage of other death substrates in apoptosis. J Biol Chem 273: 15540–15545.

Jelkmann W (2005) Effects of Erythropoietin on Brain Function. Cur. Pharmaceutical Biotech. 6: 65–79.

Jewell UR, Kvietikova I, Scheid A, Bauer C, Wenger RH, Gassmann M (2001) Induction of HIF-1alpha in response to hypoxia is instantaneous. FASEB J. 15: 1312–1314.

Jiang BH, Semenza GL, Bauer C, Marti HH (1996) Hypoxia-inducible factor 1 levels vary exponentially over a physiologically relevant range of O2 tension. Am J Physiol 271: C1172–1180.

Jönsson AC, Lindgren I, Norrving B, Lindgren A (2008) Weight loss after stroke: a population-based study from the Lund Stroke Register Stroke. 39: 918–923.

Jorgensen HS, Nakayama H, Raaschou HO, Vive-Larsen J, Stoier M, Olsen TS (1995) Outcome and time course of recovery in stroke: Part I. Outcome. The Copenhagen Stroke Study. Arch. Phys. Med. Rehabil. 76: 399–405.

Junk AK, Mammis A, Savitz SI, Singh M, Roth S, Malhotra S, Rosenbaum PS, Cerami A, Brines M, Rosenbaum DM (2002) Erythropoietin administration protects retinal neurons from acute ischemia-reperfusion injury. Proc. Natl. Acad. Sci. USA 99: 10659–10664.

Kalra L, Langhorne P (2007) Facilitating recovery: evidence for organized stroke care. J Rehab Med. 39: 97–102.

Kaneko M, Sasahara M, Takayama S, Handa J, Hazama F (1998) Expression of platelet-derived growth factor after transient forebrain ischemia in the gerbil hippocampus. Acta Neuropathol. 95: 471–478.

Karamysheva AF (2008) Mechanisms of angiogenesis. Biochemistry (Mosc). 73: 751-62.

Katoh Y, Katoh M (2006) Comparative integromics on VEGF family members. Int J Oncol. 28: 1585–1589.

Kawase M, Murakami K, Fujimura M, Morita-Fujimura Y, Gasche Y, Kondo T, Scott RW, Chan PH (1999) Exacerbation of delayed cell injury after transient global ischemia in mutant mice with CuZn superoxide dismutase deficiency. Stroke 30: 1962–1968.

Kertesz N, Wu J, Chen TH, Sucov HM, Wu H (2004) The role of erythropoietin in regulating angiogenesis. Developmental Biol. 276: 101–110.

Kilic E, Kilic U, Wang Y, Bassetti CL, Marti HH, Hermann DM (2006) The phosphatidylinositol-3 kinase/Akt pathway mediates VEGF's neuroprotective activity and induces blood brain barrier permeability after focal cerebral ischemia. Faseb J. 20: 1185–1187.

Kinouchi H, Epstein CJ, Mizui T, Carlson E, Chen SF, Chan PH (1991) Attenuation of focal cerebral ischemic injury in transgenic mice overexpressing CuZn superoxide dismutase. Proc Natl Acad Sci USA 88: 11158–11162.

Klempt ND, Sirimanne E, Gunn AJ, Klempt M, Singh K, Williams C, Gluckman PD (1992) Hypoxia-ischemia induces transforming growth factor beta 1 mRNA in the infant rat brain. Mol Brain Res. 13: 93–101.

Koizumi J, Yoshida Y, Nakazawa T, Ooneda G (1986) Experimental studies of ischemic brain edema. I. A new experimental model of cerebral embolism in which recirculation can introduced into the ischemic area. Jpn J Stroke 8: 1–8.

Kondo T, Reaume AG, Huang TT, Carlson E, Murakami K, Chen SF, Hoffman EK, Scott RW, Epstein CJ, Chan PH (1997a) Reduction of CuZn-superoxide dismutase activity exacerbates neuronal cell injury and edema formation after transient focal cerebral ischemia. J Neurosci 17: 4180–4189.

Kondo T, Reaume AG, Huang TT, Murakami K, Carlson E, Chen S, Scott RW, Epstein CJ, Chan PH (1997b) Edema formation exacerbates neurological and histological outcomes after focal cerebral ischemia in CuZn-superoxide dismutase gene knockout mutant mice. Acta Neurochir Suppl (Wein) 70: 62–64.

Kontos HA (1985) George E. Brown Memorial Lecture: oxygen radicals in cerebral vascular injury. Circ Res 57: 508–516.

Kovacs Z, Ikezaki K, Samoto K, Inamura T, Fukui M (1996) VEGF and flt. Expression time kinetics in rat brain infarct. Stroke 27: 1865–1872.

Krupinski J, Issa R, Bujny T, Slevin M, Kumar P, Kumar S, Kaluza J (1997) A putative role for platelet-derived growth factor in angiogenesis and neuroprotection after ischemic stroke in humans. Stroke 28: 564–573.

Ladomery MR, Harper SJ, Bates DO (2007) Alternative splicing in angiogenesis: the vascular endothelial growth factor paradigm. Cancer Lett. 49: 133–142.

Lallemand F, Mazars A, Prunier C, Bertrand F, Kornprost M, Gallea S, Roman-Roman S, Cherqui G, Atfi, A (2001) Smad7 inhibits the survival nuclear factor κB and potentiates apoptosis in epithelial cells. Oncogene 20: 879–884.

Landstrom M, Heldin NE, Bu S, Hermansson A, Itoh S, ten Dijke P, Heldin CH (2000) Smad7 mediates apoptosis induced by transforming growth factor β in prostatic carcinoma cells. Curr. Biol. 10: 535–538.

LaPlaca M, Raghupathi R, Verma A, Pieper AA, Saatman KE, Snyder SH, McIntosh TK (1999) Temporal patterns of poly (ADP-ribose) polymerase activation in the cortex following experiment brain injury in rat. J. Neurochem. 73: 205–213.

Lappalainen Z, Lappalainen J, Oksala NK, Laaksonen DE, Khanna S, Sen CK, Atalay M (2009) Diabetes impairs exercise training-associated thioredoxin response and glutathione status in rat brain. J Appl Physiol. 106: 461–467.

LaRochelle WJ, Jeffers M, McDonald WF, Chillakuru RA, Giese NA, Lokker NA, Sullivan C, Boldog FL, Yang M, Vernet C, Burgess CE, Fernandes E, Deegler LL, Rittman B, Shimkets J, Shimkets RA, Rothberg JM, Lichenstein HS (2001) PDGF-D, a new protease-activated growth factor. Nature Cell Biol. 3: 517–521.

Larson EB, Wang L, Bowen JD, McCormick WC, Teri L, Crane P, Kukull W (2006) Exercise is associated with reduced risk for incident dementia among persons 65 years of age and older. Ann. Intern. Med. 144: 73–81.

Lee HS, Han J, Bai HJ, Kim KW (2009a) Brain angiogenesis in developmental and pathological processes: regulation, molecular and cellular communication at the neurovascular interface. FEBS J. 276(17):4622–4635.

Lee JM, Zipfel GJ, Choi DW (1999) The changing landscape of ischemic brain injury mechanisms. Nature 399 (Supp.): A7–A14.

Lee SU, Kim DY, Park SH, Choi DH, Park HW, Han TR (2009b) Mild to moderate early exercise promotes recovery from cerebral ischemia in rats. Can J Neurol Sci. 36(4): 443–449.

Lee YI, Cho JY, Kim MH, Kim KB, Lee DJ, Lee KS (2006) Effects of exercise training on pathological cardiac hypertrophy related gene expression and apoptosis. Eur J Appl Physiol. 97: 216–224.

Lei XG, Cheng WH (2005) New roles for an old selenoenzyme: evidence from glutathione peroxidase-1 null and overexpressing mice. J Nutr 135: 2295–2298.

Leist M, Single B, Castaldi AF, Kuhle S, Nicotera P (1997) Intracellular adenosine triphosphate (ATP) concentration: a switch in the decision between apoptosis and necrosis. J. Exp. Med. 185: 1481–1486.

Lemaire C, Andreau K, Fraisse CS, Adam A, Souvannavong V (1998) Inhibition of caspase activity induces a switch from apoptosis to necrosis. FEBS Lett. 425: 266–270.

Li X, Ponten A, Aase K, Karlsson L, Abramsson A, Uutela M, Bäckström G, Hellström M, Boström H, Li H, Soriano P, Betsholtz C, Heldin CH, Alitalo K, Östman A, Eriksson U (2000) PDGF-C is a new protease-activated ligand for the PDGF α-receptor. Nature Cell Biol. 2: 302–309.

Li Y, Chopp M, Jiang N, Yao F, Zaloga C (1995a) Temporal profile of in situ DNA fragmentation after transient middle cerebral artery occlusion in the rat. J Cereb Blood Flow Metab 15: 389–397.

Li Y, Chopp M, Jiang N, Zhang ZG, Zaloga C (1995b) Induction of DNA fragmentation after 10 to 120 minutes of focal cerebral ischemia in rats. Stroke 26: 1252–1257.

Liang Q, Li W, Zhou B (2008) Caspase-independent apoptosis in yeast. Biochim Biophys Acta. 1783: 1311–9.

Liddell JR, Robinson SR, Dringen R (2004) Endogenous glutathione and catalase protect cultured rat astrocytes from the iron-mediated toxicity of hydrogen peroxide. Neurosci Lett 364: 164–167.

Lindahl T, Satoh MS, Poirier GG, Klungland A (1995) Post-translational modification of poly(ADP-ribose) polymerase induced by DNA strand breaks, Trends Biochem. Sci. 20: 405–411.

Lindahl P, Johansson BR, Levéen P, Betsholtz C (1997) Pericyte loss and microaneurysm formation in PDGF-B-deficient mice. Science 277: 242–245.

Linnik MD, Miller JA, Sprinkle-Cavallo J, Mason PJ, Thompson FY, Montgomery LR, Schroeder KK (1995) Apoptotic DNA fragmentation in the rat cerebral cortex induced by permanent middle cerebral artery occlusion. Brain Res Mol Brain Res 32: 116 –124.

Lipton P (1999) Ischemic cell death in brain neurons. Physiol Rev. 79: 1431–568.

Longa EZ, Weinstein PR, Carlson S, Cummins R (1989) Reversible middle cerebral artery occlusion without craniectomy in rats. Stroke 20: 84–91.

Los M, Mozoluk M, Ferrari D, Stepczynska A, Stroh C, Renz A, Herceg Z, Wang ZQ, Schulze-Osthoff K (2002) Activation and caspase-mediated inhibition of PARP: a

molecular switch between fibroblast nercosis and apoptosis in death receptor signaling. Mol. Biol. Cell 13: 978–988.

Los M, Stroh C, Janicke RU, Engels IH, Schulze-Osthoff K (2001) Caspases more than just killers? Trends Immunol. 22: 31–34.

Lourbopoulos A, Karacostas D, Artemis N, Milonas I, Grigoriadis N (2008) Effectiveness of a new modified intraluminal suture for temporary middle cerebral artery occlusion in rats of various weight. J Neurosci Methods. 173: 225–34.

Madeo F, Carmona-Gutierrez D, Ring J, Büttner S, Eisenberg T, Kroemer G (2009) Caspase-dependent and caspase-independent cell death pathways in yeast. Biochem Biophys Res Commun. 382: 227–31.

Maire M, Florin A, Kaszas K, Regnier D, Contard P, Tabone E, Mauduit C, Bars R, Benahmed M (2005) Alteration of transforming growth factor-beta signaling system expression in adult rat germ cells with a chronic apoptotic cell death process after fetal androgen disruption. Endocrinology, 146: 5135–5143.

Markgraf CG, Kraydieh S, Prado R, Watson BD, Dietrich WD, Ginsberg MD (1993) Comparative histopathologic consequences of photothrombotic occlusion of the distal middle cerebral artery in Sprague-Dawley and Wistar rats. Stroke 24: 286–293.

Marti HH, Risau W (1999) Angiogenesis in ischemic disease. Thromb. Haemost. 82 (Suppl.): 44–52.

Marti HH, Bernaudin M, Petit E, Bauer C (2000) Neuroprotection and angiogenesis: a dual role of erythropoietin in brain ischemia. News Physiol. Sci. 15: 225–229.

Massague´ J, Chen YG (2000) Controlling TGF-β signaling. Genes Dev. 14: 627–644.

Masuda S, Okano M, Yamagishi K, Nagao M, Ueda M, Sasaki R (1994) A novel site of erythropoietin production. Oxygen-dependent production in cultured rat astrocytes. J Biol Chem 269: 19488–19493.

Mattson MP (2000) Apoptosis in neurodegenerative disorders. Nat Rev Mol Cell Biol 1: 120–129.

Melino G, Bernassola F, Knight RA, Corasaniti MT, Mistico G, Finaz zi-Agro A (1997) S-nitrosylation regulates apoptosis. Nature 388: 432–433.

Memezawa H, Minamisawa H, Smith ML, Siesjo BK (1992) Ischemic penumbra in a model of reversible middle cerebral artery occlusion. Exp. Brain Res. 89: 67–78.

Menzies SA, Hoff JT, Betz AL (1992) Middle cerebral artery occlusion in rats: A neurological and pathological evaluation of a reproducible model. Neurosurgery 31: 100–107.

Minematsu K, Fisher M, Li L, Davis MA, Knapp AG, Cotter RE, McBurney RN, Sotak CH (1993) Effects of a novel NMDA antagonist on experimental stroke rapidly and quantitatively assessed by diffusion- weighted MRI. Neurology 43: 397–403.

Mohamed AA, Gotoh O, Graham DI, Osborne KA, McCulloch J, Mendelow AD, Teasdale GM, Harper AM (1985) Effect of pretreatment with the calcium antagonist nimodipine on local cerebral blood flow and histopathology after middle cerebral artery occlusion. Ann Neurol 18: 705–711.

Murphy AN, Fiskum G, Beal MF (1999) Mitochondria in neurodegeneration: bioenergetic function in cell life and death. J. Cereb. Blood Flow Metab. 19: 231–245.

Nagasawa H, Kogure K (1989) Correlation between cerebral blood flow and histological change in a new rat model of cerebral artery occlusion. Stroke 20: 1037–1043.

Naylor AS, Bull C, Nilsson MK, Zhu C, Björk-Eriksson T, Eriksson PS, Blomgren K, Kuhn HG (2008) Voluntary running rescues adult hippocampal neurogenesis after irradiation of the young mouse brain. Proc Natl Acad Sci U S A. 105: 14632–14637.

Nguyen N, Lee SB, Lee YS, Lee KH, Ahn JY (2009) Neuroprotection by NGF and BDNF against neurotoxin-exerted apoptotic death in neural stem cells are mediated through Trk receptors, activating PI3-kinase and MAPK pathways. Neurochem Res. 34: 942–951.

Nicholson DW, Thornberry NA (1997) Caspases: killer proteases. Trends Biochem. Sci. 22: 299–306.

Nicoletti JN, Shah SK, McCloskey DP, Goodman JH, Elkady A, Atassi H, Hylton D, Rudge JS, Scharfman HE, Croll SD (2008) Vascular Endothelial Growth Factor Is Up-Regulated after Status Epilepticus and Protects against Seizure-Induced Neuronal Loss in Hippocampus. Neuroscience 151: 232–241.

Nudo RJ, Dancause N (2007) Neuroscientific basis for occupational and physical therapy interventions. In: ND Zasler DK, RD Zafonte, eds. Brain Injury Medicine: Principles and Practice. New York, NY: Demos Publishing LLC 913–928.

Page SJ, Levine P, Leonard AC (2005) Modified constraint-induced therapy in acute stroke: a randomized controlled pilot study. Neurorehabil Neural Repair. 19: 27–32.

Page SJ, Sisto S, Levine P, McGrath R (2004) Efficacy of modified constraint-induced therapy in chronic stroke: a single blinded randomized controlled trial. Arch Phys Med Rehabil. 85: 14–18.

Page SJ, Sisto SA, Levine P, Johnston MV, Hughes M (2001) Modified constraint induced therapy: a randomized, feasibility and efficacy study. J Rehabil Res Dev. 38: 583–590.

Page SJ, Sisto SA, Johnston MV, Levine P (2002) Modified constraint-induced therapy after sub acute stroke: a preliminary study. Neurorehabil Neural Repair. 16: 223–228.

Papucci L, Formigli L, Schiavone N, Tani A, Donnini M, Lapucci A, Perna F, Tempestini A, Witort E, Morganti M, Nosi D, Orlandini GE, Zecchi Orlandini S, Capaccioli S (2004) Apoptosis shifts to necrosis via intermediate types of cell death by a mechanism depending on c- myc and bcl-2 expression Cell Tissue Res. 316: 197–209.

Park SH 2005 Fine tuning and cross-talking of TGF-beta signal by inhibitory Smads. J Biochem Mol Biol. 38: 9–16.

Patel VA, Lee DJ, Longacre-Antoni A, Feng L, Lieberthal W, Rauch J, Ucker DS, Levine JS (2009) Apoptotic and necrotic cells as sentinels of local tissue stress and inflammation: response pathways initiated in nearby viable cells. Autoimmunity 42: 317–21.

Pender MP, Nguyen KB, McCombe PA, Kerr JF (1991) Apoptosis in the nervous system in experimental allergic encephalomyelitis. J. Neurol. Sci. 104: 81–87.

Peng Z, Ren P, Kang Z, Du J, Lian Q, Liu Y, Zhang JH, Sun X (2008) Up-regulated HIF-1alpha is involved in the hypoxic tolerance induced by hyperbaric oxygen preconditioning. Brain Res. 1212: 71–78.

Pereira AC, Huddleston DE, Brickman AM, Sosunov AA, Hen R, McKhann GM, Sloan R, Gage FH, Brown TR, Small SA (2007) An in vivo correlate of exercise induced neurogenesis in the adult dentate gyrus, Proc. Natl Acad. Sci. 104: 5638–5643.

Prabhakaran K, Li L, Borowitz JL, Isom GE (2004) Caspase inhibition switches the mode of cell death induced by cyanide by enhancing reactive oxygen species generation and PARP-1 activation. Toxicol. Appl. Pharmacol. 195: 194–202.

Prehn JHM, Bindokas VP, Marcuccilli CJ, Krajewski D, Reed JC, Miller RJ (1994) Regulation of neuronal Bcl-2 protein expression and calcium homeostasis by transforming growth factor beta confers wide-ranging protection on rat hippocampal neurons. Proc Natl Acad Sci USA 91: 12599–12603.

Rami A, Bechmann I, Stehle JH (2008) Exploiting endogenous anti-apoptotic proteins for novel therapeutic strategies in cerebral ischemia. Prog Neurobiol. 85: 273–96.

Ramsden M, Berchtold NC, Patrick Kesslak J, Cotman CW, Pike CJ (2003) Exercise increases the vulnerability of rat hippocampal neurons to kainite lesion, Brain Res. 971: 239–244.

Ransohoff RM, Glabinski A, Tani M (1996) Chemokines in immunemediated inflammation of the central nervous system. Cytokine Growth Factor Rev. 7: 35-46.

Ratan RR, Siddiq A, Smirnova N, Karpisheva K, Haskew-Layton R, McConoughey S, Langley B, Estevez A, Huerta PT, Volpe B, Roy S, Sen CK, Gazaryan I, Cho S, Fink

M, LaManna J (2007) Harnessing hypoxic adaptation to prevent, treat, and repair stroke. J Mol Med. 85: 1331–1338.

Ratcliffe PJ, O'Rourke JF, Maxwell PH, Pugh CW (1998) Oxygen sensing, hypoxia-inducible factor-1 and the regulation of mammalian gene expression. J Exp Biol 201: 1153–1162.

Reigstad LJ, Varhaug JE, Lillehaug JR (2005) Structural and functional specificities of PDGF-C and PDGF-D, the novel members of the platelet-derived growth factors family. FEBS J. 272: 5723–41.

Ren RF, Flanders KC (1996) Transforming growth factor-β protects primary rat hippocampal neuronal cultures from degeneration induced by beta-amyloid peptide. Brain Res 732: 16–24.

Rigau V, Morin M, Rousset MC, de Bock F, Lebrun A, Coubes P, Picot MC, Baldy-Moulinier M, Bockaert J, Crespel A, Lerner-Natoli M (2007) Angiogenesis is associated with blood-brain barrier permeability in temporal lobe epilepsy. Brain 130: 1942–1956.

Risedal A, Zeng J, Johansson BB (1999) Early training may exacerbate brain damage after focal brain ischemia in the rat, J. Cereb. Blood Flow Metab. 19: 997–1003.

Roberts D, Smith DJ (1999) Erythropoietin concentration and arterial haemoglobin saturation with supramaximal exercise. J Sports Sci. 17: 485–493.

Roethy W, Fiehn E, Suehiro K, Gu A, Yi GH, Shimizu J, Wang J, Zhang G, Ranieri J, Akella R, Funk SE, Sage EH, Benedict J, Burkhoff D (2001) A growth factor mixture

that significantly enhances angiogenesis in vivo. J Pharmacol Exp Ther. 299(2): 494–500.

Roy M, Sapolsky R (1999) Neuronal apoptosis in acute necrotic insults: why is this subject such a mess? Trends Neurosci. 22: 419–422.

Ruemmele FM, Dionne S, Levy E, Seidman EG (1999) TNF-alpha induced IEC-6 cell apoptosis requires activation of ICE caspases whereas complete inhibition of caspase cascade leads to necrotic cell death. Biochem. Biophys. Res. Commun. 260: 159–166.

Ruocco A, Nicole O, Docagne F, Ali C, Chazalviel L, Komesli S, Yablonsky F, Roussel S, MacKenzie ET, Vivien D, Buisson A (1999) A transforming growth factor-beta antagonist unmasks the neuroprotective role of this endogenous cytokine in excitotoxic and ischemic brain injury. J Cereb Blood Flow Metab. 19: 1345–1353.

Sakanaka M, Wen TC, Matsuda S, Masuda S, Morishita E, Nagao M, Sasaki R (1998) In vivo evidence that erythropoietin protects neurons from ischemic damage. Proc. Natl. Acad. Sci. USA 95: 4635–4640.

Salceda S, Caro J (1997) Hypoxia-inducible factor 1alpha (HIF-1alpha) protein is rapidly degraded by the ubiquitin-proteasome system under normoxic conditions. Its stabilization by hypoxia depends on redoxinduced changes. J Biol Chem 272: 22642–22647.

Sasahara M, Fries JWU, Raines EW, Gown AM, Westrum LE, Frosch MP, Bonthron DT, Ross R, Collins T (1991) PDGF B-chain in neurons of the central nervous system, posterior pituitary, and in a transgenic model. Cell 64: 217–227.

Schellinger PD, Fiebach JB, Mohr A, Ringleb PA, Jansen O, Hacke W (2001a) Thrombolytic therapy for ischemic stroke—a review: part I intravenous thrombolysis. Crit Care Med 29: 1812–1818.

Schellinger PD, Fiebach JB, Mohr A, Ringleb PA, Jansen O, Hacke W (2001b) Thrombolytic therapy for ischemic stroke—a review: part II intraarterial thrombolysis, vertebrobasilar stroke, phase IV trials, and stroke imaging. Crit Care Med 29: 1819–1825.

Schmid-Elsaesser R, Zausinger S, Hungerhuber E, Baethmann A, Reulen HJ (1998) A critical reevaluation of the intraluminal thread model of focal cerebral ischemia: evidence of inadvertent premature reperfusion and subarachnoid hemorrhage in rats by laser-Doppler flowmetry. Stroke 29: 2162–2170.

Schobersberger W, Hobisch-Hagen P, Fries D, Wiedermann F, Rieder-Scharinger J, Villiger B, Frey W, Herold M, Fuchs D, Jelkmann W (2000) Increase in immune activation, vascular endothelial growth factor and erythropoietin after an ultramarathon run at moderate altitude. Immunobiology. 201: 611–620.

Schuster N, Krieglstein K (2002) Mechanisms of TGF- β-mediated apoptosis. Cell Tissue Res. 307: 1–14.

Semenza GL, Wang GL (1992) A nuclear factor induced by hypoxia via de novo protein synthesis binds to the human erythropoietin gene enhancer at a site required for transcriptional activation. Mol. Cell. Biol. 12: 5447–5454.

Semenza GL (1999) Regulation of mammalian O2 homeostasis by hypoxia-inducible factor 1. Annu. Rev. Cell Dev. Biol. 15: 551–578.

Semenza GL (2001) Hypoxia-inducible factor 1: oxygen homeostasis and disease pathophysiology. Trends Mol Med 7: 345–350.

Servais S, Couturier K, Koubi H, Rouanet JL, Desplanches D, Sornay-Mayet MH, Sempore B, Lavoie JM, Favier R (2003) Effect of voluntary exercise on H2O2 release by subsarcolemmal, and intermyofibrillar mitochondria. Free Radic. Biol. Med. 35: 24–32.

Shao G, Gao CY, Lu GW (2005) Alterations of hypoxia-inducible factor-1 alpha in the hippocampus of mice acutely and repeatedly exposed to hypoxia, Neurosignals 14: 255–261.

Shen H, Tong L, Balazs R, Cotman CW (2001) Physical activity elicits sustained activation of the cyclic AMP response element-binding protein and mitogen-activated protein kinase in the rat hippocampus. Neuroscience 107: 219–229.

Shi Y, Massague J (2003) Mechanisms of TGF-beta signaling from cell membrane to the nucleus. Cell 113: 685–700.

Shimizu S, Eguchi Y, Kamiike W, Itoh Y, Hasegawa J, Yamabe K, Otsuki Y, Matsuda H, Tsujimoto Y (1996) Induction of apoptosis as well as necrosis by hypoxia and predominant prevention of apoptosis by Bcl-2 and Bcl-XL. Cancer Res. 56: 2161–2166.

Shingo T, Sorokan ST, Shimazaki T, Weiss S (2001) Erythropoietin regulates the in vitro and in vivo production of neuronal progenitors by mammalian forebrain neural stem cells. J. Neurosci. 21: 9733–9743.

Siesjö BK, Agardh CD, Bengtsson F (1989) Free radicals and brain damage. Cerebrovasc Brain Metab Rev 1: 165–211.

Siesjo BK, Siesjo P (1996) Mechanisms of secondary brain injury. Eur J Anaesthesiol. 13: 247–268.

Sim YJ, Kim H, Kim JY, Yoon SJ, Kim SS, Chang HK, Lee TH, Lee HH, Shin MC, Shin MS, Kim CJ (2005) Long-term treadmill exercise overcomes ischemia-induced apoptotic neuronal cell death in gerbils. Physiol Behav. 84: 733–738.

Sirén AL, Fratelli M, Brines M, Goemans C, Casagrande S, Lewczuk P, Keenan S, Gleiter C, Pasquali C, Capobianco A (2001a) Erythropoietin prevents neuronal apoptosis after cerebral ischemia and metabolic stress. Proc. Natl. Acad. Sci. USA 98: 4044–4049.

Sirén AL, Knerlich F, Poser W, Gleiter CH, Brück W, Ehrenreich H (2001b) Erythropoietin and erythropoietin receptor in human ischemic/hypoxic brain. Acta Neuropathol. 101: 271–276.

Slee EA, Adrain C, Martin SJ (2001) Executioner caspase-3, -6, and -7 perform distinct, non-redundant roles during the demolition phase of apoptosis. J Biol Chem 276: 7320–7326.

Smits A, Kato M, Westermark B, Nistér M, Heldin CH, Funa K (1991) Neurotrophic activity of platelet-derived growth factor (PDGF): rat neuronal cells possess functional PDGF b-type receptors and respond to PDGF. Proc. Natl. Acad. Sci. USA 88: 8159–8163.

Soldani C, Scovassi AI (2002) Poly(ADP-ribose) polymerase-1 cleavage during apoptosis: an update. Apoptosis. 7: 321–328.

Somani SM, Husain K, Schlorff EC (1994) Response of antioxidant system to physical and chemical stress. In: Baskin, S.I., Salem, H. (Eds.), Oxidants, Antioxidants and Radicals. Taylor and Francis, Washington, pp. 125–143.

Somani SM, Ravi R, Rybak LP (1995) Effect of exercise training on antioxidant system in brain regions of rat. Pharmacol Biochem Behav 50: 635–639.

Soriano MA, Sanz O, Ferrer I, Planas AM (1997) Cortical infarct volume is dependent on the ischemic reduction of perifocal cerebral blood flow in a three vessel intraluminal MCA occlusion/reperfusion model in the rat. Brain Res. 747: 273–278.

Stranahan AM, Lee K, Martin B, Maudsley S, Golden E, Cutler RG, Mattson MP (2009) Voluntary exercise and caloric restriction enhance hippocampal dendritic spine density and BDNF levels in diabetic mice. Hippocampus. 19: 951–961.

Stroka DM, Burkhardt T, Desbaillets I, Wenger RH, Neil DAH, Bauer C, Gassmann M, Candinas D (2001) HIF-1 is expressed in normoxic tissues and displays an organ-specific regulation under systemic hypoxia, FASEB. J. 15: 2445–2453.

Swanson RA, Morton MT, Tsao-WG, Savalos RA, Davidson C, Sharp FR (1990) A semiautomated method of measuring brain infarct volume. J Cereb Blood Flow Metab 10: 290–293.

Sydserff SG, Borelli AR, Green AR, Cross AJ (2002) Effect of NXY- 059 on infarct volume after transient or permanent middle cerebral artery occlusion in the rat; studies

on dose, plasma concentration and therapeutic time window. Br J Pharmacol 135: 103–112.

Takahashi T, Ueno H, Shibuya M (1999) VEGF activates protein kinase C-dependent, but Ras-independent Raf-MEK-MAP kinase pathway for DNA synthesis in primary endothelial cells. Oncogene 18: 2221–2230.

ten Dijke P, Hill CS (2004) New insights into TGF-beta-Smad signaling. Trends Biochem Sci. 29: 265–273.

Tsai PT, Ohab JJ, Kertesz N, Groszer M, Matter C, Gao J, Liu X, Wu H, Carmichael ST (2006) A critical role of erythropoietin receptor in neurogenesis and post-stroke recovery. Journal of Neuroscience, 26: 1269–1274.

Tsujimoto Y (1997) Apoptosis and necrosis: intracellular ATP levels as a determinant for cell death modes. Cell Death Differ. 4: 429–434.

Ullerås E, Wilcock A, Miller SJ, Franklin GC (2001) The sequential activation and repression of the human PDGF-B gene during chronic hypoxia reveals antagonistic roles for the depletion of oxygen and glucose. Growth Factors. 19: 233–245.

Ulloa L, Doody J, Massague´ J (1999) Inhibition of transforming growth factor-β /SMAD signaling by the interferon-γ/STAT pathway. Nature 397: 710–713.

Ursini F, Maiorino M, Brigelius-Flohe R, Aumann KD, Roveri A, Schomburg D, Flohe L (1995) Diversity of glutathione peroxidases. Methods Enzymol 252: 38–53.

Velier JJ, Ellison JA, Kikly KK, Spera PA, Barone FC, Feuerstein GZ (1999) Caspase-8 and caspase-3 are expressed by different populations of cortical neurons undergoing delayed cell death after focal stroke in the rat. J. Neurosci. 19: 5932–5941.

Venketasubramanian N, Tan LC, Sahadevan S, Chin JJ, Krishnamoorthy ES, Hong CY, Saw SM (2005) Prevalence of stroke among Chinese, Malay, and Indian Singaporeans: a community-based tri-racial cross-sectional survey. Stroke 36: 551–556.

Vercammen D, Beyaert R, Denecker G, Goosens V, Van-Loo G, Declercq W, Grooten J. Fiers W, Vandenabeele P (1998) Inhibition of caspases increases the sensitivity of L929 cells to necrosis mediated by tumor necrosis factor. J. Exp. Med. 187: 1477–1485.

Wallisser JA, Thies RL (1999) Poly (ADP-ribose) polymerase inhibition in oxidant-stressed endothelial cells prevents oncosis and permits caspase activation and apoptosis. Exp. Cell Res. 251: 401–413.

Wen TC, Rogido M, Genetta T, Sola A (2004) Permanent focal cerebral ischemia activates erythropoietin receptor in the neonatal rat brain. Neurosci Lett. 355: 165–168.

Wenger RH (2000) Mammalian oxygen sensing, signaling and gene regulation. J. Exp. Biol. 203: 1253–1263.

Wiessner C, Allegrini PR, Ekatodramis D, Jewell UR, Stallmach T, Gassmann M (2001) Increased cerebral infarct volumes in polyglobulic mice overexpressing erythropoietin. J. Cereb. Blood Flow Metab. 21: 857–64.

Woo M, Hakem R, Soengas MS, Duncan GS, Shahinian A, Kägi D, Hakem A, McCurrach M, Khoo W, Kaufman SA, Senaldi G, Howard T, Lowe SW, Mak TW (1998) Essential contribution of caspase 3/CPP32 to apoptosis and its associated nuclear changes. Genes Dev 12: 806–819.

Wu CW, Chang YT, Yu L, Chen HI, Jen CJ, Wu SY, Lo CP, Kuo YM (2008) Exercise enhances the proliferation of neural stem cells and neurite growth and survival of neuronal progenitor cells in dentate gyrus of middle-aged mice. J Appl Physiol. 105: 1585–1594.

Wu H, Lee SH, Gao J, Liu X, Iruela-Arispe ML (1999) Inactivation of erythropoietin leads to defects in cardiac morphogenesis. Development 126: 3597–3605.

Wyllie AH, Kerr JF, Currie AR (1980) Cell death: the significance of apoptosis. Int. Rev. Cytol. 68, 251–306.

Xiao YQ, Malcolm K, Worthen GS, Gardai S, Schiemann WP, Fadok VA, Bratton DL, Henson PM (2002) Cross-talk between Erk and p38 MAPK mediates selective suppression of pro-inflammatory cytokines by TGF-β. J Biol Chem. 277: 14884–14893.

Yamaji R, Okada T, Moriya M, Naito M, Tsuruo T, Miyatake K, Nakano Y (1996) Brain capillary endothelial cells express two forms of erythropoietin receptor mRNA. Eur. J. Biochem. 239: 494–500.

Yancopoulos GD, Davis S, Gale NW, Rudge JS, Wiegand SJ, Holash J (2000) Vascular-specific growth factors and blood vessel formation. Nature 407: 242–248.

Yang G, Chan PH, Chen J, Carlson E, Chen S, Weinstein P, Epstein CJ, Kamii H (1994) Human copper-zinc superoxide dismutase transgenic mice are highly resistant to reperfusion injury after focal cerebral ischemia. Stroke 25: 165–170.

Yap E, Tan WL, Ng I, Ng YK (2008) Combinatorial-approached neuroprotection using pan-caspase inhibitor and poly (ADP-ribose) polymerase (PARP) inhibitor following experimental stroke in rats; is there additional benefit? Brain Res. 1195: 130–138.

Yoshida D, Kim K, Noha M, Teramoto A (2006) Hypoxia inducible factor 1-alpha regulates of platelet derived growth factor-B in human glioblastoma cells. J Neurooncol. 76: 13–21.

Yrjanheikki J, Tikka T, Keinanen R, Goldsteins G, Chan PH, Koistinaho J (1999) A tetracycline derivative, minocycline, reduces inflammation and protects against focal cerebral ischemia with a wide therapeutic window. Proc Natl Acad Sci USA 96: 13496–13500.

Yu L, Hebert MC, Zhang YE (2002) TGF-β receptor-activated p38 MAP kinase mediates Smad-independent TGF-β responses. EMBO J. 21: 3749–3750.

Zhang F, Signore AP, Zhou ZG, Wang SP, Cao GD, Chen J (2006) Erythropoietin Protects CA1 Neurons Against Global Cerebral Ischemia in Rat: Potential Signaling Mechanisms. J. Neurosci. Res. 83: 1241–1251.

Zhang J, Graham DG, Montine TJ, Ho YS (2000) Enhanced N-methyl-4-phenyl-1, 2,3,6-tetrahydropyridine toxicity in mice deficient in CuZn-superoxide dismutase or glutathione peroxidase. J Neuropathol Exp Neurol 59: 53–61.

Zhang ZG, Zhang L, Tsang W, Soltanian-Zadeh H, Morris D, Zhang R, Goussev A, Powers C, Yeich T, Chopp M (2002) Correlation of VEGF and angiopoietin expression with disruption of blood-brain barrier and angiogenesis after focal cerebral ischemia. J Cereb Blood Flow Metab. 22: 379–392.

Zhao Q, Memezawa H, Smith ML, Siesjo BK (1994) Hyperthermia complicates middle cerebral artery occlusion induced by an intraluminal filament. Brain Res. 649: 253–259.

Zhu Y, Ahlemeyer B, Bauerbach E, Krieglstein J (2001) TGF-β1 prevents neuronal apoptosis in rat hippocampal cultures involving inhibition of caspase-3 activation. Neurochem Int. 38: 227–235.

Zhu Y, Roth-Eichhorn S, Braun N, Culmsee C, Rami A, Krieglstein J (2000) The expression of transforming growth factor-beta1 (TGF-beta1) in hippocampal neurons: a temporary upregulated protein level after transient forebrain ischemia in the rat. Brain Res. 866: 286–298.

Zhu Y, Yang GY, Ahlemeyer B, Pang L, Che XM, Culmsee C, Klumpp S, Krieglstein J (2002) Transforming growth factor-β1 increases Bad phosphorylation and protects neurons against damage. J Neurosci 22: 3898–3909.

APPENDICES

CHAPTER SEVEN

Appendix 1

Equipment and anesthesia needed for MCAO surgery

• Shaver for general use

• Thermal blanket coupled with a rectal probe for temperature read-out

• Forceps for general use

• Micro-scissor

• Blade holder with Blade

• Skin retractor

• Hooks

• Dissecting microscope

• Illuminating lights

• Irrigation and suction set-up

• Needle and sutures

• 0.2ml/100g cocktail of ketamine and xylazine (75 mg/kg + 10 mg/kg)

Appendix 2

TTC

0.4%TTC

A stock solution of 0.4% TTC was prepared by dissolving 0.4g of TTC powder in 5ml dimethy sulphoxide (DMSO) and 95ml of distilled water. The suspension was sonicated thereafter for an hr to facilitate solution.

0.1%TTC

0.1% TTC was prepared by adding 10ml of the 0.4% TTC stock solution to 16ml 0.2M Na_2HPO_4, 4ml 0.2M NaH_2PO_4 and 10ml 8mM $MgCl_2$ (pH7.4). This solution should be protected from light.

Appendix 3

Real Time - PCR

Kit/ solutions :

Chloroform

70% and 96-100% Ethanol

Qiagen RNeasy Lipid Tissue Midi Kit (QIAzol® Lysis Reagent, Buffer RW1, Buffer RPE, RNase-free water)

Promega Reverse Transcription System (AMV Reverse Transcriptase (HC), Recombinant RNasin® Ribonuclease Inhibitor, Oligo(dT)$_{15}$ Primer, Random Primers, 1.2kb Kanamycin Positive Control RNA, dNTP Mix, Reverse Transcription 10X Buffer, $MgCl_{2,}$ Nuclease-Free Water)

Qiagen QuantiTect® SYBR® Green RT-PCR [QuantiTect SYBR Green RT-PCR Master Mix (HotStarTaq® DNA Polymerase, QuantiTect SYBR Green RT-PCR Buffer, dNTP mix, including dUTP, SYBR Green I, ROX passive reference dye, 5 mM MgCl2), QuantiTect RT Mix, a mixture of the QIAGEN® (Omniscript® Reverse Transcriptase, Omniscript® Reverse Transcriptase), RNase-Free Water]

Appendix 4

Western blotting

Homogenisation

4.5 ml of 1x PBS (pH 7.4; 4ºC) containing aprotinin (1µg/ml)

45µl of Triton-X 100

SDS-PAGE

10%, 12% or 15% Pre-casted Gel (BioRad) was used throughout the experiments.

Solutions:

Running buffer (1x)

1.51g/litre Tris base

5g/litre SDS

7.2g/litre Glycine

Transfer buffer (1x)

3.03g/litre Tris

14.4g/litre Glycine

200ml Methanol

800ml distilled water

Blocking buffer

PBS (10x) 100ml

0.1% Tween 20 1ml

5% non fat milk powder 50g

Distilled water to 1 Liter

Washing buffer

PBS (10x) 100ml

Distilled water to 1 Liter

Incubation reagents and time

Block with milk buffer for 1hr

Incubate with primary antibody overnight on a shaker

Incubate with biotinylated anti-rabbit or anti-goat secondary antibody (1:5000) (1hr)

Wash with PBS

Immunodetection of protein

ECL Plus™ Western Blotting Reagents from GE Healthcare (formerly Amersham Biosciences)

Appendix 5

Immunohistochemistry

Solutions for transcardial perfusion

Ringers solutions

4% paraformaldehyde (4g/100ml of PB)

15% sucrose (15g/10ml of PB)

Gelatinized slides

Acid-cleaned slides

1.5% gelatin and 0.15% Chrome alum solution

Buffers

PBS (pH 7.4)

Distilled water 1 Liter

Disodium Hydrogen Phosphate, Heptahydrate 13.4g

Sodium chloride 8g

PBS-TX (pH 7.4)

Distilled water 1 Liter

Disodium Hydrogen Phosphate, Heptahydrate 13.4g

Sodium chloride 8g

Triton-X 100 1ml

0.1M Acetate Buffer

1M acetate buffer 10ml

Distilled water 90ml

1M Acetate Buffer (pH 4.8)

Sodium acetate 24.6g

Distilled water 300ml